P-07-206

Forsmark site investigation

Stress measurements with hydraulic methods in boreholes KFM07A, KFM07C, KFM08A, KFM09A and KFM09B

Daniel Ask, Vattenfall Power Consultant AB

Francois Cornet, Christophe Brunet
Institut de Physique du Globe de Paris

Frederic Fontbonne, Geostress Co

November 2007

Svensk Kärnbränslehantering AB
Swedish Nuclear Fuel
and Waste Management Co
Box 250, SE-101 24 Stockholm
Tel +46 8 459 84 00

ISSN 1651-4416
SKB P-07-206

Forsmark site investigation

Stress measurements with hydraulic methods in boreholes KFM07A, KFM07C, KFM08A, KFM09A and KFM09B

Daniel Ask, Vattenfall Power Consultant AB

Francois Cornet, Christophe Brunet
Institut de Physique du Globe de Paris

Frederic Fontbonne, Geostress Co

November 2007

Keywords: AP PF 400-06-091, AP PF 400-06-083, AP PF 400-06-061, AP PF 400-06-044, MKW wireline unit, Mosnier tool, Straddle packer system, Cluster approach, Stress determination, Hydraulic fracturing (HF tests), Hydraulic tests on pre-existing fractures (HTPF tests), En echelon fractures, Boremap, Injection tests, Re-opening tests, Hydraulic jacking, Normal stress, Horizontal and vertical stresses.

Summary

Hydraulic rock stress measurements were performed in boreholes KFM07A (13 tests), KFM07C (15 tests), KFM08A (23 tests), KFM09A (16 tests), and KFM09B (18 tests) at the Forsmark candidate area, Sweden. The measurements were carried out in four separate campaigns, and a total of 87 hydraulic fracturing tests, hydraulic tests on pre-existing fractures, and sleeve fracturing tests were conducted between the 6th of June and the 21th of October, 2006.

The work involved cooperation between Vattenfall Power Consultant AB (Contractor), Institut de Physique du Globe de Paris (IPGP), and Geostress Co (both Sub-contractors). Vattenfall Power Consultant AB provided an MKW wireline system and field personnel, whereas IPGP supplied downhole equipment, data acquisition system, and field personnel. Finally, Geostress contributed with field personnel.

This report presents scope, objectives and performance of the stress measurements at the three drill sites. Further, a description is given of the employed test equipment, quality assurance, testing methodology (the so called cluster approach /Ask and Cornet 2006, 2007/), and results of stress interpretation at the Forsmark site. A more detailed account for instrument calibration, data collection, experiences of and observations made during the field work is outlined in Appendices I through III.

Despite the pronounced difficulties in collecting unambiguous data in the various boreholes, the state of stress could be determined in all investigated boreholes. However, in the absence of both true hydraulic fracturing (HF) data and hydraulic tests on pre-existing fractures (HTPF) from each drill site (only available at drill site 7), the resolution of the stress field is not always optimal. To this should be added that the stress field variation is non-linear with depth, leading to that interpolation of results over long depth intervals is not warranted. This is especially pronounced at drill site 8, but is believed to cause dispersion at all drill sites. With this respect, the cluster methodology /Ask and Cornet 2006, 2007/ for data collection is indeed favourable. However, the number of unambiguous data in each cluster, when presently disregarding information from packer-induced fractures, is not enough for an optimal resolution of all parameters within the cluster. It is the authors' opinion that with extended analysis much information could still be gained in this respect.

The stress determination for drill site 7 is the most reliable in terms of resolution of the stress field and is used below to express the state of stress at repository depth (400–500 mvd), see below. The solution was also verified by the packer-induced fractures. To our knowledge, this is the first time anyone has produced an independent check on the validity of a stress determination, which must be regarded as a unique aspect of quality assurance procedure and result verification.

400 mvd	**500 mvd**
$\sigma_h = 9.3 \pm 1.1$ MPa	$\sigma_h = 10.2 \pm 1.6$ MPa
$\sigma_H = 19.2 \pm 0.7$ MPa	$\sigma_H = 22.7 \pm 1.1$ MPa
$\sigma_v = 10.4$ MPa	$\sigma_v = 13.0$ MPa
Orientation of $\sigma_H = 124 \pm 6°$N	Orientation of $\sigma_H = 124 \pm 6°$N

Sammanfattning

Hydrauliska bergspänningsmätningar har utförts i borrhål KFM07A (13 tester), KFM07C (15 tester), KFM08A (23 tester), KFM09A (16 tester) och KFM09B (18 tester) i Forsmark. Totalt gjordes således 87 hydrauliska tester i fyra separata kampanjer mellan den 6:e juni och 21:a oktober, 2006.

Aktiviteten var ett samarbetsprojekt mellan Vattenfall Power Consultant AB (huvudkonsult), Institute de Physique du Globe de Paris (IPGP), och Geostress Co (båda dessa organisationer underkonsulter). Vattenfall Power Consultant AB tillhandahöll ett MKW wireline-system samt fältpersonal, IPGP stod för borrhålsutrustning, datainsamlingssystem och fältpersonal, medan Geostress bidrog med fältpersonal.

Denna rapport presenterar syfte, omfattning och utförande av bergspänningsmätningarna vid de tre borrplatserna. Vidare beskrivs utrustning, kvalitetssäkringsaspekter, testmetodik (den s k klustermetoden /Ask och Cornet 2006, 2007/) samt tolkningen av bergspänningarna i Forsmark. I bilagorna I till III ges en mer detaljerad redogörelse för exempelvis instrumentkalibrering, datainsamling samt allmänna erfarenheter av och observationer gjorda under fältarbetet.

Trots stora svårigheter att insamla otvetydiga data i de undersökta borrhålen kunde spänningsfältet för alla tre borrplatserna bestämmas. Som en följd av att resultat från hydrauliska tester på existerande sprickor (HTPF tester) kunde kombineras med sanna hydrauliska spräckningsdata (HF data) i endast ett av de testade borrhålen, är upplösningen på spänningsparametrarna inte alltid optimal. Till detta skall läggas att spänningsfältets förändring med djupet är icke-linjär, vilket tydligt kunde observeras under mätkampanjerna. Detta medför att interpoleringen av data över längre intervall blir problematisk. Spänningsfältets icke-linearitet är speciellt tydlig vid borrplats 8 men påverkar lösningarna i samtliga borrhål och karaktäriseras av förhöjda standardavvikelser i lösningarna. I detta avseende var den valda insamlingsmetodiken, den s k klustermetodiken /Ask och Cornet 2006, 2007/, synnerligen fördelaktig. Tyvärr är dock antalet otvetydiga data relativt få i varje kluster i nuvarande beräkningar eftersom merparten av tester med manschettinducerade sprickor inte har använts i tolkningen. Vi vill betona att vidare analys av dessa sprickor sannolikt kan leda till avsevärd förbättring av de tolkningar som presenteras i denna rapport.

Spänningsbestämningen för borrplats 7 utgör den mest tillförlitliga lösningen för förvarsdjupet 400–500 m, se nedan. Denna lösning har verifierats med hjälp av just packerinducerade sprickor, som ett illustrativt exempel. Så långt vi känner till är detta första gången någonsin som en beräknad lösning har verifierats med detta från den ordinarie beräkningsmetodiken oberoende tillvägagångssättet.

400 mvd	**500 mvd**
σ_h = 9,3 ± 1,1 MPa	σ_h = 10,2 ± 1,6 MPa
σ_H = 19,2 ± 0,7 MPa	σ_H = 22,7 ± 1,1 MPa
σ_v = 10,4 MPa	σ_v = 13,0 MPa
Orientering av σ_H = 124 ± 6°N	Orientering av σ_H = 124 ± 6°N

Contents

1 Introduction

This report describes the objectives, scope and performance of hydraulic rock stress measurements at Forsmark, Sweden. It also summarizes the collected data and presents results from stress determinations. The hydraulic tests involved Hydraulic Fracturing (HF), Hydraulic Tests on Pre-existing Fractures (HTPF), and sleeve fracturing tests in boreholes KFM07A, KFM07C, KFM08A, KFM09A, and KFM09B. The measurements are part of the activities within the investigation program at the Forsmark site and the work was carried out in compliance with the Activity Plans AP PF 400-06-091, AP PF 400-06-083, AP PF 400-06-061, and AP PF 400-06-044.

The investigated boreholes are located within the Forsmark candidate area, although the bottom of borehole KFM09A extends beyond the border of the candidate area. Drill site 7, is visualized in Figure 1-1, drill site 8 in Figure 1-2, and drill site 9 in Figure 1-3.

Controlling documents for performance of the activities are listed in Table 1-1. Both Activity Plans and Method Descriptions are SKB's internal controlling documents. To this should be added extensive internal quality operational procedures of Vattenfall Power Consultant AB, including a general Manual for testing and Quality Operating Procedures, seven Checklists, four Quality Assurance Report forms, and an object specific Quality plan.

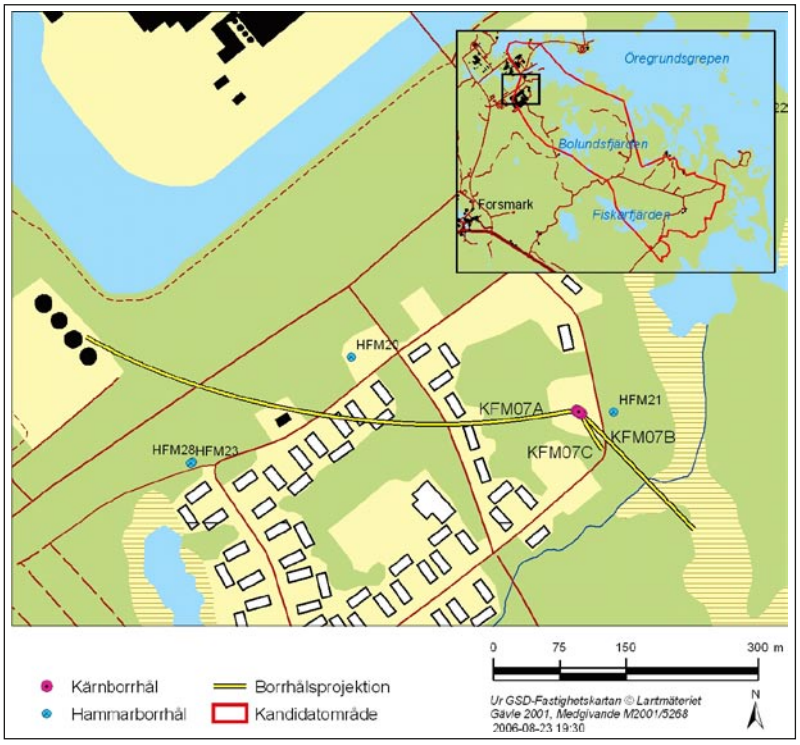

Figure 1-1. *Location of the Forsmark candidate area (the small square in the upper right corner) with drill site 7 (the large square). The projections on the ground surface of the core drilled boreholes KFM07A, KFM07B, and KFM07C at drill site 7 are shown in the large map. Also the positions of percussion drilled boreholes at and in the vicinity of the drill site are displayed in the figure.*

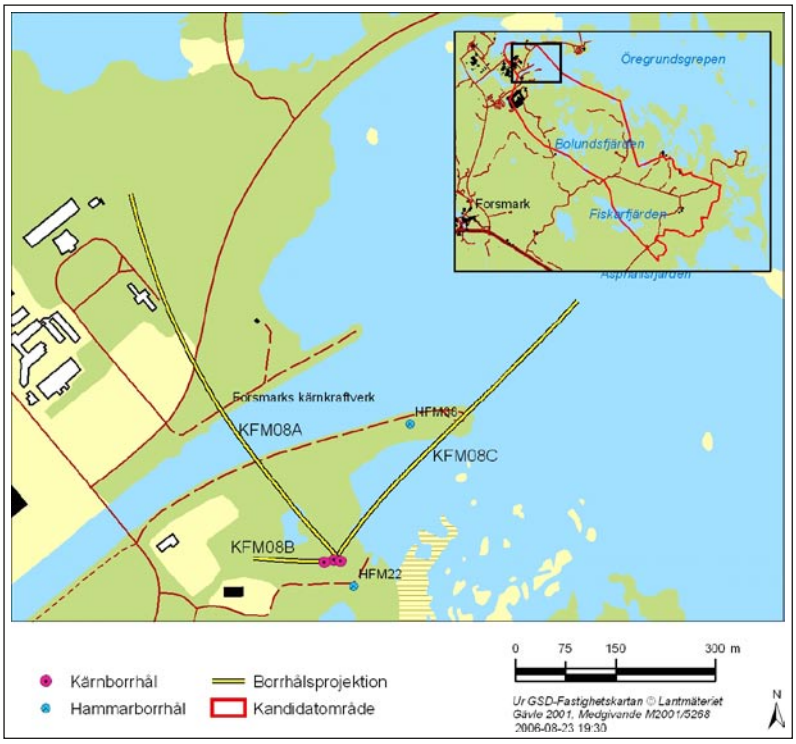

Figure 1-2. *Location of the Forsmark candidate area (the small square in the upper right corner) with drill site 8 (the large square). The projections on the ground surface of the core drilled boreholes KFM08A, KFM08B, and KFM08C at drill site 8 are shown in the large map. Also the positions of percussion drilled boreholes at and in the vicinity of the drill site are displayed in the figure.*

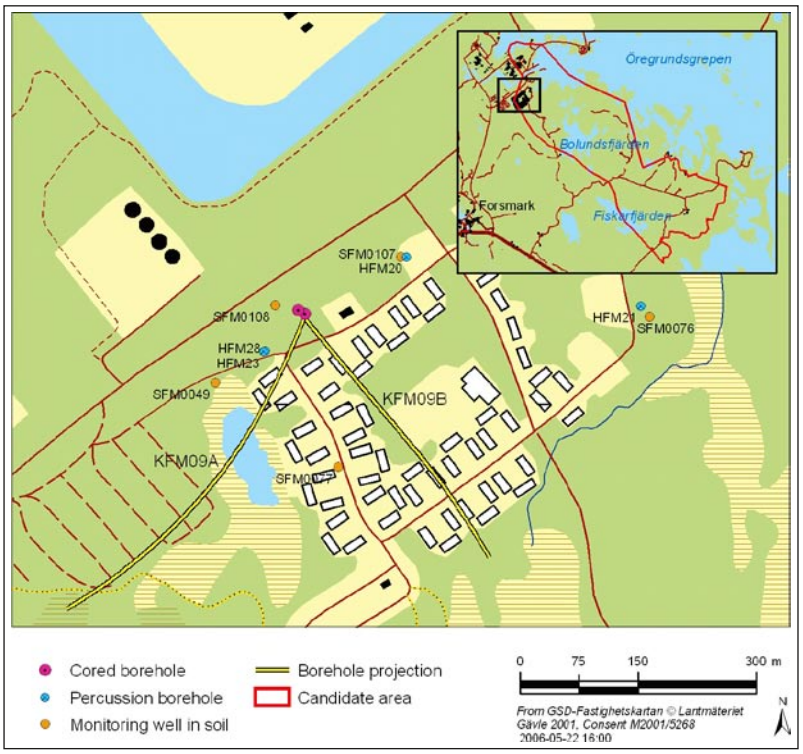

Figure 1-3. *Location of the Forsmark candidate area (the small square in the upper right corner) with drill site 9 (the large square). The projections on the ground surface of the core drilled boreholes KFM09A and KFM09B at drill site 9 are shown in the large map. Also the positions of percussion drilled boreholes and monitoring wells in soil at and in the vicinity of the drill site are displayed in the figure.*

Table 1-1. Controlling documents for performance of the activities.

Activity Plan	Number	Version
Rock stress measurements with hydraulic fracturing (HF) and hydraulic testing of pre-existing fractures (HTPF) in boreholes KFM07A and KFM07C	AP PF 400-06-091	1.0
Rock stress measurements with hydraulic fracturing (HF) and hydraulic testing of pre-existing fractures (HTPF) in borehole KFM08A	AP PF 400-06-083	1.0
Rock stress measurements with hydraulic fracturing (HF) and hydraulic testing of pre-existing fractures (HTPF) in borehole KFM09A	AP PF 400-06-061	1.0
Rock stress measurements with hydraulic fracturing (HF) and hydraulic testing of pre-existing fractures (HTPF) in borehole KFM09B	AP PF 400-06-044	1.0
Rock stress measurements with hydraulic methods	SKB MD 182.003e	2.0
Instructions for cleaning borehole equipment and certain surface equipment	SKB MD 600.004e	1.0

Borehole KFM07A extends to 1,001.55 mbl (metres borehole length) and is at ground surface directed 261.47° (clock-wise from North) and has at the borehole collaring a dip of 59.29° from the horizontal. The borehole has at borehole bottom flattened out to a dip of 46.53°. The relatively strong inclination entails that the total vertical depth reach is about 821 mvd (metres vertical depth). The numbers of different tests performed in borehole KFM07A are presented in Table 1-2.

Borehole KFM07C extends to 500.34 mbl and is at ground surface directed 142.71° (clock-wise from North) and has a dip of 85.33° from the horizontal at the collaring and 84.22° at the borehole bottom. The borehole reaches a total vertical depth of about 494 mvd. The numbers of different tests conducted in borehole KFM07C are presented in Table 1-2.

Borehole KFM08A extends to 1,001.19 mbl and is at ground surface directed 321.00° (clock-wise from North) and has a dip of 60.85° from the horizontal at the borehole collaring, flattening out to 37.66° at the borehole bottom. The relatively strong inclination entails that the total vertical depth reach is about 759 mvd. The numbers of different tests performed in borehole KFM08A are presented in Table 1-2.

Borehole KFM09A extends to 799.67 mbl and is at ground surface directed 200.08° (clock-wise from North) and has a dip of 59.46° from the horizontal at the borehole collaring and 40.79° at the borehole end. The relatively strong inclination entails that the total vertical depth reach is about 621 mvd. The numbers of different tests performed in borehole KFM09A are presented in Table 1-2.

Borehole KFM09B extends to 616.45 mbl and is at ground surface directed 140.83° (clock-wise from North) and has a dip of 55.08° from the horizontal at collaring, flattening out to 42.85° at the end. Again, the relatively strong inclination entails that the total vertical depth reach is only about 472 mvd. The number of tests conducted in borehole KFM09B is presented in Table 1-2.

The work involved cooperation between Vattenfall Power Consultant AB (Contractor), Institut de Physique du Globe de Paris (IPGP), and Geostress Co (both Sub-contractors). Vattenfall Power Consultant AB provided a MKW wireline system and field personnel, IPGP supplied downhole equipment, data acquisition system, and field personnel, and finally, Geostress contributed with field personnel.

The methodology of testing and analysis, which is based on the ISRM suggested methods for rock stress estimation by hydraulic fracturing and hydraulic tests on pre-existing fractures /Haimson and Cornet 2003/, is outlined in Chapter 5.

Table 1-2. Tests conducted at Forsmark.

Investigated borehole	Hydraulic fracturing (HF)	Hydraulic tests on pre-existing fractures (HTPF)	Sleeve fracturing (SF)
KFM07A	0	13	0
KFM07C	8	7	2
KFM08A	5	18	0
KFM09A	3	2	0
KFM09B	15	14	0
Total	31	54	2

2 Scope, objectives and structure of presentation

Large scale stress determination measurements with the HF- and HTPF techniques, performed in four separate campaigns, have been undertaken during the summer and autumn of year 2006 for the Forsmark candidate site (5 boreholes on three different drill sites) and another campaign at the Oskarshamn (Laxemar) candidate site (one borehole). This report presents scope, objectives and performance of the stress measurements at the three drill sites at the Forsmark site. Further, a description is given of the employed test equipment, quality assurance, testing methodology (the so called cluster approach /Ask and Cornet 2006, 2007/), and results of stress interpretation. A more detailed account for instrument calibration, data collection, experiences of and observations made during the field work is outlined in Appendices I through III.

The hydraulic rock stress measurements at the Forsmark site were conducted between 6th of June and 21st of October, 2006. The measurements were carried out in four separate campaigns and a total of 87 hydraulic fracturing tests, hydraulic tests on pre-existing fractures, and sleeve fracturing tests were performed.

The objectives of the hydraulic stress measurements were to (i) decrease uncertainty in data on in situ state of stress, (ii) increase the understanding of how local geological site conditions may affect the state of stress, and (iii) provide input for site descriptive modelling on the state of stress at the site.

The more method specific objectives were to:

- Test the effectiveness of the HTPF tool in the rock mass at the Forsmark site.
- Work out an effective strategy for stress determination with the hydraulic methods within the SKB Site Investigation Program.
- Identify what types of fractures that seem feasible for HTPF.
- Identify possible decoupling zones along the boreholes.
- Test the capacity of the equipment for HF in competent, unfractured rock at a vertical depth of at least 400–500 m.
- Determine the state of stress at the borehole location, from 100 m depth and at least down to a vertical depth of 500 m.

The results of the stress determination involve presentation for single boreholes, and a combined solution for multiple boreholes at single drill sites. The presentation of results is restricted to the work done and the raw data results obtained. No in-depth attempts are made to put the data into a geological/tectonic context nor to discuss similarities/deviations observed with other types of stress data. However, a specific chapter (Chapter 7) is devoted to the commonly observed packer-induced sub-horizontal fractures in the investigated boreholes and the implications of these fractures for the present study.

3 Description of the testing equipment

3.1 Overwiew of equipment components

The surface equipment is based on an upgraded MKW (MessKabelWinde) wireline unit of Vattenfall Power Consultant AB, with which the downhole tool is moved within the borehole on a seven conductor geophysical logging cable and a winch system (Figure 3-1). The downhole tool involves a combined straddle packer and HTPF electrical imaging tool of Institut de Physique du Globe de Paris (IPGP).

The suggested wireline system, together with the HTPF tool of IPGP for fracture orientation and characterization, optimizes the testing performance. A schematic view of the system is given in Figure 3-2.

3.2 Pump equipment

The high-pressure water pump is a three-plunger Hermetic (type AH30) with a maximum pressure of 100 MPa. The pump delivers 17 l/min at a pressure of 75 MPa. The pump is remotely controlled by revolutions per minute, which enables a very large interval of flows at high pressures that are required for reliable quasi-static re-opening and hydraulic jacking (step-pressure) tests.

Figure 3-1. *Photo of the upgraded MKW wireline unit of Vattenfall Power Consultant AB during operation in borehole KFM08A.*

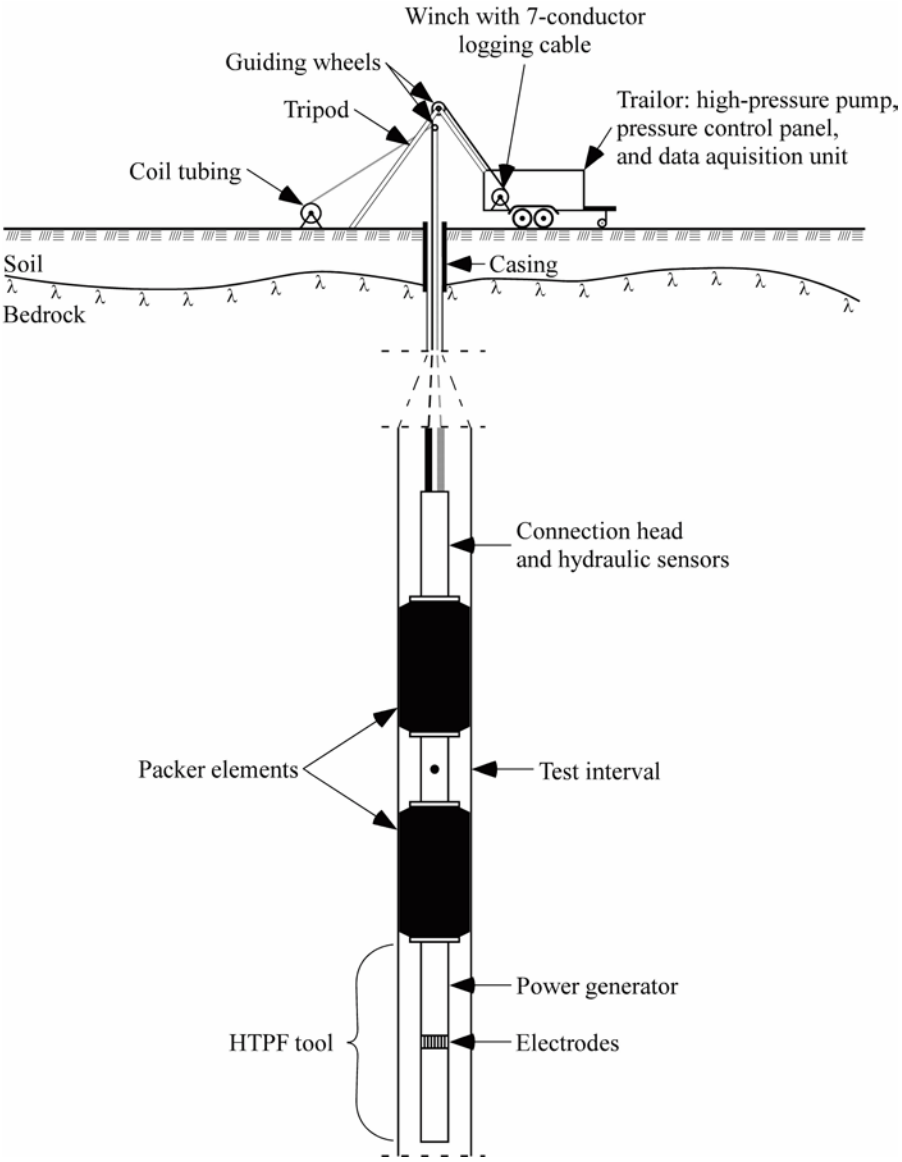

Figure 3-2. *Schematic overview of the wireline equipment with straddle packer and HTPF tool.*

3.3 Wireline system/tube system

The wireline system (Figure 3-1) is driven by a Hatz diesel engine (type 3 L30S), which through the Mannesmann-Rexroth hydraulic pump system (type HS-17-G 905-3-0) drives the high-pressure water pump (see above) and the winch (upgraded to MKW-1500).

The logging cable is a seven-conductor Rochester 3/8” (type 7-H-375A) with a breaking strength of 5.8 tons.

The coiled tubings, one for the straddle packer (OD 1/4”, service pressure 100 MPa) and one for the test section (OD 3/8”, service pressure 50 MPa), are made of seamless stainless steel. Although not determined at the time of this project, the suggested system is known to have a high stiffness (compressibility of the order 10^{-11} m^3/Pa).

3.4 Packer system

The straddle packer is equipped with steel-reinforced packer elements (TAM, OD = 67 mm; Figure 3-3). The sealing length is about 1 m, the length of the test section about 1.0 m in a 76 mm borehole, and the maximum service differential pressure is 33 MPa (burst pressure close to 50 MPa).

3.5 Equipment used to determine and document position in the borehole and orientation of fractures

The fracture orientation data are collected using the HTPF tool /Mosnier and Cornet 1989/, which combines the possibility of running tests through a wireline activated straddle packer with that of obtaining electrical images of the fractures intersecting the borehole (Figure 3-4). The electrical imaging technique has been adopted from Mosnier's azimuthal laterolog /Mosnier 1982/. During measurement, an alternating electric voltage is applied between a distant electrode (the armour of the logging cable) and a number of electrodes set in various azimuths on a ring placed at the centre of the tool. The electric current emitted (or received) by each of the electrodes on the central ring is proportional to the conductance of that part of the borehole wall facing the electrode. Focusing electrodes located on both sides of the electrode ring ensure that electric current lines are normal to the borehole wall. The results can be displayed either as polar diagrams or graphically as horizontal bands made by juxtaposed squares (one square per electrode). Because the intersection of a plane with a cylinder is an ellipse, planar fractures are easily detected by their sinusoidal shape. As the tool orientation is known, with the aid of two tilt meters (accuracy of 0.5°) and 3 magnetometers (accuracy of 3° to 4°) inside the tool, both dip and strike of the fractures can be determined /Cornet 1993/. The tool is run at least twice over a test section, and the repeatability can be used to determine the fracture orientation within half a degree for dip and 5 degrees for azimuth. Because the intensity of the injected electrical current can be adapted, it is possible either to highlight very tiny fractures, or to work on very conductive fractures. This provides a dynamic view that is not accessible to direct core examination as shown in Figure 3-5 below.

A very strong benefit of the HTPF tool is the ability to make differential plots of the test section before and after the injection test, which clearly demonstrates which fracture that has been stimulated. However, it was not necessary to employ the methodology at Forsmark.

Figure 3-3. *The straddled packer system showing its large deformability implying that it may operate in wells with variable diameters.*

Figure 3-4. *The straddle packer and the HTPF tool. The top of the downhole assembly is shown in the lower, left corner and terminates with the upper packer element. The second and third parts include the lower packer element and a weight used in inclined boreholes (mounted below the HTPF tool), respectively. The fourth part is the HTPF tool where the thicker central part contains the electrodes.*

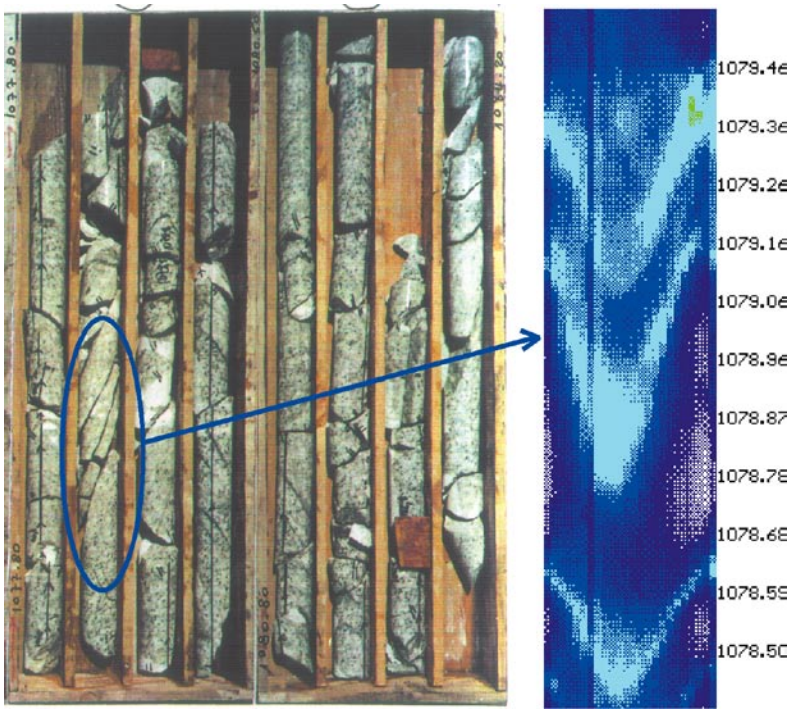

Figure 3-5. *Comparison of fractures between drill cores and HTPF tool. Cores appear very broken while electrical images show that the fractures are in fact quite tight in situ. The tightness of fractures is established during permeability tests.*

3.6 Data recording

The data were collected using a data acquisition system (PC and DQPad6020E, 16-channels, 12 bit resolution) that integrates simultaneously the surface data (injection flow rate, injection pressure, depth of test as provided by depth reader of logging cable) and downhole data (electrical images, downhole pressure for both interval and packers, plus tool orientation). Furthermore, a backup system was also brought to the field (PC and 2 Intab PC-loggers 3150, 8-channels, 12 bit resolution). This provided an excellent redundancy that ensured retrieving data.

Packer and interval pressures were monitored at ground surface by pressure gauges (EFE pressure transducers, type P925R, 0–40 MPa, precision 0.03%) and downhole (EFE, type P922A, 0–50 MPa). The flow was measured at surface with a high precision mass flow meter (Micro Motion Rosemount D12 with max 5 l/m, 39 MPa, and precision 0.004 g/cc).

4 Quality assurance and equipment calibrations

4.1 General

To ensure that data are collected with an optimum quality, a number of quality assurance measures are undertaken prior to, during, and after field work (Figure 4-1).

Prior to departure for the field, all system components are systematically tested for functionality and key components for data collection are calibrated (Table 4-1). Once all components have been approved, all equipment is carefully packed according to pre-established packing lists.

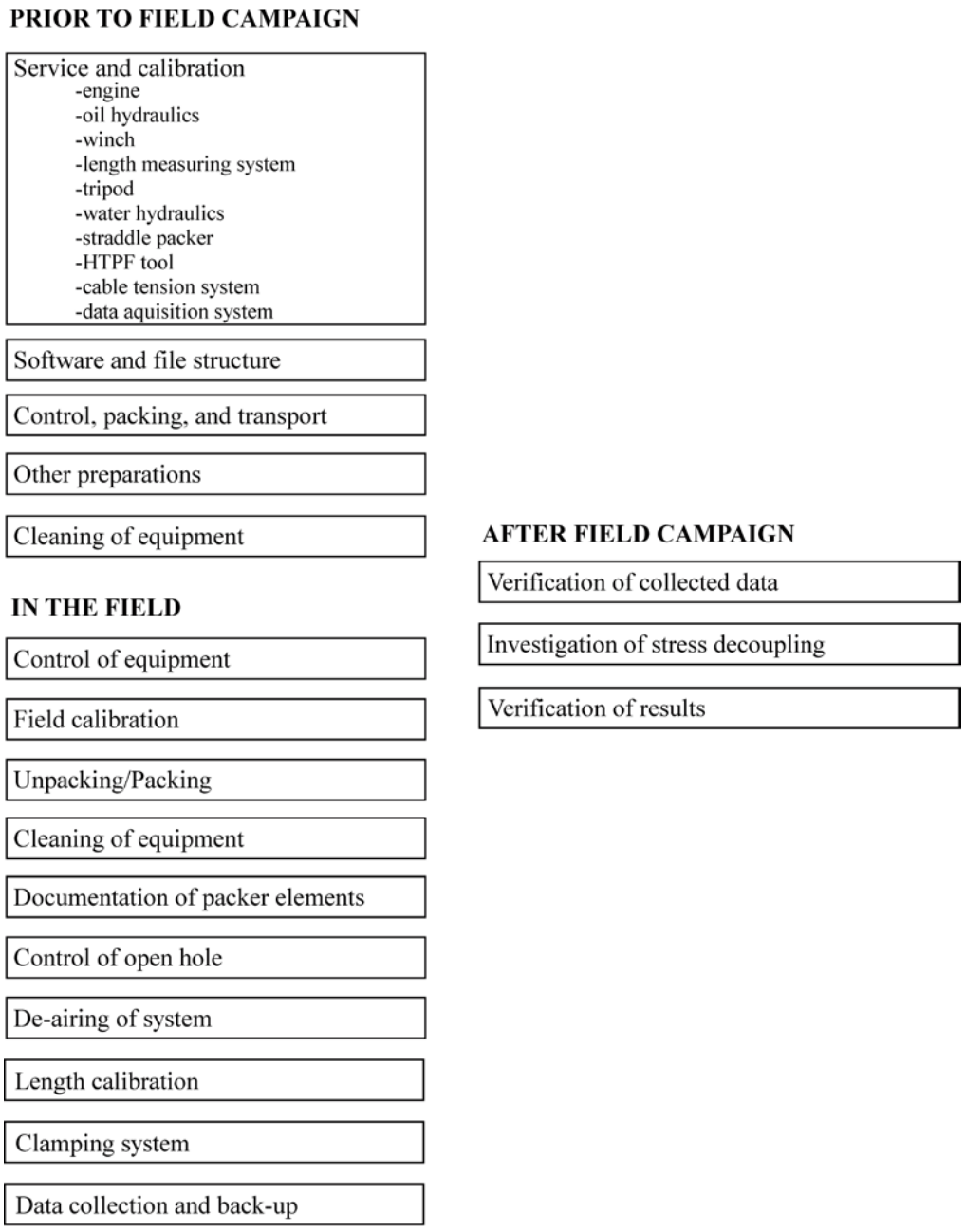

Figure 4-1. *Schematic overview of quality assurance procedures during hydraulic stress measurements.*

Table 4-1. Calibration list of key components.

Calibration item	Prior to field campaign	During field campaign	After field campaign
Downhole pressure gauge	Yes	Optional	Yes
Surface pressure gauges	Yes	Optional	–
Flow meter	Yes	Optional	–
Tilt meters	Yes	Yes	Yes
Magnetometers	Yes	Yes	Yes
Length system	–	Yes	–
Cable tension system	Yes	Yes	–

In the field, the functionality and the packing is once again verified. Field calibrations of pressure and flow gauges are also undertaken, if recommended by the client.

After field work, the functionality of key components is once again verified. The most important steps of the quality assurance procedures are outlined below. A more detailed description can be found in /Ask 2006ab/.

4.2 Calibration of equipment

4.2.1 Overall quality of data recording

There are a few independent means to verify that the overall data recording has been successful. This involves readings of orientation devices and of downhole pressures as the tool is lowered and hoisted in the borehole.

The values of the magnetic field inclination, as determined from magnetometers, offers a completely independent check on the digitization procedure used for the downhole data acquisition and surface data recording. The quality procedure has identified a general systematic discrepancy above about 250 m depth at the Forsmark site. This is due to a 50 Hz electrical noise that is collected by our tool resulting from ground currents.

This is a site specific phenomenon, which has never been observed in any of our previous field campaigns (we measured up to 10 volts of 50 Hz current between our tripod and the wellhead), except in borehole KLX12A in Laxemar, where similar conditions were encountered /Ask et al. 2007/. The noise (ground currents) results in a digitization problem close to the surface, causing the timer that samples the data to be slightly off phase, and a small error is introduced. This noise affects all downhole sensors. This implied that, for tests conducted above 250 m depth, collected data were given special attention.

The results from the magnetometers and inclinometers may also be used to verify reproducibility. This involves comparisons of derived fracture orientations with those of the BIPS, but more importantly, we compare our determination of magnetic field inclination (angle with vertical) with that of the Uppsala magnetic field observatory (Appendices I to III). Thus, we have established that our orientation determination for the tool is reliable and reproducible and well within expected errors.

The other independent control of successful data recording is correlated with the observed variations in downhole pressure during lowering and hoisting in the borehole. These variations, which were investigated after completed field campaign, can be compared with the theoretical weight of the water column in the borehole and indicate that no discrepancies were found during measurements at the Forsmark site.

4.2.2 Pressure transducers, flow meter, tilt meters, and magnetometers

Prior to the measurements, the pressure transducers are calibrated against a reference load cell and the flow meters by volume (mass) determination per time unit prior to field measurements. The results from the calibrations are given in Appendices I to III, which include the following items:

- Calibration of downhole pressure transducer in the test section.
- Calibration of pressure transducer in the packers.
- Calibration of surface transducers.
- Calibration of flow meter.
- Calibration of orientation devices. These components were checked for functionality and calibrated several times during the campaign: prior to departure to the field, before entering each borehole, and after completed measurements. Moreover, after the field campaign, the electrical imaging logs are used to provide independent data on dip and azimuth of the well (see 4.2.1 above).

4.2.3 Length measurement

For the sake of stress determination, the knowledge of absolute depth to within a few metres is quite sufficient. But because the objective is to relate images of features on the HTPF logs with those observed on cores, an adjustment to some decimetre is necessary.

Initially, the reference grooves in the borehole were intended to be identified with the HTPF electrical imaging tool (Mosnier tool; /Mosnier 1982, Mosnier and Cornet 1989/). However, the grooves proved to be too small for identification with the tool and a different strategy had to be adopted.

Instead, we compared the electrical imaging log with the cores and the BIPS images for a few unique features in each well. Once identified, by interpolation, equivalence is proposed between HTPF logs and BIPS/Boremap depths for the complete borehole length. Thereafter, each pre-existing fracture tested was correlated with the equivalent fracture observed on the cores. In addition, the tested fracture was photo documented in the core boxes. This comparison entails that the length calibration between the two systems is within 2 dm for drill site 7, 1 dm for KFM08A, and 2 dm for drill site 9. The results of the length calibrations are summarized in Table 4-2.

Note that measurement positions are given as the borehole length of the centre of the test section (which is not necessarily the exact depth of tested fractures) as well as converted to corresponding vertical depth.

Table 4-2. Result of length calibration.

Borehole	Calibration equation
KFM07A	BIPS length = 1.001 · electrical imaging length
KFM07C	BIPS length = 1.000 · electrical imaging length
KFM08A	BIPS length = 1.005 · electrical imaging length
KFM09A	BIPS length = 0.7 + 0.994 · electrical imaging length
KFM09B	BIPS length = 0.995 · electrical imaging length

4.2.4 Cable tension measurement

The cable tension (or weight) measuring device, which is a safety measure to prevent pulling off the geophysical cable by mistake if stuck in the borehole, has an accuracy of 10 kg and its functionality was tested prior to departure and in the field by attaching a weight.

4.2.5 Fracture orientation methods

In principle, the fracture orientations (here expressed as the normal to the fracture plane) can in this specific assignment be determined with three different methods:

- Based on magnetometers and inclinometers of the HTPF tool.
- Based on SKB's deviation measurements of the well (the optical Maxibor method or the magnetic Flexit method) and tool face (inclinometers) of the HTPF tool.
- Based on SKB's Boremap system (Maxibor or Flexit deviation measurements) and tool face of the BIPS tool.

In the result files (Appendices I to III), the results using method 2 are displayed (based on the Maxibor method). The reason for this choice of method is primarily twofold: (i) the well deviation data from SKB were judged more reliable than those of the magnetometers of the Mosnier tool; (ii) the Boremap system cannot be used for induced fractures and at the time of this report, the Boremap system was not proven to yield more reliable results than that of method 2. In addition, it is not recommended to use different systems for fracture orientation determinations as the different methods likely yield different uncertainties in the fracture orientation. If employed, this would introduce a weighting factor in the data during stress inversion, i.e. induced fractures are given higher or lower weight during inversion as compared with pre-existing fractures.

Regrettably, after this study was commenced, a decision was taken to up-date SKB's well deviation measurements, entailing that for many boreholes Maxibor measurement would be exchanged to Flexit measurements as the official deviation measurement files in SKB's database Sicada. This up-date affects the fracture orientations of both the HTPF tool and in Boremap as they are based on deviation data. As a result of this, a study was initiated attempting to quantify the corresponding error for the HTPF tool. The result is presented in Appendices I to III and indicates that the error is very small and, in practice, negligible for the sake of stress determination. Note that in Appendices I to III, the Boremap orientations based on the new Flexit well deviation data are presented, whereas the orientations of the HTPF tool are based on Maxibor.

4.3 Verification of indata for stress calculation

4.3.1 Fracture orientations

The reliability of the fracture orientation determination rests on three features:

- The proper recording of all parameters that characterize the position of the tool in the well (borehole length, and azimuth and dip values from 3 magnetometers, 2 inclinometers).
- The good understanding of tool manufacturing and its consistency with data processing routines.
- The repeatability of orientations during comparisons of multiple scans of the same fracture.

The reliability of orienting sensors (inclinometers and magnetometers) is provided by the repeatability of observations. Further comparison with independent data provides evaluation of accuracy of tool orientation. For boreholes KFM07A and KFM07C below about 225 mvd, we are always within 3 and 2°, respectively, with the Uppsala observatory determinations of the magnetic field inclination. As mentioned, above this depth, electric noise is disturbing all downhole sensors. Moreover, the inclinometers are reproducible (comparison between pre- and

post-logs) and values always fall within 2 and 1° for boreholes KFM07A and KFM07C, respectively. For well azimuth, the corresponding values are 5 and 6°, respectively. For KFM08A, repeatability of well inclination and azimuth is within a few degrees and the magnetic field inclination determinations are always within 2.5° of Uppsala observatory measurements for all depths greater than 400 m. For drill site 9, repeatability is better than 2° on inclinations and 6° on borehole azimuth between the various reconnaissance logs and post logs. Magnetic field inclination determinations are always within 2.5° of Uppsala observatory measurements, for all depths greater than 300 m. Position in well is calibrated on that of the BIPS images and drill cores.

Unambiguous fracture orientation data involve proper recording of tool positioning, repeatability of different logs, and clearly visible fracture traces.

4.3.2 Normal stresses

The normal stress determination is based on shut-in pressure determinations, because /Cornet et al. 2003/ observed that the normal stress may be overestimated during the opening phase of a hydraulic jacking test. The normal stress is determined using two methods suggested by ISRM /Haimson and Cornet 2003/ and involves only cycles where the injected volume is in the range of 2 to 5 litres into the formation.

Quasi-static reopening pressure tests have been conducted, but their primary purpose is to minimize chances of creating new fractures as well as of rotations of the fracture planes. The value of the reopening pressure is also an interesting source of "qualitative" information. When it is equal to the shut-in pressure value, it suggests that the fracture is sub-parallel to the borehole axis. This is later verified by the fracture imaging. In this case the quasi-static reopening measurement provides a useful complementary measurement of the normal stress. However, in many an instance, this quasi-static reopening pressure has been found significantly larger than the shut-in pressure. When this occurs, it suggests that the fracture is inclined with respect to the borehole axis. This is later verified by the post-frac image. Accuracy of the pressure transducers is provided both by initial and field calibrations and by the pressure recorded in the well, when packers are deflated.

Specific to the Forsmark site, two additional quality assurance features have been introduced. The first one refers to the influence of fractures generated by the packers, at the interface between the packers and the pressurized interval. During several tests (in particular in KFM09A (Appendix III)), these fractures remain opened by the packer, when pressure drops in the interval and prevents proper shut-in measurements. The other quality assurance aspect considered was related to fluid percolating to the borehole, below the straddle packer (e.g. the deepest tests in KFM08A; Appendix II). This results in a progressive increase in the shut-in pressure that is not linked to the fracture extension but to the change in stress close to the well, through the coupling imposed by the packers. Significance of "back-up pressure" can be evaluated from cable tension variations recorded during testing.

Note that normal stresses are denoted using a geomechanical sign convention with compressive stresses taken as positive.

Unambiguous normal stress data involve repeatable and clearly defined shut-in values from tests involving 2 to 5 litres of injected water volume and that show a pronounced flow-back after completed testing.

5 Methodology for data collection

5.1 General line of work

The general line of work in the boreholes at Forsmark involves the following steps:

1. Mobilization.
2. Verification of open hole, i.e. logging with dummy.
3. Reconnaissance log of entire borehole.
4. Length calibration.
5. Selection of suitable test sections.
6. Injection testing.
7. Post-logging of test section.
8. Demobilization.

Below, the most important steps of the work, items 3 and 6, are outlined.

5.2 Reconnaissance log and selection of suitable test sections

Because the notion of rock stress is a concept of continuum mechanics, it is necessary to identify volumes where the continuity hypothesis is verified. In other words, bodies that may be approximated by a continuum need to be identified. Moreover, because the stress at a specific point involves six components, the determination of the regional stress field includes determination of six functions for the domain under consideration. This requires integrating measurements conducted at points that sample properly the continuum volume of interest.

The first interpretation of the continuity hypothesis is given by the reconnaissance log with the HTPF tool (Appendices I to III). During the reconnaissance log, the intensity of the injected electrical current is adjusted to highlight very tiny fractures (which are suitable for hydraulic injection testing), which means that very conductive fractures, i.e. potential stress decoupling zones, are clearly outlined by a significant change of resistivity. The first evaluation provided by the HTPF tool is used for selection of suitable test sections.

Given the non-linear and scattered stress profiles derived from previous overcoring stress data /e.g. Sjöberg et al. 2005/, application of a standard profiling approach would be hampered by the non-linearity. Instead, the methodology chosen for the tests at Forsmark involved the cluster approach /e.g. Ask and Cornet 2006, 2007/. This implies that measurements are grouped in clusters with the aim of determination of the full stress tensor. The objective of each individual cluster is to collect sufficient HF and HTPF data in a small enough volume to permit complete stress determination without considering stress gradients. This results in a minimum of parameters at each cluster but also has the benefit of that the continuity hypothesis may be more easily evaluated by comparisons of full tensors from multiple clusters along a borehole. The adopted methodology thus includes three steps:

- Identification of domains where the continuity hypothesis is validated preliminarily.
- Combination of HF and HTPF measurements in a clustered procedure so that each cluster corresponds to a small enough volume to permit complete stress determination without considering stress gradients.
- Integration of results from all clusters so as to establish the validity of the continuity hypothesis and determine the complete stress field within the domain of interest with proper attention to decoupling zones.

It is important to identify the depth where the stress determination is desired: one objective at the Forsmark campaign has been to focus on placing clusters at planned repository depth at the Forsmark site.

5.3 Injection testing

5.3.1 General

The applied injection tests were a combination of hydraulic fracturing (HF) and hydraulic testing on pre-existing fractures (HTPF), which are described below. We emphasize that the execution and interpretation of the two methods are consistent with the ISRM recommendations /Haimson and Cornet 2003/.

In wells that are inclined with respect to a principal stress direction, hydraulic fracturing will not yield axial fractures, but fractures of en echelon type. /Peska and Zoback 1995/ have shown that such tests are very useful for constraining the maximum horizontal principal stress magnitude.

HTPF measurements are commonly used to constrain the magnitude of primarily σ_H but also σ_v, once σ_h has been solved with hydraulic fracturing technique. However, because of the limitations in the HF technique in inclined wells, the cluster approach will depend very much on the success rate of the HTPF technique.

5.3.2 Hydraulic fracturing (HF) tests

The overall purpose of the hydraulic fracturing test, in case of a vertical borehole aligned with a principal stress direction, is to determine the horizontal stress magnitudes and orientations. However, in thrust regimes, the fracture plane rotates during propagation, giving an estimate of the vertical stress component. If the minimum horizontal stress can be determined by other means, the HF test provides an estimate of the maximum horizontal stress based on the break-down pressure, rock tensile strength, and a hypothesis of the pore pressure effect.

We have adopted the following scheme to conduct HF tests:

- Permeability test involving a rapid pressurization of the test section up to between 1–3 MPa and subsequent monitoring of the pressure decay for about 5 to 10 minutes. Release of test section pressure.
- Rapid pressurization of the test section so that peak pressure is obtained in 1–3 min. When breakdown is reached, the pumping is stopped and the pressure decline is monitored. About 5 minutes after fracture closure (shut-in), the test section is vented. In the beginning of the venting, the test interval is closed back and the rise in pressure is monitored. When the initial permeability test has shown that the rock is fairly impervious, this action provides a means to verify that the fluid pressure has been injected into the rock mass and that no significant by-passing to the borehole has occurred.
- Standard quasi static slow re-opening test (hydraulic jacking/step-rate pressure test) with about 5 pressure steps, starting way below the previous shut-in reading and going up in 2 MPa steps, until the fracture is clearly open. This is followed by a standard shut-in test. We consequently have not adopted fast flow rate re-opening tests for evaluating the maximum horizontal principal stress magnitude, because it is difficult to ascertain that the pore pressure has reached its original value and because theories based on the re-opening pressure are associated with great uncertainties /e.g. Ratigan 1992, Ito et al. 1999, Rutqvist et al. 2000/.
- Hydraulic jacking followed by shut-in until repeatable normal stresses are produced.
- If the normal stresses are not self consistent (repeatable), a cyclic jacking /e.g. Rutqvist, 1995/ and thereafter a rapid re-opening followed by shut-in is conducted (not necessary at the Forsmark site).

Some estimate of the maximum horizontal stress may be retrieved from the breakdown pressure reading when the rock tensile strength has been determined with some confidence.

5.3.3 Hydraulic tests on pre-existing fractures (HTPF)

Generally, HTPF measurements are used to constrain the magnitude of primarily σ_H, but also σ_v, once σ_h has been solved with hydraulic fracturing technique. The HTPF tests aim at opening and stimulating pre-existing planes of weakness with, preferably, a large range of fracture directions and inclinations /Cornet 1993/.

We have adopted the same testing procedure as for the HF tests, but with one major difference: the flow rate during the opening phase should be chosen much smaller to enhance the possibility of re-opening as the fluid has time to penetrate the fracture plane and add an additional stress component.

For the HTPF technique, the choice of suitable fractures for HTPF testing is crucial. Generally, for this type of test, isolated fractures are sought, implying that the nearest neighbouring fracture should be at least 1 m above or below the tested fracture. Moreover, individual tests should be separated by c. 2 m to avoid the local stress change caused by the neighbouring test as a result of the mechanical opening of a fracture. The chosen fractures for HTPF testing should also be distributed with a large variety of dip and dip directions for a reliable resolution of all stress components during stress inversion. The objective is to take advantage of optimally oriented pre-existing fractures, even if they are in a very limited quantity. If more directions are available, the resolution of proposed methodology will be improved. Preferably, the chosen fractures should be at least partially opened or coated with weak fracture minerals, which, using a low flow rate test, enhances the possibility for re-opening as the fluid has time to penetrate the fracture plane and add an additional stress component. In this respect, the HTPF tool has great benefits, as it directly outlines the fractures suitable for testing. What remains to ascertain is that the fractures are isolated and that the full stress tensor can be solved in each cluster.

With the HTPF method, the stress tensor is evaluated so as to fit best all measured data according to a misfit function that characterizes the quality of the fit. The misfit function is a non-dimensional feature that describes the discrepancy between observed and computed values as determined with a calculated stress model. The misfit must include errors associated with all measured parameters, i.e. errors in both normal stress and in fracture orientation. The solution is defined as the stress model that minimizes the misfit function, i.e. the model that is closest to all the measurements.

If HTPF tests are close enough to HF tests, integration of HF and HTPF data is conducted on the hypothesis of a uniform stress field.

When tests have been run at large distances from one another, the solution requires a parameterization of the stress field in the rock mass. The choice of parameterization for stress calculation depends on the number of measurement points and the range of orientations of the tested fractures. A commonly applied parameterization of the stress field involves the assumption of linear stress variation along the borehole axis, i.e. the stress at point X_m is expressed as a linear function of the stress at point X_o with a stress gradient, α, along the borehole axis according to:

$$\sigma(X_m) = \sigma(X_O) + (X_m - X_O) \cdot \alpha \tag{5-1}$$

In its general form, it involves 12 model parameters and requires a minimum of 14–15 tests for its solution (because measurements are never exact and always involve some uncertainty, it is always desirable to conduct more tests than there are unknown model parameters). It is to be noted here that if the borehole is inclined to a principal stress direction by more than 15 to 20°, en echelon fractures result from HF tests. /Peska and Zoback 1995/ have shown that such tests are very useful for constraining the maximum horizontal principal stress magnitude.

When the borehole is vertical and there are no lateral stress variations, the vertical stress remains principal at all depths and the system involves only 10 unknown model parameters (/Haimson and Cornet 2003/; the theory is outlined in more detail in Section 6.2). HF tests, in vertical wells, provide directly six parameters: principle directions and their variation with depth and the minimum horizontal stress component and its gradient (in strike-slip regimes) or the vertical component and its gradient (in thrust regimes). The remaining parameters are subsequently solved by HTPF technique.

5.3.4 Sleeve fracturing

As a result of the difficulty to induce axial fractures in borehole KFM07C, it was decided to use the sleeve fracturing technique /Stephansson 1983ab/ in a relatively shallow homogeneous rock section. The intention with the test was to avoid generating sub-horizontal fractures at the contact between packers and the straddled interval. The tests involved inflating the packers up to about 35 MPa in three cycles, thereby inducing fractures with the packer. Because the packer counteracts the tangential stresses around the well, the test normally results in inducement of axial fractures, especially as the test does not involve any fluid percolation.

However, the lack of fluid percolation implies that the induced fractures have a very limited depth into the borehole wall. For this reason, the downhole tool was hoisted about 1 m so that the test section interval was located exactly over the earlier position of the upper packer element. At this position, a standard HF test was conducted, aiming at propagating the packer induced fracture. Thereafter, the test section was post-logged with the electrical imaging tool.

5.4 Observed problems during injection testing

Early on in the injection testing at drill site 9 (Appendix III), it became clear that the pre-existing fractures do not easily open because of a relatively strong fracture sealing. For this reason the testing time had to be extended to include a more pronounced percolation process during the first quasi-static re-opening tests. However, the primary problem with the strong fracture sealing is that the pressure to open the fracture is significantly higher compared with a fracture that is already open. This had a large effect on the testing results, because it became clear that sub-horizontal fractures were induced at pressures just moderately higher than the corresponding theoretical vertical stress at the location in question. Hence, unless the chosen pre-existing fracture could be re-activated before reaching the level of the theoretical vertical stress, sub-horizontal fractures would be induced.

The physical explanation for the observed induced sub-horizontal fractures is presently not fully understood, but a successful interpretation methodology for inclined wells is presented in Chapter 7. However, to our surprise, such fractures have also been found in vertical boreholes at drill site 7 at Forsmark (Appendix I) and at drill site 12 at Laxemar, Oskarshamn /Ask et al. 2007/, implying a more complex theory of development.

During the measurements in borehole KFM08A (Appendix II) and the first test in borehole KFM07C (Appendix I), the tool was sometimes displaced during the injection testing as a result of pressure build-up behind the downhole tool. This was especially pronounced in the three first and deepest tests. The reason for this pressure build-up is not fully understood but it is probably a combination of several factors. First of all, the bedrock is completely impervious (i.e. all pre-existing fractures are sealed) and pressure cannot escape if trapped below the tool. Hence, already the inflation of the packer would increase the pressure behind the tool, although not to such a degree that the tool would move. During injection in to the test section, additional pressure build-up behind the tool could result from: (i) short-circuiting through fractures. Because the well is inclined about 60° from the horizontal and the dominating fracture sets are sub-vertical and sub-horizontal, there is a possibility for the injected water to pass through these fractures and below the tool; and (ii) leakage through the packer. A common observation at the Forsmark site is spiral grooves on the cores and borehole walls. Hence, the packers may not have sealed the test section properly, allowing water to enter the well section behind the tool.

6 Results from stress inversion

6.1 General line of work

The general line of work in all boreholes included a run-through of all tests to identify the tests that are judged most reliable. Indeed, many tests are associated with features that reduce their reliability as estimates of the state of stress at the site. Factors that reduce the reliability of the tests involve primarily multiple fractures in the test section, non-optimal fracture orientation (poorly resolved fracture orientation or unclear image of the fracture), and poor flow-back after completed testing.

The major observed problem in the collected data involves the existence of fractures induced by the packer, even though a very careful pressurizing procedure had been adopted. These packer-induced fractures raise some difficulty for some of the tests but, at the same time, provide an independent means to validate the stress field that has been determined (see further Chapter 7).

Normal stresses are denoted using a geomechanical sign convention with compressive stresses taken as positive. All orientations represent the normal to the fracture plane, positive downwards, and are given with respect to geographic North according to coordinate system RT90 2.5 gon W 0: –15 for x and y and RHB70 for z, using a right-hand rule notation. Measurement positions are given as the borehole length of the centre of the test section as well as converted to corresponding vertical depth.

In Appendices I to III, we outline those data that have been considered as reliable for the sake of stress determination, which we denominate unambiguous data. “Unambiguous data” implies that the test involves both reliable fracture orientation and normal stress determination. Hence, the fracture orientation data involve proper recording of tool positioning, repeatability of different logs, and clearly visible fracture traces. Unambiguous normal stress data involve repeatable and clearly defined shut-in values from tests involving 2 to 5 litres of injected water volume, and show a pronounced flow-back after completed testing.

The majority of the presented inversions are based on unambiguous data, but the solution may not necessarily involve all of the unambiguous data. However, once a solution was obtained for this set of data, a few additional ambiguous tests could be added without altering the result. The sole purpose of adding additional data is to decrease uncertainties in the obtained solution without altering stress magnitudes or orientations. An exception to this general line of work is borehole KFM08A, in which the solution must be based on ambiguous data in order to derive a solution. Moreover, the solution for borehole KFM07C is based on average standard deviations on the measured parameters instead on the calculated in order to achieve convergence. The inversions involved testing of different fracture alternatives to derive the most reliable solution as well as a few tests where different normal stresses were encountered (Tests 7 and 13 in borehole KFM07A). At drill sites 7 and 9, which both included two investigated boreholes, the state of stress was also calculated using a combined data set.

Few of the single well inversions are completely satisfactory with respect to all model parameters and the corresponding numerical quality of the solutions. However, when data from various boreholes are integrated together, the situation is significantly improved, especially for drill site 7. Later, in Section 7.3, it is shown that one of the solutions for this drill site fits well the geometry of packer induced fractures. Hence for drill site 7, it is considered that the proposed solution is well constrained and uniquely validated.

6.2 Method for inversion

The inversion procedure is based on a least squares measure of misfit and the Tarantola-Valette gradient algorithm /Tarantola and Valette 1982, Cornet and Valette 1984/. It assumes a linear variation of the stress field throughout the volume sampled by the tests considered for the inversion.

When tests have been run at large distances from one another, the solution requires a parameterization of the stress field in the rock mass. The choice of parameterization for stress calculation depends on the number of measurement points and the range of orientations of the tested fractures. A commonly applied parameterization of the stress field involves the assumption of linear stress variation along the borehole axis, i.e. the stress at point X_m is expressed as a linear function of the stress at point X_o with a stress gradient, α, along the borehole axis according to Equation 5-1.

In its general form, it involves 12 model parameters (Equation (6-1)) and requires a minimum of 14–15 tests for its solution (because measurements are never exact and always involve some uncertainty, it is always desirable to use more tests than there are unknown model parameters). If lateral stress gradients can be neglected, the stress field is characterized by 12 parameters according to

$$\sigma\left(X^m\right)=\sigma\left(X\right)+\left(z^m-z\right)\alpha^{[z]} \tag{6-1}$$

For hydraulic fracturing/HTPF data, the fracture normal stress can be expressed as:

$$\left[\sigma\left(X^m\right)\vec{n}^m\right]\vec{n}^m=\sigma_{normal}^{m} \tag{6-2}$$

where n^m is the normal of the m^{th} fracture plane and includes the dip direction ϕ^m and the dip φ^m of the normal to the m^{th} fracture plane with respect to the vertical direction. With these definitions, Equation (6-2) can be formulated in matrix form according to:

$$\sigma_{n}^{m}=\left(\left[SB\cdot S^o\cdot SB^T+\left(z^m-z\right)\cdot AB\cdot A^o\cdot AB^T\right]\vec{n}^m\right)\vec{n}^m \tag{6-3}$$

where matrices S° and A° represent the stress and gradient tensors, SB includes the Euler angles E_1 to E_3, which describe S° in the geographical frame of reference, AB includes Euler angles E_4 to E_6, which describe A° in the S° frame of reference, z^m is the depth of the m^{th} fracture, and z is the chosen calculation depth (normally the average depth of the data set; /Ask 2004/).

The inversion is performed using a method developed by /Cornet 1993/, based on the least squares criterion /Tarantola and Valette 1982, Cornet and Valette 1984/. In this method, *a priori* knowledge of the unknown model parameters is assumed to exist, which can be formulated in terms of expected value, variance and covariances. In practice, large error bars are placed on assumed central values for the unknown parameters. The hydraulic fracturing and HTPF data consist of four components: the depth, z^m, of the m^{th} fracture plane, the dip direction, ϕ^m, and the dip, φ^m, of the normal to the m^{th} fracture plane with respect to the vertical direction, and the fracture normal stress, σ_n^m. Thus, for a 12-parameter problem, hydraulic fracturing and HTPF data involve 4m+12 = M components for m measurements.

A vector π_o can be created which includes *a priori* values according to:

$$\pi_0=col\begin{bmatrix}\left(z_o,\phi_o,\varphi_o,\sigma_{no}\right)^1,\ldots,\left(z_o,\phi_o,\varphi_o,\sigma_{no}\right)^M,\\ E_1,E_2,E_3,E_4,E_5,E_6,S_1,S_2,S_3,\alpha_1,\alpha_2,\alpha_3\end{bmatrix} \tag{6-4}$$

The corresponding covariance matrix is denominated C_o and is diagonal, because measurements and unknown parameters are assumed independent /Cornet 1993/. The correspondingly computed, or *a posteriori,* vector is of the form:

$$\pi = col\begin{bmatrix}(z,\phi,\varphi,\sigma_n)^1,\ldots,(z,\phi,\varphi,\sigma_n)^M,\\ E_1,E_2,E_3,E_4,E_5,E_6,S_1,S_2,S_3,\alpha_1,\alpha_2,\alpha_3\end{bmatrix} \quad (6\text{-}5)$$

A vector function f(π) may be introduced in which the m^{th} component is defined by:

$$f^m(\pi) = \sigma_n^m - \left(\left[SB\cdot S^o\cdot SB^T + \left(z^m - z\right)\cdot AB\cdot A^o\cdot AB^T\right]n^m\right)n^m \quad (6\text{-}6)$$

The solution of the inverse problem is defined by the minimum of:

$$\left(\pi-\pi_o\right)^T C_o^{-1}\left(\pi-\pi_o\right) \quad (6\text{-}7)$$

The problem is a conditional least square, i.e. the minimum of Equation (6-7) is sought as to satisfy the condition f(π) = 0. /Tarantola and Valette 1982/ demonstrated that this could be solved using the iterative algorithm based on the fixed-point method:

$$\pi_{n+1} = \pi_o + C_o F_n^T\left(F_n C_o F_n^T\right)^{-1}\left[F_n\left(\pi_n-\pi_o\right) - f\left(\pi_n\right)\right] \quad (6\text{-}8)$$

where F is a matrix of partial derivatives of f(π) valued at point π.

6.3 Inversion results for borehole KFM07A

The best solution for KFM07A involves 7 model parameters (horizontal stresses and their variation with depth, the vertical stress gradient, and the orientation of the horizontal stresses with depth) and 12 data in the interval 270–670 mvd. It solves accurately the stress magnitudes (vertical stress gradient = 0.0239 MPa/m; although somewhat low) but the orientation is less resolved (Table 6-1; Figure 6-1). All calculated parameters are within one standard deviation of the measured (Table 6-2). The solution for borehole KFM07A suggests that thrust regime prevails. The average ratio σ_H/σ_h is 1.4, and the average ratios σ_v/σ_h and σ_H/σ_v are 0.7 and 1.9, respectively. The large uncertainty of σ_h towards depth renders the ratios more uncertain. For the interval 270–470, where the uncertainties are acceptable, the following is obtained: $\sigma_H/\sigma_h = 1.3$, $\sigma_v/\sigma_h = 0.6$, and $\sigma_H/\sigma_v = 2.0$. The orientation of σ_H was found to rotate from 127 to 155°N in the interval and is generally quite poorly constrained.

Table 6-1. Best solution for borehole KFM07A.

Depth [mvd]	Parameter	σ_H [MPa]	σ_h [MPa]	σ_v [MPa]	Orient σ_H [°N]
270	Magnitude	15.2	13.1	6.5	127
	Std	0.5	0.8	0.1	14.1
	95% conf. int.	14.2–16.2	11.5–14.7	6.3–6.7	99–155
370	Magnitude	17.6	14.1	8.9	144
	Std	0.1	0.4	0.1	5.3
	95% conf. int.	17.4–17.8	13.3–14.9	8.7–9.1	133–155
470	Magnitude	20.2	14.9	11.2	151
	Std	0.3	0.9	0.2	7.3
	95% conf. int.	19.6–20.8	13.1–16.7	10.8–11.6	136–166
570	Magnitude	22.9	15.6	13.6	154
	Std	0.6	1.4	0.2	10.0
	95% conf. int.	21.7–24.1	12.8–18.4	13.2–14.0	134–174
670	Magnitude	25.6	16.2	16.0	155
	Std	0.8	2.0	0.3	11.6
	95% conf. int.	24.0–27.2	12.2–20.2	15.4–16.6	129–175

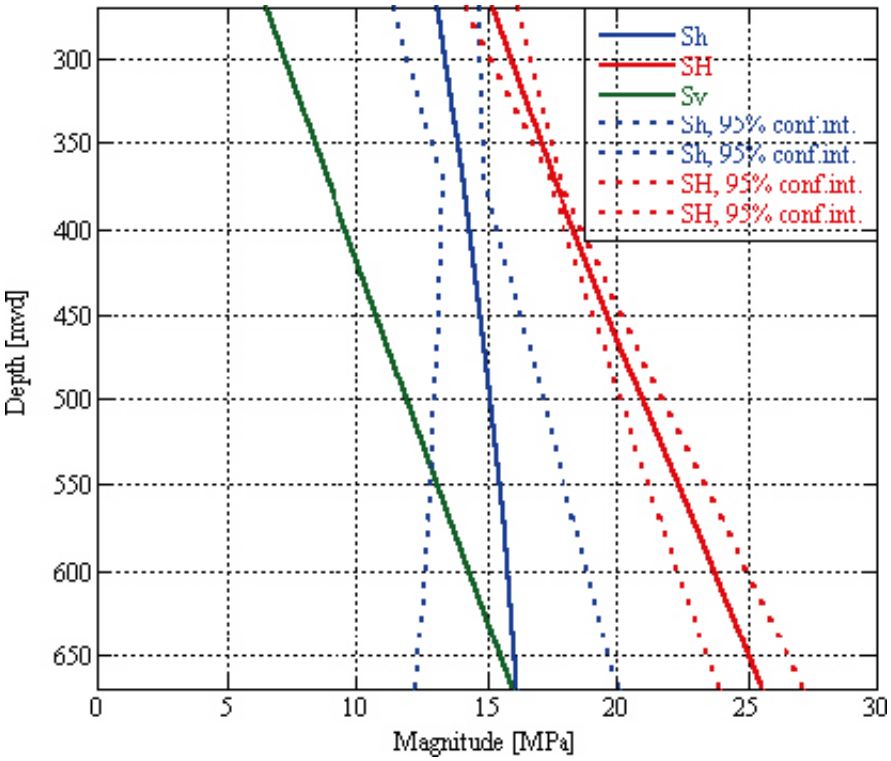

Figure 6-1. *Best solution obtained for borehole KFM07A, involving 7 model parameters and 12 measurement points between 270–670 mvd.*

Table 6-2. A priori and a posteriori data in best solution for borehole KFM07A.

Depth [mvd]	Test no	Az_{meas} [°N]	Az_{calc} [°N]	Error [°N]	STD_{Az}	Dip_{meas} [°N]	Dip_{calc} [°N]	Error [°N]	STD_{Dip}	$\sigma_{n,meas}$ [MPa]	$\sigma_{n,calc}$ [MPa]	Error [MPa]	$STD_{\sigma n}$ [MPa]
663.5	1*	87.0	83.9	3.1	10.5	27.0	26.6	0.4	4.0	16.0	16.1	0.1	0.3
636.5	2	166.0	163.7	2.3	21.5	88.0	88.0	0.0	5.5	24.5	24.5	0.0	0.2
597.0	3*	2.0	1.6	0.4	4.5	12.0	16.7	4.7	5.5	15.0	14.9	0.1	0.2
493.0	5*	120.0	119.8	0.2	10.5	12.0	10.9	1.1	6.0	12.0	12.1	0.1	0.3
487.5	6*	10.0	10.0	0.0	8.5	13.0	12.9	0.1	4.5	12.0	12.0	0.0	0.1
481.0	7*	254.0	257.1	3.1	13.0	82.0	82.3	0.3	7.0	15.4	15.3	0.1	0.5
427.5	8	332.0	332.2	0.2	5.0	72.0	70.5	1.5	4.0	18.0	18.1	0.1	0.3
387.0	9*	319.0	318.9	0.1	5.0	85.0	84.8	0.2	4.0	17.9	17.9	0.0	0.1
368.0	10*	271.0	273.7	2.7	8.5	86.0	86.1	0.1	3.5	15.5	15.5	0.0	0.2
343.0	11*	33.0	33.5	0.5	5.5	82.0	81.8	0.2	3.5	14.0	14.0	0.0	0.3
326.0	12*	151.0	150.1	0.9	5.0	89.0	89.1	0.1	3.0	16.4	16.4	0.0	0.1
271.5	13*	129.0	129.2	0.2	7.5	79.0	78.0	1.0	3.5	14.4	14.9	0.5	0.6

Unambiguous data are marked with "*".

6.4 Analysis of sleeve fracturing data and true hydraulic fracturing data in borehole KFM07C

General

In borehole KFM07C, most hydraulic fracturing tests resulted in sub-horizontal fractures, similar to those in the other boreholes investigated in Forsmark (Appendices I to III). This result was unexpected in the near-vertical borehole KFM07C, but it was also encountered in the near vertical borehole KLX12A at the Oskarshamn site (Laxemar; /Ask et al. 2007/). This result was obtained despite various attempts with different pressurization rate. As a result, it was decided to employ the sleeve fracturing technique /e.g. Stephansson et al. 1983ab, Desroches and Kurkjian 1999/ at the last two hydraulic fracturing sections in borehole KFM07C (Tests 14 and 15).

The general idea was to fracture the rock by inflating the packer to about 35 MPa overpressure. Such fracturing generally leads to axial fractures due to the geometry of straddle-packer testing. However, the induced fractures have a very limited depth from the borehole wall and need further propagation to enhance the image from the Mosnier tool after completed testing (see e.g. Appendix I). Thus, after completed sleeve fracturing, the straddle-packer was hoisted so that the test section coincided with the position of the upper packer during the sleeve fracturing test. Thereafter, a conventional hydraulic fracturing test was conducted, aiming at propagating the already existing vertical structure. This approach proved to be successful and resulted in clearly visible axial fractures (Appendix I).

Results from sleeve fracturing

In the sleeve fracturing technique, the magnitude of the horizontal stresses perpendicular to the borehole is determined from the recorded pressure versus injected volume charts. The main advantage of the method is that the stresses can be determined without introducing fluids in the rock mass during the fracture initiation phase. Hence, the problems associated with the re-opening pressure in the conventional hydraulic fracturing test is thereby avoided. On the other hand, the fractures have a limited depth from the borehole wall and it is often difficult to pinpoint breakdown and re-opening pressures from the recorded pressure versus volume charts.

In Figure 6-2 and Figure 6-3, the pressure versus time plot for Tests 14 and 15 in borehole KFM07C are given. In the following figures (Figure 6-4 to Figure 6-9), the pressure versus injected volume is presented, including interpretation of key parameters. Clearly, identifying the various critical pressures in sleeve fracturing data is not straightforward and involves some subjectivity. The results are further summarized in Table 6-3.

Regrettably, for both tests, the flow rate was not perfectly constant, resulting in small kinks in the pressure versus flow and pressure versus volume plots. Hence, these are sorted out from the pressure versus volume plots. Moreover, to fully understand the curves, information of the packer behaviour during pressurization would have been fruitful. In the absence of this information, it is assumed that the stiffness of the packer is a linear function of packer pressure above 5 MPa.

For Test 14, the flow rate was increased at a pressure of about 26 MPa (i.e. 260 bars; 1 MPa = 10 bars) and thereafter reduced, leading to a kink on the packer pressure versus volume plot. However, a reduction in stiffness is thereafter observed, which is interpreted as a possible breakdown (30.8 MPa; Figure 6-4). The following cycles indicate a re-opening at 11.3 and 11.8 MPa (Figure 6-5 and Figure 6-6), respectively. In addition, the second cycle includes a kink as a result of flow rate change (at 30.8 MPa) and the third cycle indicates a breakdown at 33.5 MPa.

For Test 15, the flow rate was adjusted several times during the first cycle. Yet, a distinct breakdown could be identified at 32.2 MPa (Figure 6-7). The following cycles indicate a re-opening at 10.6 and 11.1 MPa (Figure 6-8 and Figure 6-9), respectively, and cycle two a possible secondary breakdown at 30.9 MPa.

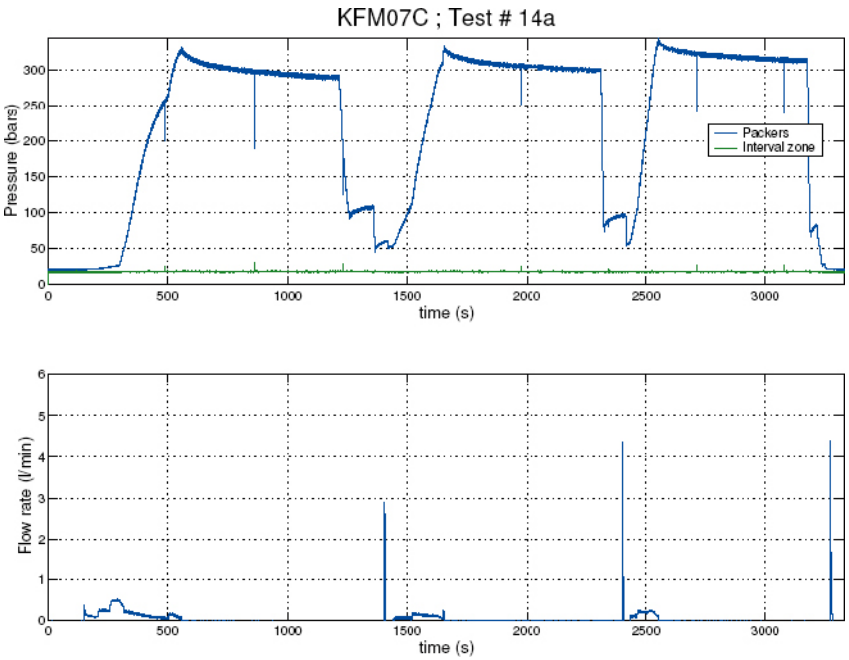

Figure 6-2. *Sleeve fracturing test one at 197 mvd in borehole KFM07C.*

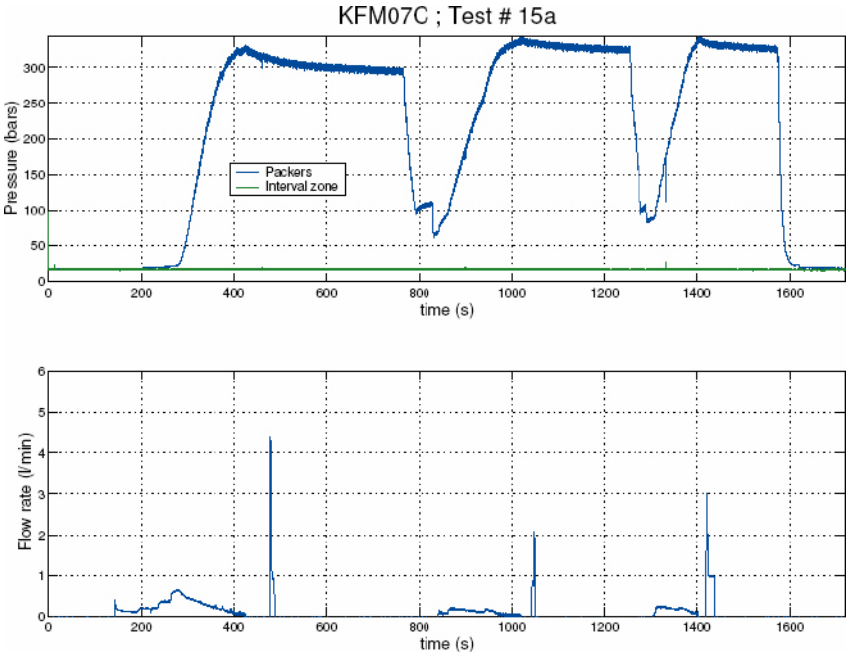

Figure 6-3. *Sleeve fracturing test two at 174 mvd in borehole KFM07C.*

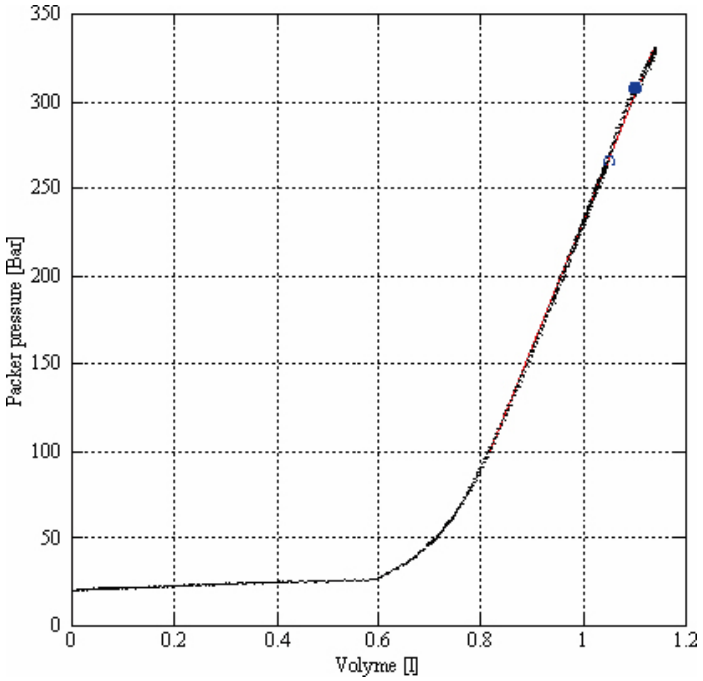

Figure 6-4. *Sleeve fracturing test at 197 mvd in borehole KFM07C, first cycle. Linear fit is displayed with red line, possible breakdown full symbol (at 30.8 MPa), and kink of curve as a result of flow rate change is displayed with empty symbol.*

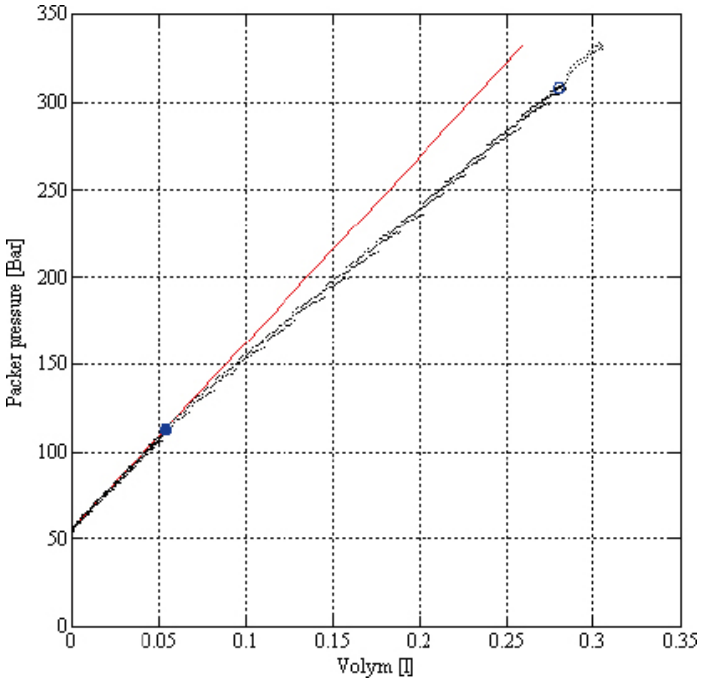

Figure 6-5. *Sleeve fracturing test at 197 mvd in borehole KFM07C, second cycle. Linear fit is displayed with red line, re-opening (at 11.3 MPa) with full symbol, and kink of curve as a probable result of flow rate change (at 30.8 MPa) is displayed with empty symbol.*

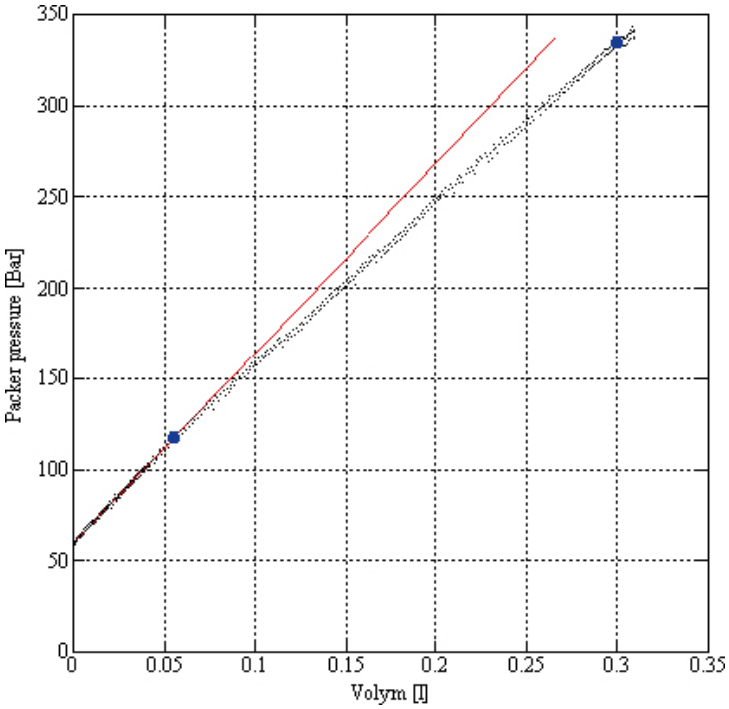

Figure 6-6. *Sleeve fracturing test at 197 mvd in borehole KFM07C, third cycle. Linear fit is displayed with red line, re-opening (at 11.8 MPa) and secondary breakdown (at 33.5 MPa) with full symbols.*

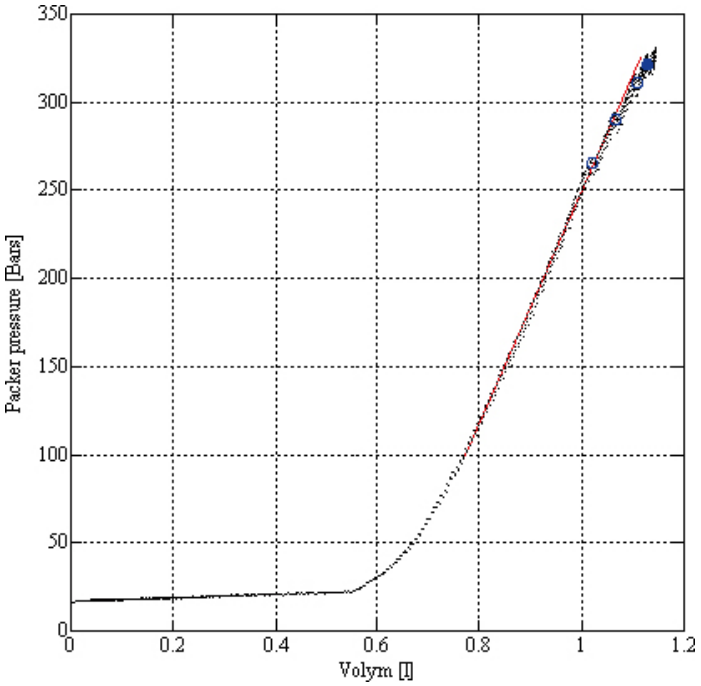

Figure 6-7. *Sleeve fracturing test at 174 mvd in borehole KFM07C, first cycle. Linear fit is displayed with red line, breakdown (at 32.2 MPa) with full symbol, and multiple kinks (at 26.5, 28.8, and 31.1 MPa) as a result of varying flow rate with empty symbols.*

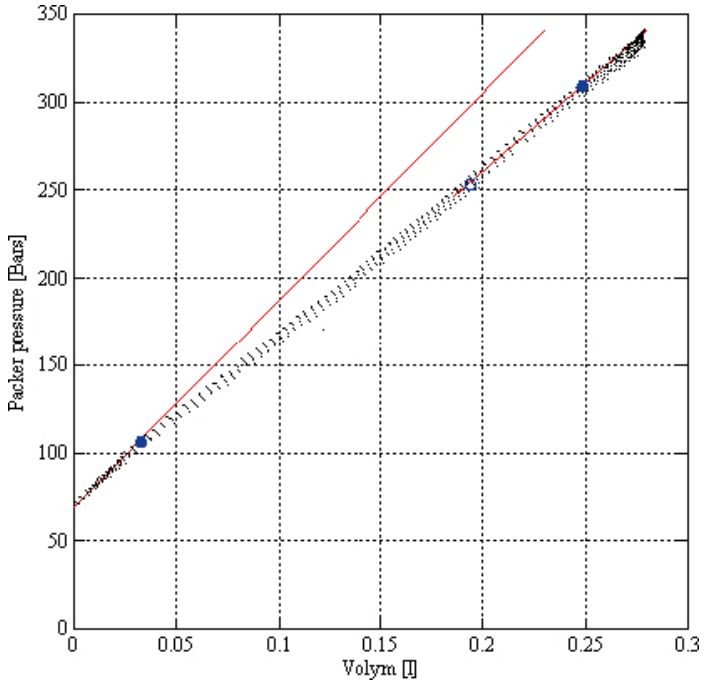

Figure 6-8. *Sleeve fracturing test at 174 mvd in borehole KFM07C, second cycle. Linear fit is displayed with red line, re-opening (at 10.6 MPa) and a possible secondary breakdown (at 30.9 MPa) with full symbols, and kink of curve as a probable result of flow rate change (at 25.3 MPa) is displayed with empty symbol.*

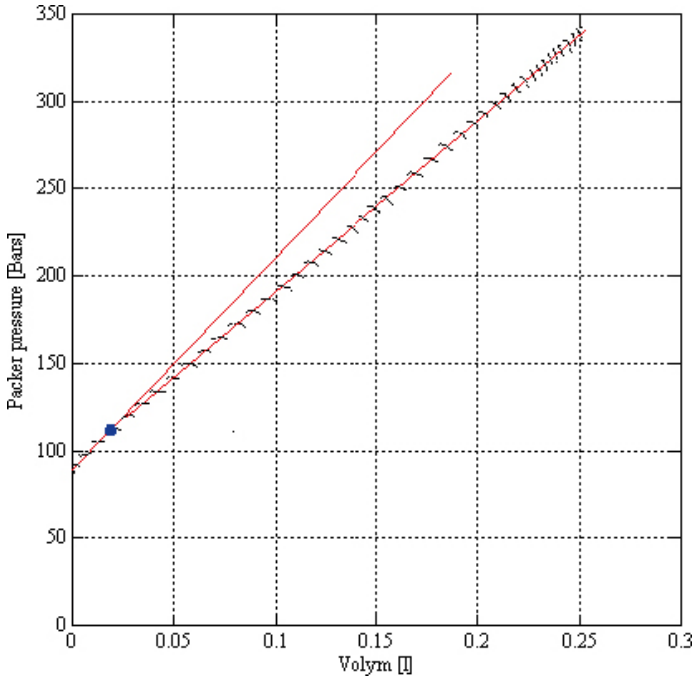

Figure 6-9. *Sleeve fracturing test at 174 mvd in borehole KFM07C, third cycle. Linear fit is displayed with red line and re-opening (at 11.1 MPa) with full symbol.*

Table 6-3. Critical parameters determined in sleeve fracturing data.

Test	Vert. depth [m]	$P_{b,sf}$ [MPa]	$P_{r1,sf}$ [MPa]	$P_{r2,sf}$ [MPa]
14	197	30.8?	11.3	11.8
		33.5		
15	174	32.2	10.6	11.1
		30.9?		

Two of the breakdown pressures are associated with uncertainties (at 30.8 and 30.9 MPa, respectively), whereas the other two are rather well pronounced (at 33.5 and 32.2 MPa, respectively). The re-opening pressures are quite well defined and well grouped between 10.6–11.8 MPa. The average parameters for the sleeve fracturing tests become:

At 197 mvd:	At 174 mvd:
$P_{b,sf}$ = 33.5 MPa	$P_{b,sf}$ = 32.2 MPa
$P_{r,sf}$ = 11.6 MPa	$P_{r,sf}$ = 10.9 MPa

where $P_{b,sf}$ and $P_{r,sf}$ are the breakdown and re-opening pressures for the sleeve fracturing tests, respectively. The modified fracturing equation by /Bredehoeft et al. 1976/ yields:

$$\sigma_H = 3\sigma_h - P_{r,sf} \tag{6-9}$$

where σ_h and σ_H are the minimum and maximum horizontal stresses. Thus, we obtain the following at 197 and 174 mvd:

$\sigma_H = 3*\sigma_h - 11.6$ MPa = {using σ_h from conventional HF below} = 10.6 MPa

$\sigma_H = 3*\sigma_h - 10.9$ MPa = {using σ_h from conventional HF below} = 11.3 MPa

The sleeve fracturing tests may also be used to estimate the tensile strength as the difference between breakdown and re-opening pressure. The data at 197 and 174 mvd would then suggest a tensile strength as high as 21.9 and 21.3 MPa, respectively.

Results from conventional hydraulic fracturing

The subsequent hydraulic fracturing test at the location of the sleeve fracturing tests yielded the following result (Figure 6-10 and Figure 6-11):

At 197 mvd:	At 174 mvd:
$P_{b,hf}$ = 32.1 MPa	$P_{b,hf}$ = 13.1 MPa (non-distinct)
$P_{shut\text{-}in,hf} = \sigma_h$ = 7.4 MPa	$P_{shut\text{-}in,hf} = \sigma_h$ = 7.4 MPa
Orientation of σ_H: 128°N	Orientation of σ_H: 121°N

where $P_{b,hf}$ and $P_{shu\text{-}in,hf}$ are the breakdown and shut-in pressures for the conventional hydraulic fracturing tests, respectively. The classical hydraulic fracturing equation entails that (neglecting pore pressure):

$$\sigma_H = 3\sigma_h - P_{b,hf} + T - a * P_p \tag{6-10}$$

where σ_h and σ_H are the minimum and maximum horizontal stresses, T is the tensile strength, P_p is pore pressure, and a is an unknown constant between 0 and 1.

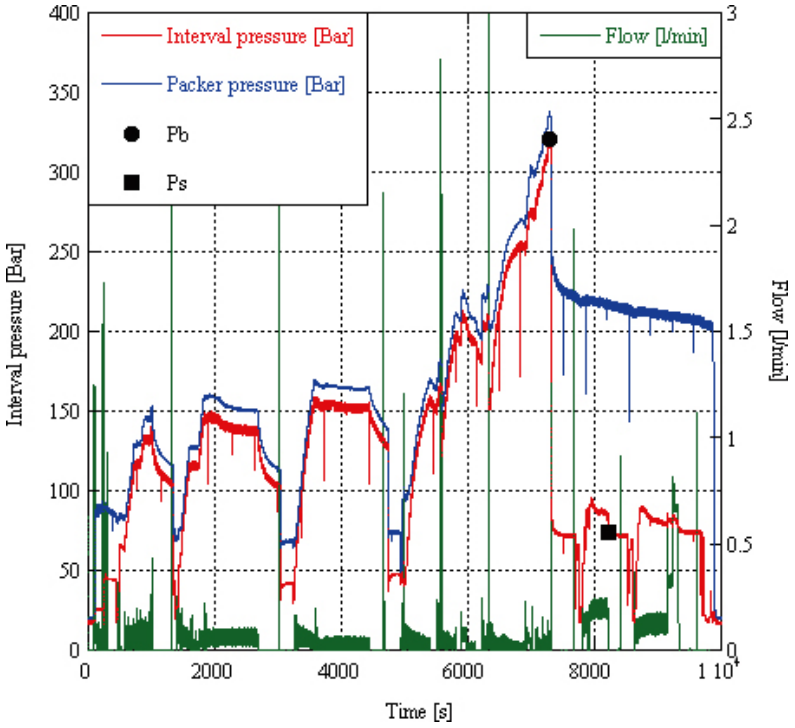

Figure 6-10. *Conventional hydraulic fracturing at 197 mvd in borehole KFM07C, with interpretation of breakdown (P_b = 32.1 MPa) and shut-in pressures (P_s = 7.4 MPa).*

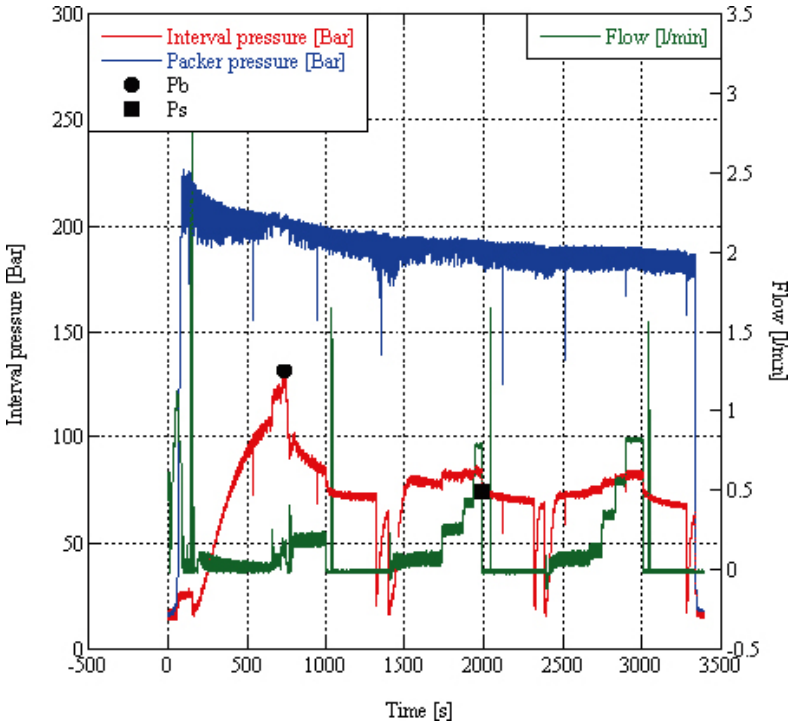

Figure 6-11. *Conventional hydraulic fracturing at 174 mvd in borehole KFM07C, with interpretation of breakdown (P_b = 13.1 MPa but non-distinct) and shut-in pressures (P_s = 7.4 MPa).*

The pore pressure is unknown because the permeability, in the extension zone close to the borehole before failure occurs, is stress dependent. The extreme values occur for (1) a = 0, P_p value arbitrary; and (2) a = 1 and $P_p = P_{b,hf}$, giving the maximum and minimum magnitudes for σ_H, respectively. In the following, we assume that pore pressure effects may be neglected, i.e. we will estimate the upper limit for the magnitude of σ_H.

Using the hydraulic fracturing data at 197 mvd and the tensile strength estimate from the corresponding sleeve fracturing test yields:

$\sigma_H = 3*7.4 – 32.1 + 21.9 = 12.0$ MPa

The breakdown at 174 mvd is non-distinct and the borehole pressure behaviour is non-linear. This result is interpreted as that a fracture is already opened in the test section, e.g. the fractures induced and/or opened by the sleeve fracturing test, which significantly lowers the breakdown pressure. Thus, conventional hydraulic fracturing theory cannot be applied.

Because the maximum horizontal stress magnitude derived from the sleeve fracturing, which is independent of pore pressure effects, and conventional hydraulic fracturing data is within 1.4 MPa, this is regarded as a strong constraint for the stress field in borehole KFM07C between 170 and 200 mvd.

6.5 Inversion results for borehole KFM07C

A solution for borehole KFM07C was not possible with the measured uncertainties on the data. Hence, uncertainties of 3.0° and 2.0° for azimuth and dip were employed as well as 0.3 MPa uncertainty in normal stress. Yet, convergence was most difficult to achieve and the solution finally obtained is poor, except for magnitude of minimum horizontal stress (Table 6-4; Figure 6-12). No rotation is assumed and the vertical gradient was set to 0.0260 MPa/m. All calculated parameters are within one standard deviation of the measured parameters (Table 6-5).

The solution for borehole KFM07C also suggests that thrust regime prevails. The average ratio σ_H/σ_h is 2.0, and the average ratios σ_v/σ_h and σ_H/σ_v are 0.8 and 2.7, respectively (note that the vertical stress gradient was assumed to equal 0.0260 MPa/m). Acceptable uncertainties are only obtained at 420 mvd, where the ratios become: $\sigma_H/\sigma_h = 1.5$, $\sigma_v/\sigma_h = 0.9$, and $\sigma_H/\sigma_v = 1.8$. The orientation of σ_H was found to be 134°N but with a relatively large span of the 95% confidence interval (117–151°N).

Table 6-4. Best solution for borehole KFM07C.

Depth [mvd]	Parameter	σ_H [MPa]	σ_h [MPa]	σ_v [MPa]	Orient σ_H [°N]
180	Magnitude	18.7	7.0	4.7	134
	Std	9.1	0.5	–	8.5
	95% conf. int.	0.5–36.9	6.0–8.0	–	117–151
300	Magnitude	18.9	9.8	7.8	134
	Std	4.4	0.4	–	8.5
	95% conf. int.	10.1–27.7	9.0–10.6	–	117–151
420	Magnitude	19.2	12.7	10.9	134
	Std	1.7	0.5	–	8.5
	95% conf. int.	15.8–22.6	11.7–13.7	–	117–151

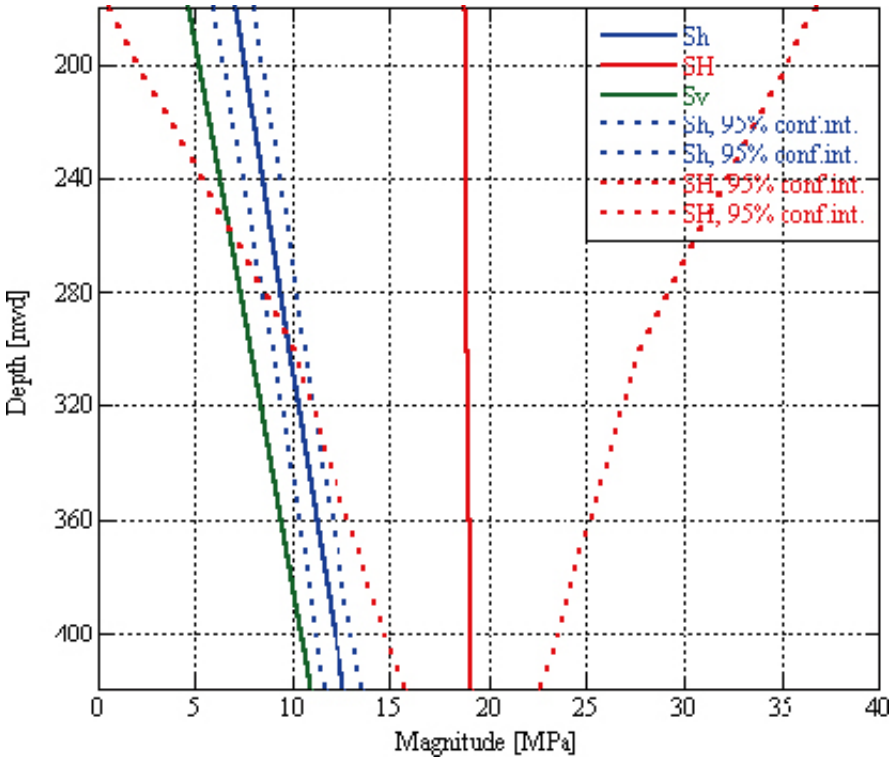

Figure 6-12. *Best solution obtained for borehole KFM07C, involving 5 model parameters and 6 measurement points between 180-420 mvd.*

Table 6-5. A priori and a posteriori data in best solution for borehole KFM07C.

Depth [mvd]	Test no	Az_{meas} [°N]	Az_{calc} [°N]	Error [°N]	STD_{Az}	Dip_{meas} [°N]	Dip_{calc} [°N]	Error [°N]	STD_{Dip}	$\sigma_{n,meas}$ [MPa]	$\sigma_{n,calc}$ [MPa]	Error [MPa]	$STD_{\sigma n}$ [MPa]
416.5	2*	202.0	202.0	0.0	3.0	44.0	44.0	0.0	2.0	12.1	12.1	0.0	0.3
394.0	4	166.0	167.0	1.0	3.0	66.0	66.0	0.0	2.0	16.0	16.0	0.0	0.3
388.0	5*	228.0	228.0	0.0	3.0	48.0	48.0	0.0	2.0	11.1	11.1	0.0	0.3
235.5	12*	218.0	217.6	0.4	3.0	30.0	30.6	0.6	2.0	7.1	6.7	0.4	0.3
196.4	14*	38.0	38.3	0.3	3.0	88.0	88.0	0.0	2.0	7.4	7.5	0.1	0.3
173.5	15*	31.0	31.1	0.1	3.0	87.0	87.0	0.0	2.0	7.4	7.4	0.0	0.3

Unambiguous data are marked with "*".

6.6 Combined stress inversion result of boreholes KFM07A and KFM07C

For the combination of data at drill site 7, two approaches were used. The first is denominated an unconstrained solution, meaning that standard inversion is applied where the hydraulic data are used to constrain all model parameters. The second approach, on the other hand, is denominated a constrained solution. In this case, the knowledge of the stress state at 170–200 mvd from the sleeve fracturing and subsequent hydraulic fracturing is used. Thus, for this approach, a new solution was searched, in which σ_H = 12.0 MPa, σ_h = 7.4 MPa, and σ_H oriented 125°N at about 190 mvd is satisfied.

The best unconstrained solution for drill site 7 involves 7 parameters and 13 data in the interval 170–490 mvd. It solves quite nicely the stress down to about 400 mvd, where the uncertainties are increasing more rapidly (Table 6-6; Figure 6-13). The vertical gradient was found relatively high (0.0297 MPa/m) as opposed to the other inversions at the Forsmark site. Three azimuths are outside the range of one standard deviation, but within two standard deviations (Table 6-7).

The unconstrained solution for drill site 7 suggests that σ_h is approximately of the same order of magnitude as σ_v down to about 300 mvd, but becomes the minor stress below this depth. The average ratio σ_H/σ_h is 2.7, and the average ratios σ_v/σ_h and σ_H/σ_v are 1.2 and 2.4, respectively. At the depth interval where the uncertainties are minimized (250–330 mvd), the following is obtained: $\sigma_H/\sigma_h = 2.7$, $\sigma_v/\sigma_h = 1.1$, and $\sigma_H/\sigma_v = 2.4$. The orientation of σ_H was found to be stable over the interval, 117–118°N, and displaying a 95% confidence interval in the range 106–128°N.

The constrained solution, with known orientation and stress magnitude at 190 mvd, consists of solving only the stress gradients for σ_H, σ_h, and σ_v, as well as a possible rotation of the stresses with depth. The solution involves 9 data in the interval 170–490 mvd, but because none involves sub-horizontal fractures, the vertical stress gradient was assumed to be equal to the theoretical weight of the overburden rock mass (0.026 MPa/m).

As it turns out, the constrained solution is quite similar to the unconstrained with respect to the magnitude of σ_h and the orientation of σ_H, whereas the stress gradient for σ_H is considerably larger compared with the unconstrained solution. At greater depth, the solutions are basically equivalent (Table 6-8; Figure 6-14). The fit between *a priori* and *a posteriori* data (Table 6-9) is considerably better in the constrained solution, entailing that this solution should be favoured. In Section 7.3, an attempt to verify these solutions by adding information from packer induced sub-horizontal fractures will be attempted.

Table 6-6. Best unconstrained solution for boreholes KFM07A and KFM07C.

Depth [mvd]	Parameter	σ_H [MPa]	σ_h [MPa]	σ_v [MPa]	Orient σ_H [°N]
170	Magnitude	19.4	7.0	5.0	117
	Std	1.3	0.8	0.4	5.6
	95% conf. int.	16.8–22.0	5.4–8.6	4.2–5.8	106–128
250	Magnitude	20.0	7.3	7.4	118
	Std	0.8	0.7	0.6	4.4
	95% conf. int.	18.4–21.6	5.9–8.7	6.2–8.6	109–127
330	Magnitude	20.5	7.7	9.8	118
	Std	0.8	0.9	0.7	3.4
	95% conf. int.	18.9–22.1	5.9–9.5	8.4–11.2	111–125
410	Magnitude	21.1	8.1	12.2	118
	Std	1.2	1.2	0.9	3.0
	95% conf. int.	18.7–23.5	5.7–10.5	10.4–14.0	112–124
490	Magnitude	21.6	8.4	14.6	118
	Std	1.9	1.6	1.1	3.4
	95% conf. int.	17.8–25.4	5.2–11.6	12.4–16.8	111–125

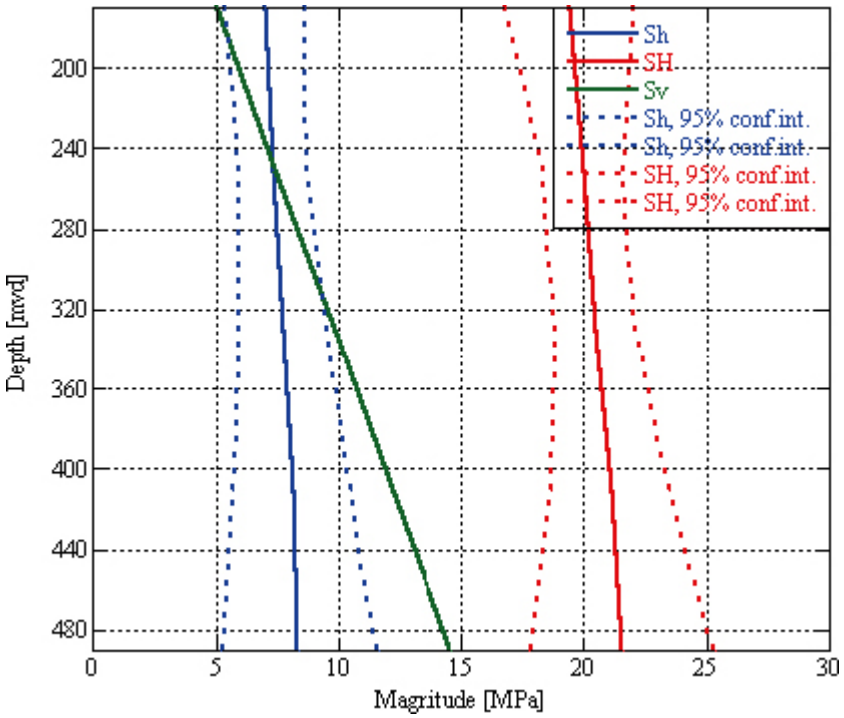

Figure 6-13. *Best unconstrained solution obtained for boreholes KFM07A and KFM07C, involving 7 model parameters and 13 measurement points between 170–490 mvd.*

Table 6-7. A priori and a posteriori data in best unconstrained solution for boreholes KFM07A and KFM07C.

Depth [mvd]	Borehole	Test no	Az_{meas} [°N]	Az_{calc} [°N]	Error [°N]	STD_{Az}	Dip_{meas} [°N]	Dip_{calc} [°N]	Error [°N]	STD_{Dip}	$\sigma_{n,meas}$ [MPa]	$\sigma_{n,calc}$ [MPa]	Error [MPa]	$STD_{\sigma n}$ [MPa]
493.0	KFM07A	5*	237.0	238.8	1.8	9.0	86.0	86.0	0.0	6.0	12.0	12.0	0.0	0.3
487.5	KFM07A	6*	237.0	238.5	1.5	6.5	78.0	77.9	0.1	5.5	12.0	12.0	0.0	0.1
481.0	KFM07A	7*	254.0	254.6	0.6	13.0	82.0	82.0	0.0	7.0	15.4	15.4	0.0	0.5
427.5	KFM07A	8	332.0	325.7	6.3	5.0	72.0	73.3	1.3	4.0	18.0	17.9	0.1	0.3
387.0	KFM07A	9*	319.0	326.2	7.2	5.0	85.0	84.5	0.5	4.0	17.9	17.9	0.0	0.1
368.0	KFM07A	10*	271.0	258.1	12.9	8.5	86.0	85.9	0.1	3.5	15.5	15.5	0.0	0.2
326.0	KFM07A	12*	151.0	152.1	1.1	5.0	89.0	89.0	0.0	3.0	16.4	16.4	0.0	0.1
271.5	KFM07A	13*	129.0	126.5	2.5	7.5	79.0	79.6	0.6	3.5	19.5	19.4	0.1	0.3
400.0	KFM07C	3*	187.0	188.9	1.9	9.0	50.0	50.4	0.4	5.5	10.4	10.4	0.0	0.1
388.0	KFM07C	5*	228.0	235.0	7.0	13.0	48.0	47.8	0.2	6.0	11.1	11.1	0.0	0.2
235.5	KFM07C	12*	218.0	214.9	3.1	22.5	30.0	29.7	0.3	10.5	7.1	7.1	0.0	0.2
196.5	KFM07C	14*	38.0	36.8	1.2	11.0	88.0	88.0	0.0	1.0	7.4	7.4	0.0	0.1
173.5	KFM07C	15*	31.0	38.2	7.2	14.5	87.0	87.0	0.0	1.5	7.4	7.4	0.0	0.1

Unambiguous data are marked with "*".

Table 6-8. Best constrained solution for boreholes KFM07A and KFM07C.

Depth [mvd]	Parameter	σ_H [MPa]	σ_h [MPa]	σ_v [MPa]	Orient σ_H [°N]
190	Magnitude	12.0	7.4	4.9	125
	Std	–	–	0.1	–
	95% conf. int.	–	–0	4.9–5.1	–
290	Magnitude	15.5	8.3	7.5	125
	Std	0.4	0.5	0.2	3.5
	95% conf. int.	14.7–16.3	7.3–9.3	7.1–7.9	118.0–132.0
390	Magnitude	18.9	9.2	10.1	124
	Std	0.7	1.1	0.2	5.2
	95% conf. int.	17.5–20.3	7.0–11.4	9.7–10.5	113.6–134.4
490	Magnitude	22.4	10.1	12.7	124
	Std	1.1	1.6	0.3	6.1
	95% conf. int.	20.2–24.6	6.9–13.3	12.1–13.3	111.8–136.2

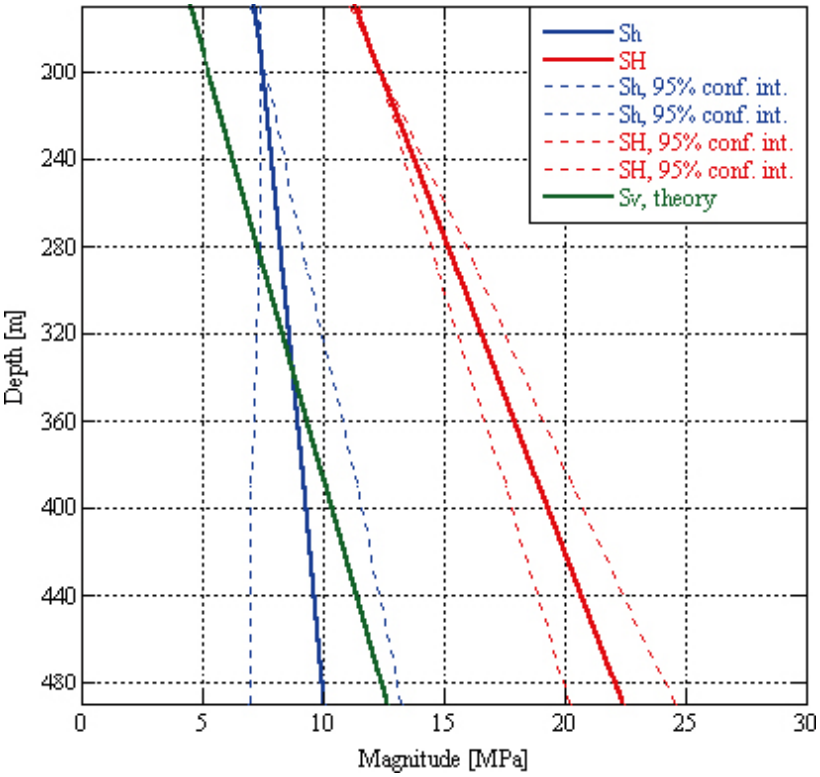

Figure 6-14. *Best constrained solution obtained for boreholes KFM07A and KFM07C, involving 3 model parameters and 9 measurement points between 170–490 mvd.*

Table 6-9. A priori and a posteriori data in best constrained solution for boreholes KFM07A and KFM07C.

Depth [mvd]	Borehole	Test no	Az_{meas} [°N]	Az_{calc} [°N]	Error [°N]	STD_{Az}	Dip_{meas} [°N]	Dip_{calc} [°N]	Error [°N]	STD_{Dip}	$\sigma_{n,meas}$ [MPa]	$\sigma_{n,calc}$ [MPa]	Error [MPa]	$STD_{\sigma n}$ [MPa]
493.0	KFM07A	5*	237.0	237.0	0.0	9.0	86.0	86.0	0.0	6.0	12.0	12.0	0.0	0.3
487.5	KFM07A	6*	237.0	237.3	0.3	6.5	78.0	78.0	0.0	5.5	12.0	12.0	0.0	0.1
481.0	KFM07A	7*	254.0	256.5	2.5	13.0	82.0	82.0	0.0	7.0	15.4	15.4	0.0	0.5
427.5	KFM07A	8	332.0	328.3	3.7	5.0	72.0	73.3	1.3	4.0	18.0	17.9	0.1	0.3
387.0	KFM07A	9*	319.0	321.8	2.8	5.0	85.0	84.5	0.5	4.0	17.9	17.9	0.0	0.1
368.0	KFM07A	10*	271.0	272.1	1.1	8.5	86.0	86.0	0.0	3.5	15.5	15.5	0.0	0.2
271.5	KFM07A	13*	129.0	129.3	0.3	7.5	79.0	78.8	0.2	3.5	14.4	14.5	0.1	0.6
196.5	KFM07C	14*	38.0	36.8	1.2	11.0	88.0	88.0	0.0	1.0	7.4	7.5	0.1	0.1
173.5	KFM07C	15*	31.0	24.1	6.9	14.5	87.0	87.0	0.0	1.5	7.4	7.4	0.0	0.1

Unambiguous data are marked with "*".

6.7 Inversion results for borehole KFM08A

Borehole KFM08A involves two 6 parameter solutions (horizontal stresses and their variation with depth, the vertical stress gradient, and the orientation of the horizontal stresses assuming no rotation with depth): (i) 570–720 mvd and 7 data; and (ii) 420–490 mvd and 7 data. The solution for the lower interval is fair except for the σ_H-magnitude (Table 6-10; Figure 6-15), whereas for the upper interval, the orientation of σ_H is poorly resolved (Table 6-11; Figure 6-15). The solutions are widely different and the vertical stress gradients were found to be 0.0217 and 0.0199 MPa/m, for the lower and upper solutions, respectively (thus somewhat low; Table 6-10 and Table 6-11). For both data sets, the calculated parameters are within one standard deviation of the measured parameters (Table 6-12 and Table 6-13).

The solutions for borehole KFM08A suggest that strike-slip regime prevails below 580 mvd, whereas $\sigma_h \approx \sigma_v$ in the interval 420–490 mvd (note that the more shallow solution indicates decreasing magnitude of σ_h with increasing depth but uncertainties are increasing with depth). The average ratios σ_H/σ_h are 2.4 and 1.3 for the deeper and shallower solutions, respectively. The average ratios σ_v/σ_h and σ_H/σ_v are 1.4 and 1.7, respectively, for the deeper solution. Corresponding values for the shallower solutions are 0.8 and 1.6, respectively. Again, the large uncertainty of primarily σ_H towards depth makes the ratios σ_H/σ_h and σ_H/σ_v meaningless. The orientation of σ_H was found to be 153°N and 122°N for the deep and shallow solutions, respectively.

Table 6-10. Best solution for borehole KFM08A, 580–720 mvd.

Depth [mvd]	Parameter	σ_H [MPa]	σ_h [MPa]	σ_v [MPa]	Orient σ_H [°N]
580	Magnitude	20.1	8.4	12.6	153
	Std	0.7	1.8	0.6	4.2
	95% conf. int.	18.7–21.5	4.8–12.0	11.4–13.8	145–161
650	Magnitude	24.5	10.1	14.1	153
	Std	2.5	1.6	0.7	4.2
	95% conf. int.	19.5–29.5	6.9–13.3	12.4–15.5	145–161
720	Magnitude	28.9	11.8	15.6	153
	Std	5.0	2.5	0.8	4.2
	95% conf. int.	18.9–38.9	6.8–16.8	14.0–17.2	145–161

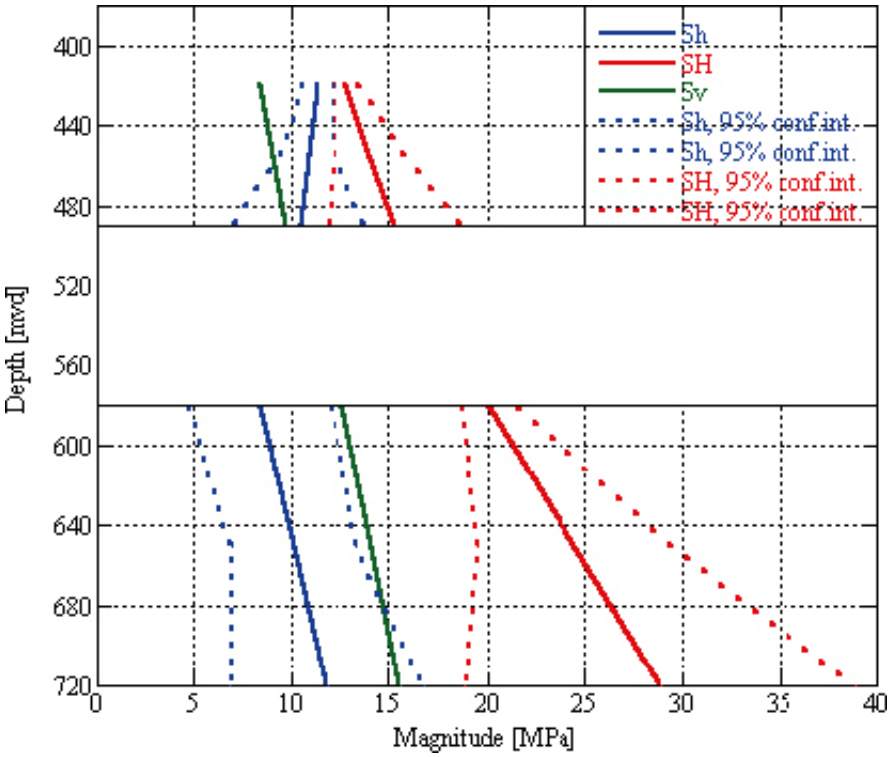

Figure 6-15. *Best solutions obtained for boreholes KFM08A: (1) 580–720 mvd with 6 model parameters and 7 measurement points; and (2) 420–490 mvd with 6 model parameters and 7 measurement points.*

Table 6-11. Best solution for borehole KFM08A, 420–490 mvd.

Depth [mvd]	Parameter	σ_H [MPa]	σ_h [MPa]	σ_v [MPa]	Orient σ_H [°N]
420	Magnitude	12.8	11.3	8.4	122
	Std	0.3	0.4	0.3	9.1
	95% conf. int.	12.2–13.4	10.5–12.1	7.8–9.0	104–140
455	Magnitude	14.0	10.8	9.0	122
	Std	0.9	0.7	0.3	9.1
	95% conf. int.	12.2–15.8	9.4–12.2	8.4–9.6	104–140
490	Magnitude	15.3	10.4	9.7	122
	Std	1.7	1.7	0.3	9.1
	95% conf. int.	11.9–18.7	7.0–13.8	9.1–10.3	104–140

Table 6-12. A priori and a posteriori data in best solution for borehole KFM08A, 580–720 mvd.

Depth [mvd]	Test no	Az_{meas} [°N]	Az_{calc} [°N]	Error [°N]	STD_{Az}	Dip_{meas} [°N]	Dip_{calc} [°N]	Error [°N]	STD_{Dip}	$\sigma_{n,meas}$ [MPa]	$\sigma_{n,calc}$ [MPa]	Error [MPa]	$STD_{\sigma n}$ [MPa]
719.5	1*	212.0	213.3	1.3	5.0	78.0	78.0	0.0	4.0	16.0	16.0	0.0	0.1
692.5	4*	187.0	181.2	5.8	21.0	20.0	20.7	0.7	4.0	16.1	16.1	0.0	0.2
689.0	5	26.0	21.1	4.9	5.5	81.0	81.3	0.3	5.5	18.1	18.1	0.0	0.1
604.5	6*	226.0	227.8	1.8	8.0	35.0	35.8	0.8	4.5	12.0	11.8	0.2	0.5
595.5	7	9.0	10.1	1.1	5.5	89.0	89.0	0.0	3.5	16.6	16.6	0.0	0.1
583.0	9	284.0	285.7	1.7	6.5	61.0	61.1	0.1	5.5	13.6	13.6	0.0	0.2
576.5	10	324.0	323.5	0.5	6.0	68.0	67.3	0.7	5.5	18.5	18.5	0.0	0.1

Unambiguous data are marked with "*". Additional, less reliable, had to be included in order to solve the stress field.

Table 6-13. A priori and a posteriori data in best solution for borehole KFM08A, 420–490 mvd.

Depth [mvd]	Test no	Az_{meas} [°N]	Az_{calc} [°N]	Error [°N]	STD_{Az}	Dip_{meas} [°N]	Dip_{calc} [°N]	Error [°N]	STD_{Dip}	$\sigma_{n,meas}$ [MPa]	$\sigma_{n,calc}$ [MPa]	Error [MPa]	$STD_{\sigma n}$ [MPa]
490.0	12*	261.0	260.1	0.9	8.5	82.0	81.9	0.1	7.5	13.0	13.0	0.0	0.4
476.0	14	42.0	41.9	0.1	27.0	12.0	12.0	0.0	5.0	9.5	9.5	0.0	0.3
470.0	15*	124.0	124.0	0.0	13.5	21.0	21.0	0.0	3.5	10.0	10.0	0.0	0.4
436.5	16	10.0	10.1	0.1	4.5	89.0	89.0	0.0	3.5	11.4	11.4	0.0	0.2
432.0	17	302.0	302.0	0.0	6.5	65.0	67.7	2.7	5.5	12.6	12.5	0.1	0.2
426.5	18	214.0	214.0	0.0	4.0	81.0	81.0	0.0	3.5	11.2	11.2	0.0	0.3
416.5	19	129.0	129.1	0.1	3.5	86.0	85.9	0.1	3.0	12.5	12.6	0.1	0.3

Unambiguous data are marked with "*". Additional, less reliable, had to be included in order to solve the stress field.

6.8 Inversion results for borehole KFM09A

The best solution for KFM09A involves 6 model parameters (horizontal stresses and their variation with depth, the vertical stress gradient, and the orientation of the horizontal stresses assuming no rotation with depth) and 8 data in the interval 470–540 mvd. It solves the vertical stress (0.0218 MPa/m; although somewhat low) and relatively well the orientation of maximum horizontal stress (Table 6-14; Figure 6-16). However, the magnitudes of the horizontal stresses are poorly resolved. All calculated parameters are within one standard deviation of the measured (Table 6-15), entailing that the solution is reliable mathematically speaking.

The solution suggests that strike-slip regime ($\sigma_H < \sigma_v < \sigma_h$) prevails, that the average ratio σ_H/σ_h is as high as 4.8, and the average ratios σ_v/σ_h and σ_H/σ_v are 4.0 and 1.2, respectively. However, the large uncertainty of the stress magnitudes renders these numbers almost meaningless. At 500 mvd, where the uncertainties are minimized, the following is obtained: $\sigma_H/\sigma_h = 4.6$, $\sigma_v/\sigma_h = 3.9$, and $\sigma_H/\sigma_v = 1.2$. The orientation of σ_H was found to be 108°N with a 95% confidence interval in the span 101–115°N.

Table 6-14. Best solution for borehole KFM09A.

Depth [mvd]	Parameter	σ_H [MPa]	σ_h [MPa]	σ_v [MPa]	Orient σ_H [°N]
450	Magnitude	11.9	1.8	9.8	108
	Std	2.4	3.3	0.3	3.6
	95% conf. int.	7.1–16.7	–4.8–8.4	9.2–10.4	101–115
475	Magnitude	12.4	2.3	10.3	108
	Std	1.8	2.6	0.3	3.6
	95% conf. int.	8.8–16.0	–2.9–7.5	9.7–10.9	101–115
500	Magnitude	12.9	2.8	10.9	108
	Std	1.8	2.3	0.4	3.6
	95% conf. int.	9.3–16.5	–1.8–7.4	10.3–11.5	101–115
525	Magnitude	13.2	3.4	11.4	108
	Std	2.3	2.6	0.4	3.6
	95% conf. int.	8.6–17.8	–1.8–8.6	10.6–12.2	101–115
550	Magnitude	13.8	3.9	12.0	108
	Std	3.2	3.3	0.4	3.6
	95% conf. int.	7.4–20.2	–2.7–10.5	11.2–12.8	101–115

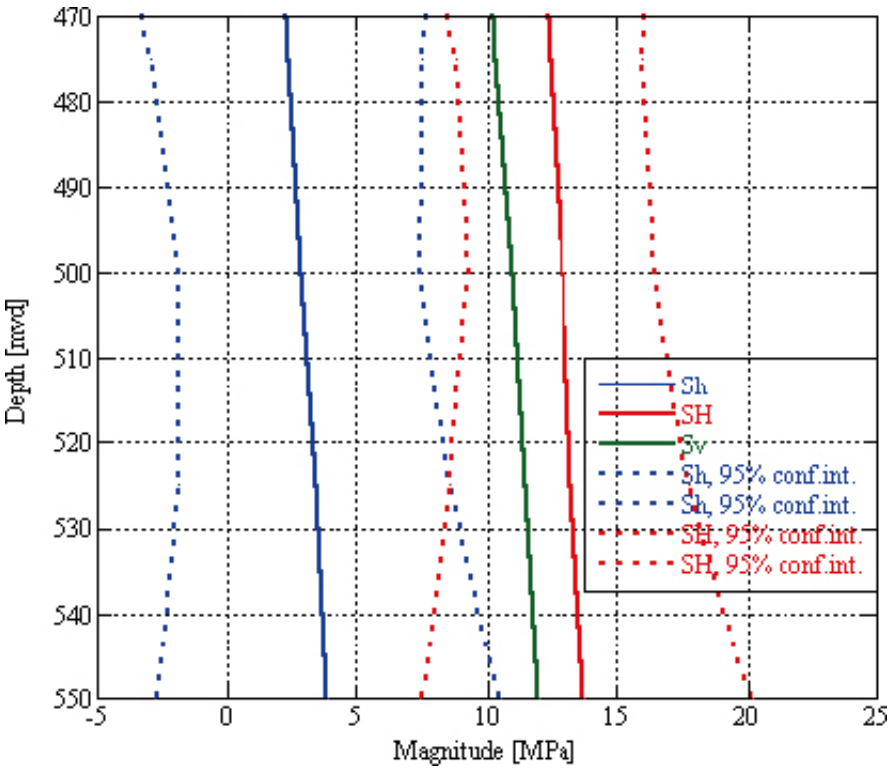

Figure 6-16. *Best solution obtained for borehole KFM09A, involving 6 model parameters and 8 measurement points between 470–540 mvd.*

Table 6-15. A priori and a posteriori data in best solution for borehole KFM09A.

Depth [mvd]	Test no	Az_{meas} [°N]	Az_{calc} [°N]	Error [°N]	STD_{Az}	Dip_{meas} [°N]	Dip_{calc} [°N]	Error [°N]	STD_{Dip}	$\sigma_{n,meas}$ [MPa]	$\sigma_{n,calc}$ [MPa]	Error [MPa]	$STD_{\sigma n}$ [MPa]
540.5	1*	102.0	101.9	0.1	8.5	14.0	14.0	0.0	2.0	11.7	11.9	0.2	0.7
538.5	2*	114.0	114.0	0.0	5.8	21.0	21.0	0.0	3.0	11.9	11.8	0.1	0.5
517.5	3*	67.0	67.4	0.4	2.3	87.0	87.0	0.0	1.5	10.0	8.9	1.1	1.6
502.0	4*	66.0	65.3	0.7	2.5	90.0	90.0	0.0	1.5	8.1	8.3	0.2	0.5
496.0	6*	153.0	153.0	0.0	1.8	79.0	79.0	0.0	1.8	7.9	7.9	0.0	1.0
500.5	7	63.0	63.0	0.0	7.8	14.0	14.0	0.0	1.5	10.7	10.7	0.0	0.7
493.0	8*	276.0	276.0	0.0	2.3	79.0	79.0	0.0	2.0	12.0	12.2	0.2	1.5
473.5	9*	72.0	72.2	0.2	2.3	84.0	84.0	0.0	1.5	9.5	8.9	0.6	1.5

Unambiguous data are marked with "*".

6.9 Inversion results for borehole KFM09B

The best solution for KFM09B involves 7 model parameters (horizontal stresses and their variation with depth, the vertical stress gradient, and the orientation of the horizontal stresses with depth) and 12 data in the interval 270–430 mvd. It solves accurately the vertical stress (0.0224 MPa/m; although somewhat low) and relatively well the minimum horizontal stress and the orientation of maximum horizontal stress (Table 6-16; Figure 6-17). However, maximum horizontal stress is poorly resolved. All calculated parameters are within one standard deviation of the measured (Table 6-17).

The solution for KFM09B suggests that strike-slip regime prevails to about 300 mvd, followed by thrust regime ($\sigma_H < \sigma_h < \sigma_v$) at least down to 430 mvd. The average ratio σ_H/σ_h is as high as 4.6, and the average ratios σ_v/σ_h and σ_H/σ_v are 1.0 and 4.0, respectively. However, the large uncertainty of primarily σ_H makes the ratios σ_H/σ_h and σ_H/σ_v basically meaningless. The orientation of σ_H was found to be stable over the interval at 133°N and with a 95% confidence interval in the span 122–144°N.

Table 6-16. Best solution for borehole KFM09B.

Depth [mvd]	Parameter	σ_H [MPa]	σ_h [MPa]	σ_v [MPa]	Orient σ_H [°N]
270	Magnitude	25.6	3.0	6.0	133
	Std	5.6	2.2	0.2	3.5
	95% conf. int.	8.8–42.4	–3.6–9.6	5.6–6.4	123–144
310	Magnitude	28.1	5.6	6.9	133
	Std	4.7	1.6	0.2	3.3
	95% conf. int.	14.0–42.2	0.8–10.4	6.5–7.3	123–143
350	Magnitude	30.6	8.2	7.8	133
	Std	4.3	1.2	0.2	3.2
	95% conf. int.	17.7–43.5	4.6–11.8	7.4–8.2	123–143
390	Magnitude	33.0	10.8	8.7	133
	Std	4.4	1.2	0.3	3.3
	95% conf. int.	19.8–46.2	7.2–14.4	8.1–9.3	123–143
430	Magnitude	35.5	13.4	9.6	133
	Std	5.1	1.6	0.3	3.6
	95% conf. int.	20.2–50.8	8.6–18.2	0.9–10.2	122–144

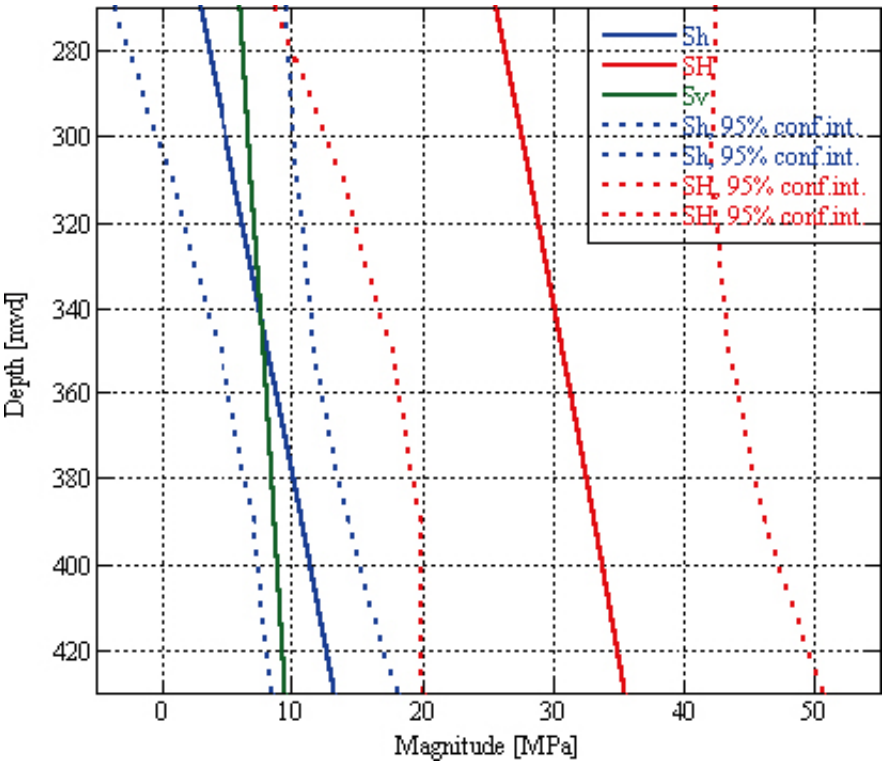

Figure 6-17. *Best solution obtained for borehole KFM09B, involving 7 model parameters and 8 measurement points between 270–430 mvd.*

Table 6-17. A priori and a posteriori data in best solution for borehole KFM09B.

Depth [mvd]	Test no	Az_{meas} [°N]	Az_{calc} [°N]	Error [°N]	STD_{Az}	Dip_{meas} [°N]	Dip_{calc} [°N]	Error [°N]	STD_{Dip}	$\sigma_{n,meas}$ [MPa]	$\sigma_{n,calc}$ [MPa]	Error [MPa]	$STD_{\sigma n}$ [MPa]
428.2	1*	59.0	58.9	0.1	1.8	53.0	52.9	0.1	1.5	12.9	13.0	0.1	0.7
419.8	2*	76.0	76.2	0.2	1.5	83.0	83.0	0.0	1.5	20.0	19.3	0.7	1.5
405.5	3*	345.0	341.8	3.2	16.3	12.0	12.7	0.7	2.5	10.2	10.0	0.2	0.5
399.0	4	4.0	3.0	1.0	3.5	22.0	22.2	0.2	1.0	10.7	10.6	0.1	0.3
374.0	5*	64.0	64.0	0.0	6.3	38.0	38.0	0.0	3.5	10.0	10.0	0.0	0.5
367.0	6*	341.0	343.8	2.8	9.0	14.0	13.6	0.4	1.3	9.0	9.2	0.2	0.3
345.0	7*	342.0	341.0	1.0	16.0	14.0	14.2	0.2	2.3	10.0	8.8	1.2	2.5
334.0	8	39.0	39.1	0.1	5.0	16.0	16.0	0.0	1.5	7.3	7.4	0.1	0.5
318.0	9*	262.0	262.0	0.0	1.5	85.0	85.0	0.0	1.3	15.0	15.1	0.1	1.5
292.5	10*	283.0	281.4	1.6	6.3	22.0	21.2	0.8	2.3	8.2	8.4	0.2	0.5
273.0	12*	199.0	199.1	0.1	1.5	89.0	89.0	0.0	1.3	6.7	6.8	0.1	1.0
265.5	13*	38.0	37.4	0.6	16.0	11.0	10.9	0.1	1.8	5.9	5.8	0.1	0.3

Unambiguous data are marked with "*".

6.10 Combined inversion results for boreholes KFM09A and KFM09B

The best solution for drill site 9 involves 7 model parameters (horizontal stresses and their variation with depth, the vertical stress gradient, and the orientation of the horizontal stresses with depth) and 18 data in the interval 265–500 mvd. It solves accurately the vertical stress (0.0230 MPa/m; although somewhat low) and the minimum horizontal stress. The orientation of maximum horizontal stress is also quite well resolved (Table 6-18; Figure 6-18). However, maximum horizontal stress is only relatively accurate above 440 mvd, whereas it is less resolved below this depth. All calculated parameters are within one standard deviation of the measured, except two (the normal stress for Test 7 in KFM09A and Test 15 in KFM09B; Table 6-19) that are well within two standard deviations.

The solution for drill site 9 suggests that σ_h is of the same order of magnitude as σ_v for the interval 265–500 mvd. The average ratio σ_H/σ_h is 3.1, and the average ratios σ_v/σ_h and σ_H/σ_v are 1.0 and 3.2, respectively. Again, the large uncertainty of primarily σ_H makes the ratios σ_H/σ_h and σ_H/σ_v meaningless. At 320 mvd, where the uncertainties are minimized, the following is obtained: $\sigma_H/\sigma_h = 2.8$, $\sigma_v/\sigma_h = 1.0$, and $\sigma_H/\sigma_v = 2.8$. The orientation of σ_H was found to be relatively stable over the interval, 133–126°N, and displaying a 95% confidence interval in the range 120–130°N when disregarding the uppermost 50 m of the solution.

Table 6-18. Best solution for boreholes KFM09A and KFM09B.

Depth [mvd]	Parameter	σ_H [MPa]	σ_h [MPa]	σ_v [MPa]	Orient σ_H [°N]
260	Magnitude	11.7	5.5	6.0	133
	Std	2.7	1.0	0.2	8.6
	95% conf. int.	6.3–17.1	3.5–7.5	5.6–6.4	116–150
320	Magnitude	20.5	7.3	7.4	128
	Std	2.2	0.7	0.2	3.4
	95% conf. int.	16.1–24.9	5.9–8.7	7.0–7.8	121–135
380	Magnitude	29.4	9.1	8.7	127
	Std	3.3	0.4	0.2	2.8
	95% conf. int.	22.8–36.0	8.3–9.9	8.3–9.1	121–133
440	Magnitude	38.3	10.9	10.1	126
	Std	4.9	0.4	0.3	3.2
	95% conf. int.	28.5–48.1	10.1–11.7	9.5–10.7	120–132
500	Magnitude	47.1	12.7	11.5	126
	Std	6.6	0.6	0.3	3.7
	95% conf. int.	33.9–60.3	11.5–13.9	10.9–12.1	119–133

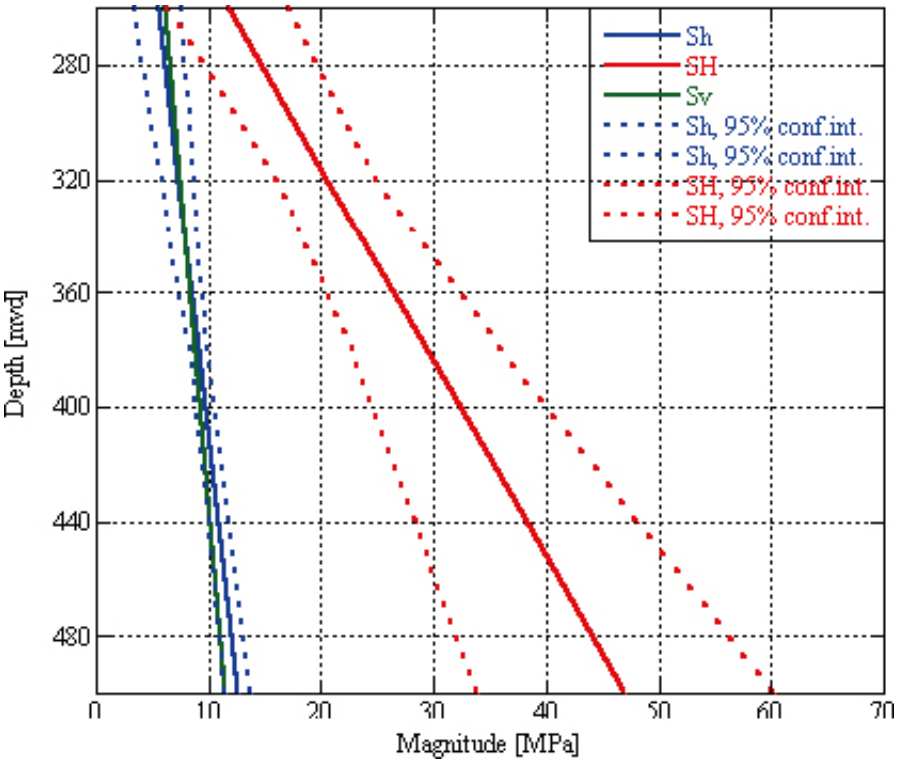

Figure 6-18. *Best solution obtained for boreholes KFM09A and KFM09B, involving 7 model parameters and 18 measurement points between 260–500 mvd.*

Table 6-19. A priori and a posteriori data in best solution for boreholes KFM09A and KFM09B.

Depth [mvd]	Borehole	Test no	Az_{meas} [°N]	Az_{calc} [°N]	Error [°N]	STD_{Az}	Dip_{meas} [°N]	Dip_{calc} [°N]	Error [°N]	STD_{Dip}	$\sigma_{n,meas}$ [MPa]	$\sigma_{n,calc}$ [MPa]	Error [MPa]	$STD_{\sigma n}$ [MPa]
428.2	KFM09B	1*	59.0	59.1	0.1	1.8	53.0	53.0	0.0	1.5	12.9	12.8	0.1	0.7
419.8	KFM09B	2*	76.0	75.9	0.1	1.5	83.0	83.0	0.0	1.5	20.0	20.3	0.3	1.5
405.5	KFM09B	3*	345.0	342.3	2.7	16.3	12.0	12.4	0.4	2.5	10.2	10.1	0.1	0.5
399.0	KFM09B	4	4.0	1.3	2.7	3.5	22.0	22.4	0.4	1.0	10.7	10.3	0.4	0.3
374.0	KFM09B	5*	64.0	62.5	1.5	6.3	38.0	37.7	0.3	3.5	10.0	10.1	0.1	0.5
367.0	KFM09B	6*	341.0	343.2	2.2	9.0	14.0	13.7	0.3	1.3	9.0	9.1	0.1	0.3
345.0	KFM09B	7*	342.0	341.1	0.9	16.0	14.0	14.1	0.1	2.3	10.0	8.6	1.4	2.5
334.0	KFM09B	8	39.0	39.0	0.0	5.0	16.0	16.0	0.0	1.5	7.3	7.7	0.4	0.5
318.0	KFM09B	9*	262.0	262.3	0.3	1.5	85.0	85.0	0.0	1.3	15.0	13.4	1.6	1.5
273.0	KFM09B	12*	199.0	199.1	0.1	1.5	89.0	89.0	0.0	1.3	6.7	7.0	0.3	1.0
265.5	KFM09B	13*	38.0	38.3	0.3	16.0	11.0	11.0	0.0	1.8	5.9	6.1	0.2	0.3
386.0	KFM09B	15	257.0	258.8	1.8	2.8	22.0	22.5	0.5	1.0	11.4	10.3	1.1	0.5
500.5	KFM09A	7	63.0	59.3	3.7	7.8	14.0	13.7	0.3	1.5	10.7	11.9	1.2	0.7
493.0	KFM09A	8*	99.0	95.6	3.4	12.5	18.0	15.8	2.2	4.0	12.0	13.3	1.3	1.5
456.0	KFM09A	10	212.0	211.7	0.3	2.5	85.0	85.0	0.0	1.8	11.7	11.6	0.1	0.5
453.0	KFM09A	11	31.0	31.8	0.8	3.5	79.0	79.0	0.0	1.3	11.2	11.4	0.2	0.5
293.0	KFM09A	14	62.0	62.5	0.5	2.5	87.0	87.0	0.0	1.5	8.3	8.0	0.3	0.7

Unambiguous data are marked with "*".

7 The packer-induced sub-horizontal fractures

The individual test results for all investigated boreholes at the Forsmark candidate site indicate that a large number of sub-horizontal fractures have been induced (Appendices I to III). These fractures sometimes appear in the test section, although they are more commonly located at the end of the test section (i.e. at the packer ends) and sometimes underneath the packers. Hence, a majority of these fractures are packer induced. In a few tests, multiple sub-horizontal fractures were created (e.g. about 14 fractures in Test 4 in borehole KFM09B; Figure 7-1).

The induced sub-horizontal fractures cause two significant problems: (i) during the injection testing; and (ii) during the evaluation of the tests. The packer-induced fractures were created when the pressure in the test section was just moderately larger (a few bars) than the theoretical weight of the overburden rock mass. This implies that a major constraint for injection testing prevailed and that sub-horizontal fractures were induced in all cases where the fracture did not re-activate before reaching this critical pressure. We find it likely that the relatively moderate testing depth in combination with the inclined boreholes (c. 60–40° from the horizontal plane for all wells but KFM07C) is not favourable for hydraulic stress measurements. This phenomenon has apart from the Oskarshamn site, as far as we know, not been found elsewhere. This means that it is either specific to the Forsmark and Oskarshamn sites, or perhaps more likely, it has not been detected before due to limitations in fracture determination methods (which normally involve impression packer technique).

The problem during evaluation of the tests relates to the fact that the opening of a fracture changes the stress field locally, but leaves the normal stress unaffected. Hence, for multiple fractures in the test section, the fracture normal stresses can be unambiguously determined only when the fractures are parallel.

By the appearance of the sub-horizontal fractures on the electrical imaging logs, many fractures seem to have experienced no or very limited fluid percolation, although visual inspection is a somewhat speculative approach. This would imply that, similar to drilling induced fractures /Brudy and Zoback 1993, Peska and Zoback 1995, Zoback et al. 2003/ or fractures induced by sleeve fracturing technique /Stephansson 1983ab/, they do not extend far into the rock. If this would be true, they would not distort the stress field as much as fully propagated fractures. Because the effect of the sub-horizontal fractures has not been investigated fully at this stage, HTPF tests that have changed the resistivity image of the aimed pre-existing fracture but that also include sub-horizontal fractures, were assigned “potentially successful re-opening” in Appendices I to III.

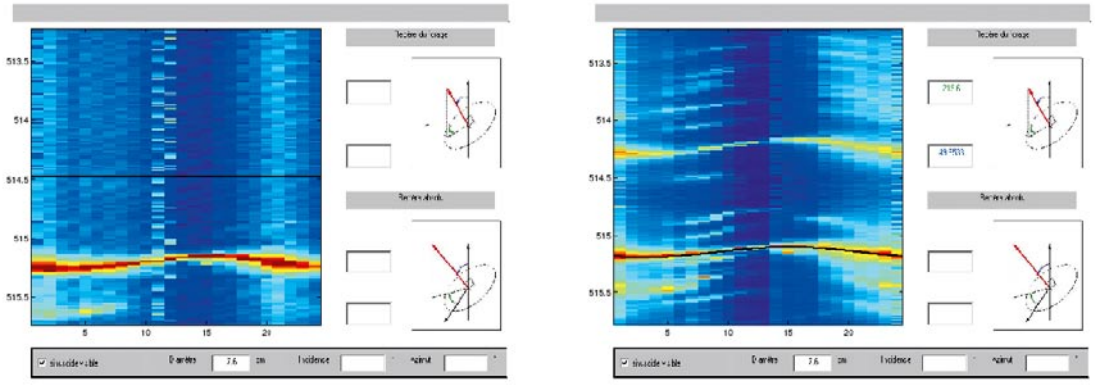

Figure 7-1. *Multiple induced sub-horizontal fractures during testing at 514.9 mbl in borehole KFM09B. The left and right images correspond to the results from the reconnaissance log and the post-log, respectively.*

By the results in the preceding chapter, it is clear that local heterogeneities introduce some dispersion in the results that require a combination of both true hydraulic fracturing tests and HTPF tests. However, true hydraulic fracturing tests can only be completed in boreholes that are parallel to a principal stress direction. None was available at drill sites 8 or 9, hence the difficulty for the complete stress determination at these two sites. It should be emphasized that when both true hydrofrac tests and HTPF tests are run in the same borehole or in two closely located boreholes, the influence of the local heterogeneity remains tractable. This is the essence of the cluster approach /Ask and Cornet 2006, 2007/ that was proven successful at drill site 12 in Oskarshamn.

However, as will be shown in this chapter, the packer-induced fractures also contain useful information that could contribute considerably to the knowledge of the present state of stress at the Forsmark site. Because the development of the sub-horizontal fractures is a function of the state of stress, we may validate the above solutions with a proper failure criterion. This will be attempted in this chapter by applying a special computer code developed by Prof. Francois Cornet, Institut de Physique de Globe de Paris (IPGP). The code was initially developed for en-echelon fractures, which are tensile failures commonly observed in boreholes not fully aligned with one principal stress direction, but it was extended to investigate failure also by shear. We emphasize that the code is not a strict inversion program but merely a tool of investigating a domain of solutions for both tensile failure and shear failure according to the Coulomb failure criterion.

7.1 Appearance of packer induced fractures

As previously noted, the packer-induced fractures appear primarily at the packer ends, although they also sometimes appear underneath the packers or inside the test section. This relative positioning has consequences for what pressure should be used in their analysis, i.e. the test section pressure or the packer pressure (which are normally about 10 bars higher than the section pressure). In Figure 7-1, we show an example of when multiple sub-horizontal fractures have been induced.

The observed sub-horizontal fractures in boreholes KFM07A and KFM07C are presented in Table 7-1. In Figure 7-2, the normals to the fracture planes are presented, indicating a relatively large scatter in orientations. However, when disregarding dip-values larger than 30°, most of the normals are oriented 75–120°. Noteworthy is that sub-horizontal fractures have a fairly large uncertainty on orientation as compared with more inclined fractures. This fact is a result of a geometrical problem, independent of equipment used to determine fracture orientations.

Table 7-1. Analysis of sub-horizontal fractures in boreholes KFM07A and KFM07C.

Borehole	Depth [mvd]	Test no	Azimuth [°N]	STD_{Az} [°N]	Dip [°]	STD_{Dip} [°]	Bh dipdir [°N]	Bh dip. [°]
KFM07A	663.5	1	87	10.5	27	4.0	288	38
KFM07A	636.5	2	151	12.0	28	5.5	287	37
KFM07A	597.0	3	2	4.5	12	5.5	285	36
KFM07A	518.5	4	119	24.5	19	5.0	282	36
KFM07A	493.0	5	120	10.5	12	6.0	280	35
KFM07A	487.5	6	10	8.5	13	4.5	280	35
KFM07A	481.0	7	100	45.0	7	4.0	280	35
KFM07A	427.5	8	96	24.0	16	3.0	278	35
			114	30.0	19	9.5		
KFM07A	387.0	9	177	13.5	27	6.5	276	34
KFM07A	368.0	10	101	23.0	27	4.5	276	34
KFM07A	343.0	11	83	25.0	23	5.0	274	34
KFM07A	326.0	12	120	13.5	19	3.0	273	34
KFM07A	371.5	13	27	11.5	41	6.5	271	33
KFM07C	421.0	1	110	10.0	18	43.0	146	6
KFM07C			137	17.5	30	4.5	146	6
KFM07C	416.5	2	180	90.0	8	4.0	146	6
KFM07C	400.0	3	101	23.0	14	4.5	147	6
KFM07C	394.0	4	220	7.0	38	5.0	148	6
KFM07C			225	11.5	42	4.5	148	6
KFM07C	388.0	5	180	90.0	10	5.5	148	6
KFM07C	340.5	6	325	24.0	12	4.5	148	6
KFM07C	312.0	7	35	17.5	33	6.5	149	6
KFM07C	300.5	8	77	38.5	21	9.0	149	6
KFM07C	293.0	9	180	90.0	8	43.0	149	6
KFM07C	271.5	10	180	90.0	10	5.0	149	6
KFM07C	246.0	11	225	15.0	20	5.5	150	6
KFM07C	235.5	12	218	22.5	30	10.5	150	6
KFM07C	223.5	13	180	90.0	9	5.0	150	6
KFM07C	196.5	14	45	19.0	22	6.0	150	6
KFM07C	173.5	15	185	9.5	29	4.0	150	6
			211	5.5	53	3.0	150	6

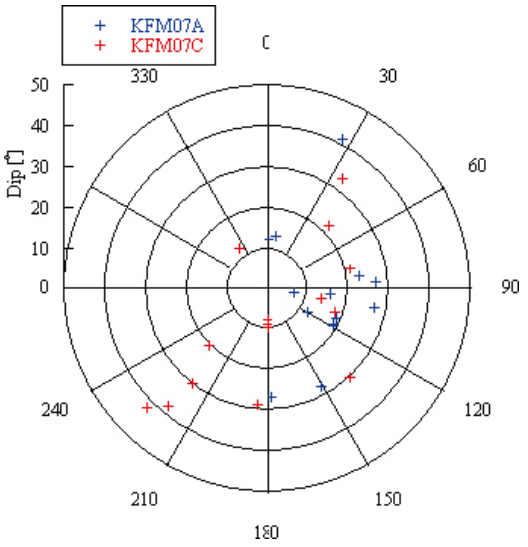

Figure 7-2. *Polar plot of the normals to the sub-horizontal fractures in boreholes KFM07A and KFM07C.*

7.2 Theory

When a borehole is inclined by more than 20° from any of the principal stress directions, only the radial ($\sigma_{\rho\rho}$) stress component, at the borehole wall, is principal (and equal to the applied pressure; /Hiramatsu and Oka 1968/). The two other principal stress components are inclined with respect to the tangential (θ) axis and the axial (Z) axis. The stress field around the borehole is given by:

$$\sigma_{\rho\rho} = (1 - r^2/\rho^2)(\sigma_{11} + \sigma_{22})/2 + (1 - 4r^2/\rho^2 + 3r^4/\rho^4)\begin{bmatrix} 1/2(\sigma_{11} - \sigma_{22})\cos 2\theta + \\ +\sigma_{12}\sin 2\theta \end{bmatrix} \quad (7\text{-}1)$$

$$\sigma_{\theta\theta} = (1 + r^2/\rho^2)(\sigma_{11} + \sigma_{22})/2 - (1 + 3r^4/\rho^4)[1/2(\sigma_{11} - \sigma_{22})\cos 2\theta + \sigma_{12}\sin 2\theta] \quad (7\text{-}2)$$

$$\sigma_{zz} = \sigma_{33} - 4\nu(r^2/\rho^2)[1/2(\sigma_{11} - \sigma_{22})\cos 2\theta + \sigma_{12}\sin 2\theta] \quad (7\text{-}3)$$

$$\sigma_{\theta z} = (1 + r^2/\rho^2)(\sigma_{23}\cos\theta - \sigma_{31}\sin\theta) \quad (7\text{-}4)$$

$$\sigma_{z\rho} = (1 - r^2/\rho^2)(\sigma_{31}\cos\theta + \sigma_{32}\sin\theta) \quad (7\text{-}5)$$

$$\sigma_{\rho\theta} = (1 + 2r^2/\rho^2 - 3r^4/\rho^4)[1/2(\sigma_{22} - \sigma_{11})\sin 2\theta + \sigma_{12}\cos 2\theta] \quad (7\text{-}6)$$

where σ_{11} to σ_{33} correspond to the far field stress components, ν is Poisson's ratio, θ is the angular coordinate, r is the borehole radius, and ρ is the radial distance taken from the centre of the borehole. Stresses at the borehole wall are obtained by setting ρ = r. Hence, when a pressure is applied in the borehole, this results in "en echelon" cracking (Figure 7-3). This was first discussed by /Daneshy 1973/ and since then, the geometry of en echelon fractures has been considered for constraining the far field stress state /Brudy and Zoback 1993, Peska and Zoback 1995/.

Equations (7-1) to (7-6) have been used for analysing results at the French Underground Research Laboratory for nuclear waste repository (the Bure site). The code assumes that five of the stress components (the minimum horizontal principal stress magnitude and its orientation together with the weight of overburden, given the vertical direction is assumed to be principal) are known. It determines for various incremental values of the far field maximum principal stress magnitude, the magnitude of the non-radial principal stress components, at the borehole wall, for incremental

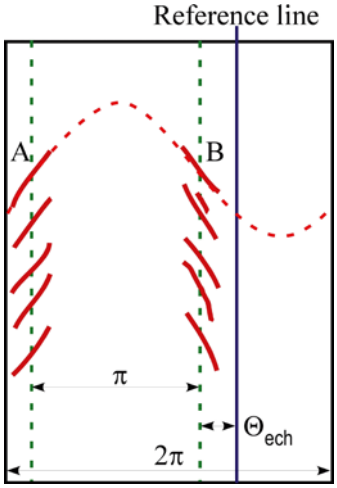

Figure 7-3. *Definition of "en echelon" fractures and identification of characteristic angles. Failure is assumed to occur at the diametrically opposed points B and A, when the normal stress to the plane, at this location, reaches the tensile strength of the rock (or that of a weakness plane).*

values of the angular coordinate θ of points distributed along the intersection of the plane of interest with the borehole wall (ρ = r in Equations (7-1) to (7-6)), according to the following equation:

$$(\sigma_{\min}, \sigma_{\max}) = 1/2\left[\sigma_{\theta\theta} + \sigma_{zz} \pm \sqrt{\left[(\sigma_{\theta\theta} - \sigma_{zz})^2 + \right] 4\sigma_{\theta z}{}^2}\right] \quad (7\text{-}7)$$

Thus, it is possible to determine the angular coordinate for which the minimum principal stress, at the borehole wall, reaches its minimum value. This is the angular coordinate where en echelon rupture is supposed to occur. In addition, it is verified that, for this angular coordinate, the normal stress supported by the observed failure plane reaches its smallest (negative) value and that the shear stress supported by the failure plane at this location is very close to zero. This ensures that the observed plane is indeed a plane of tensile rupture. Because the angular coordinate for which both conditions are satisfied simultaneously is very sensitive to the magnitude of the maximum horizontal principal stress, this is taken as a means to determine the maximum horizontal principal magnitude, independently of any consideration of pore pressure or tensile strength of the rock.

To determine whether the fracture was induced by shear, the angular coordinate of maximum effective shear stress [$\tau - \mu\ (\sigma_n - P_w)$] in the plane of the fracture may be investigated. If the angular coordinates correspond to the maximum effective shear, it would suggest that the rupture occurred by shear. The Coulomb criterion, as expressed in principal stress components is given by:

$$S_1(\sqrt{(1+\mu^2)} - \mu) - S_3(\sqrt{(1+\mu^2)} + \mu) + 2\mu P_w = K \quad (7\text{-}8)$$

where S_1 and S_1 are major and minor principal stress around the borehole, μ is the intrinsic friction coefficient, and P_w is the well pressure (which is either the test section pressure or the packer pressure depending on the location of the fracture). If the angular coordinate for which the effective shear is maximum coincides with the coordinate where the shear stress on the fracture plane reaches the Coulomb stress, the fracture is caused by shear failure.

7.3 Application to drill site 7

The application of the en echelon theory was made by using the two solutions obtained for the combined data set at drill site 7 (Section 6.6). The primary purpose of the study is to show the useful information that may be derived by the appearance of packer-induced fractures, but also to pinpoint which of the two possible solutions for drill site 7 that is preferable. To limit the number of calculations, Poisson's ratio was set to 0.25, and the intrinsic friction was set to 0.9. As illustrative examples, we use first Tests 14 and 15 in borehole KFM07C (i.e. the sleeve fracturing tests that also resulted in sub-horizontal or inclined fractures). In the following, the constrained solution from Section 6.6 is used:

Test 14, in borehole KFM07C

σ_h = 7.5 MPa; σ_v = 5.1 MPa; orientation of σ_H = 125°N; azimuth of the normal to the fracture plane = 45°N; dip of the normal to the fracture plane = 22° (Table 7-1); P_b = 33.5 MPa; borehole dip direction = 149.7°N; borehole dip = 5.8° (with respect to vertical direction), Poisson's ratio = 0.25; intrinsic friction coefficient = 0.9.

Test 15, in borehole KFM07C

σ_h = 7.3 MPa; σ_v = 4.5 MPa; orientation of σ_H = 125°N; azimuth of the normal to the fracture plane = 211°N; dip of the normal to the fracture plane = 53° (Table 7-1); P_b = 32.2 MPa; borehole dip direction = 150.0°N; borehole dip = 5.7° (with respect to vertical direction), Poisson's ratio = 0.25; intrinsic friction coefficient = 0.9.

The angular coordinates for the fracture in Test 14 were found to be –12 and 168° and –31 and 148° for Test 15, both expressed in the borehole frame of reference. Thereafter, the angular coordinate was investigated for values of σ_H ranging between 8 and 50 MPa. However, for the observed angular coordinate, the shear component is far from being null when the normal stress supported by the observed failure plane reaches its smallest value. This result indicates that the observed plane is not caused by tension.

To determine whether the fracture was induced by shear, the angular coordinate of maximum effective shear stress in the plane of the fracture was investigated. If the angular coordinate for which the effective shear is maximum coincides with the coordinate where the shear stress on the fracture plane reaches the Coulomb stress, the fracture is caused by shear failure.

For Test 14, the maximum effective shear occurs around the angular coordinate of 156–164° for σ_H magnitudes larger than about 14 MPa. The Coulomb stress equals the shear stress when σ_H reaches 13.7 MPa and the angular coordinate of 155°. Similarly, for Test 15, this is valid when σ_H reaches 13.2 MPa, which corresponds to an angular coordinate of 155°. Thus, the angular coordinates for Tests 14 and 15 are 13° and 7° from the anticipated. Moreover, the σ_H-magnitudes for Tests 14 and 15 are 1.5 and 1.8 MPa from the anticipated value of the constrained solution for drill site 7 (σ_H = 12.2 MPa and 11.4 MPa for Tests 14 and 15, respectively).

We continue with three more examples, that verify the constrained solution at larger depth, and choose Test 7 in KFM07C and Test 8 in KFM07A (two fractures with similar orientation).

Test 7, in borehole KFM07C

σ_h = 8.5 MPa; σ_v = 8.1 MPa; orientation of σ_H = 125°N; azimuth of the normal to the fracture plane = 35°N; dip of the normal to the fracture plane = 33° (Table 7-1); P_b = 8.5 MPa; borehole dip direction = 148.7°N; borehole dip = 5.7° (with respect to vertical direction), Poisson's ratio = 0.25; intrinsic friction coefficient = 0.9. These data give angular coordinates of –21 and 159° in the borehole frame of reference.

Test 8, in borehole KFM07A, fracture 96/16 (Table 7-1)

σ_h = 9.5 MPa; σ_v = 11.1 MPa; orientation of σ_H = 125°N; azimuth of the normal to the fracture plane = 96°N; dip of the normal to the fracture plane = 16°; P_b = 17.0 MPa; borehole dip direction = 274.9°N; borehole dip = 34.0° (with respect to vertical direction), Poisson's ratio = 0.25; intrinsic friction coefficient = 0.9. These data give angular coordinates of –27 and 153° in the borehole frame of reference.

Test 8, in borehole KFM07A, fracture 114/19 (Table 7-1)

σ_h = 9.5 MPa; σ_v = 11.1 MPa; orientation of σ_H = 125°N; azimuth of the normal to the fracture plane = 114°N; dip of the normal to the fracture plane = 19°; P_b = 17.0 MPa; borehole dip direction = 274.9°N; borehole dip = 34.0° (with respect to vertical direction), Poisson's ratio = 0.25; intrinsic friction coefficient = 0.9. These data give angular coordinates of –26 and 154° in the borehole frame of reference.

For Test 7 in borehole KFM07C, the maximum effective shear occurs around the angular coordinate of 158–159° and the Coulomb stress equals the shear stress when σ_H reaches 18.7 MPa (σ_H = 16.3 MPa in the constrained solution, i.e. angular error of 0–1° and 2.4 MPa). For Test 8, fracture 96/16, in borehole KFM07A, the maximum effective shear occurs around the angular coordinate of 131–137° for σ_H magnitudes larger than about 14.3 MPa. Pinpointing the solution gives σ_H = 15.3 MPa at the angular coordinate of 133°, which should be compared with σ_H = 16.7 MPa in the constrained solution and the angular coordinate of 153° (i.e. angular error of 20° and 1.4 MPa). For Test 8, fracture 114/19, in borehole KFM07A, the maximum effective shear occurs around the angular coordinate of 129–135° for σ_H magnitudes larger than about 14.3 MPa. Pinpointing the solution is less clear in this case compared with previous examples,

but for angular coordinates between 144 and 154°, σ_H varies between 16.5 and 23.6 MPa, which should be compared with σ_H = 16.7 MPa in the constrained solution and angular coordinate of 154°.

To investigate the sensitivity of the proposed theory, a simplified sensitivity analysis was undertaken. With simplified, we mean that one parameter was varied at a time, as compared with a more thorough investigation that involves simultaneous variation of multiple parameters. The primary reason for this decision is that the program at this stage is not a strict inversion program but rather a tool for investigating a domain of solutions. A complete sensitivity analysis would therefore involve considerable time. Yet, a simplified analysis gives a hint of which parameters that have the strongest influence on the result.

The sensitivity analysis involved variations of σ_h with ± 0.3 MPa, σ_v with ± 0.3 MPa, breakdown pressure P_b with ± 1.5 MPa, orientation of σ_H with ± 3°, dip and azimuth of the normal to the fracture plane with ± 3°, dip and azimuth of the well with ± 2°, Poisson's ratio ± 0.04°, and of the intrinsic friction coefficient with ± 0.2.

The results are presented in Figure 7-4 to Figure 7-6 for Tests 7, 14, and 15 in borehole KFM07C and generally indicate that, for the specified ranges of the investigated parameter, the theory is only moderately sensitive. The largest variation of angular coordinate is observed for Tests 14 and 15 with 17° and 15°, respectively, whereas it is only 5° for Test 7. The azimuth of the fracture is the most difficult parameter to pinpoint and is a result of a geometrical problem independent upon measurement method. In a 76 mm borehole, the perimeter is 239 mm, which corresponds to 360°. Hence, if the azimuth is pinpointed 5–10 mm off its true value (which is quite possible for a sub-horizontal fracture), the corresponding error is as large as 8–15°.

Concerning the σ_H-magnitude, Test 7 displays the largest scatter (10.6 MPa), whereas the scatter in σ_H-magnitude for Tests 14 and 15 are considerably smaller (1.0 and 0.9 MPa, respectively). Conclusively, the proposed methodology indicates that the precision of the σ_H-magnitude and the angular coordinate generally is high. The exception is Test 7, which is sensitive to variations in the intrinsic friction coefficient. On the other hand, the accuracy of the methodology is only moderate.

The analysis is not clear as to which parameters that control the solution. The results for Test 7 are primarily sensitive, in decreasing order or importance, to variations of intrinsic friction coefficient, Poisson's ratio and fracture azimuth. Correspondingly, Test 14 is mostly sensitive to variations in Poisson's ratio, orientation of σ_H, intrinsic friction coefficient, σ_v, and borehole azimuth. Finally, Test 15 is primarily sensitive to variations in orientation of σ_H, borehole azimuth, P_b, and intrinsic friction coefficient.

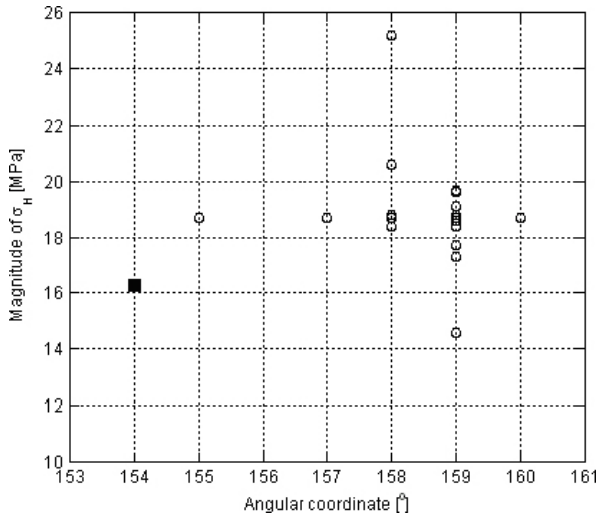

Figure 7-4. *Results from simplified sensitivity analysis for Test 7 in borehole KFM07C. The results from varying the involved parameters are displayed with empty circles whereas the anticipated result is marked with a filled square.*

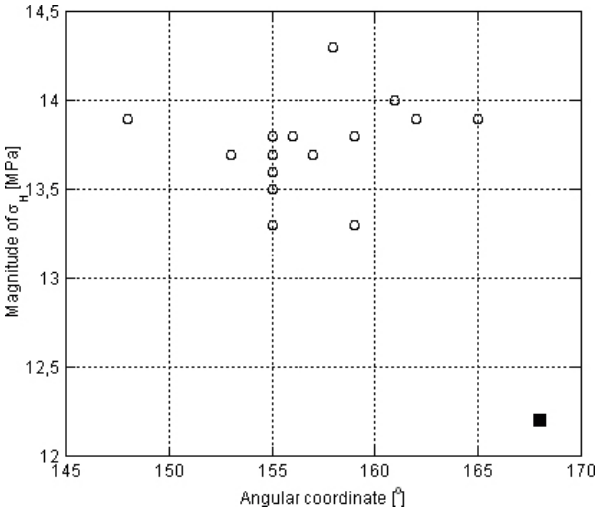

Figure 7-5. *Results from simplified sensitivity analysis for Test 14 in borehole KFM07C. The results from varying the involved parameters are displayed with empty circles whereas the anticipated result is marked with a filled square.*

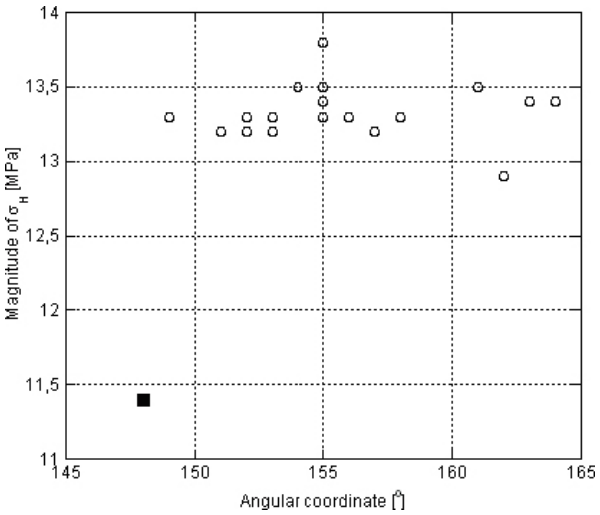

Figure 7-6. *Results from simplified sensitivity analysis for Test 15 in borehole KFM07C. The results from varying the involved parameters are displayed with empty circles whereas the anticipated result is marked with a filled square.*

Given the many parameters involved in this analysis, and based on the results of the simplified sensitivity analysis, it is considered that this observed agreement between calculated and anticipated angular coordinates and σ_H-magnitudes demonstrates the validity of the methodology and of the constrained solution at these depths. The values of the different parameters can be slightly varied so as to fit precisely the observed angles or σ_H-magnitude. But given this result combines eight different parameters (the six components of the stress field, the fracture orientation and the well orientation), it would have been impossible to generate from a random process a set of 8 parameters that would fit simultaneously the three independent equations that characterize the normal stress supported by the sub horizontal fracture plane, the critical Coulomb shear failure and the shear component supported at the wellbore by the observed fracture plane. Hence, we consider that the stress field at drill site 7 is well validated and that the constrained solution is preferable. This result further suggests that a new method may be applied for solving unresolved stress components, especially for the case when only data from single and inclined wells are available. This proposition is however outside the scope of the present work.

8 Discussion and conclusions

8.1 General

Hydraulic rock stress measurements were performed in boreholes KFM09A (16 tests), KFM09B (18 tests), KFM08A (23 tests), KFM07A (13 tests), and KFM07C (15 tests) at the Forsmark candidate area, Sweden. The measurements were carried out in four separate campaigns and a total of 87 hydraulic fracturing tests and hydraulic tests on pre-existing fractures were conducted between the 6th of June and the 21th of October, 2006.

Despite the pronounced difficulties in collecting unambiguous data in the various boreholes, the state of stress could be determined in all investigated boreholes. All obtained solutions are presented in Figure 8-1 to Figure 8-6 (without confidence intervals). The majority of the inversion results indicates in the interval 150–750 mvd that σ_H, σ_h, and the orientation of σ_H are in the ranges 12–25 MPa, 6–13 MPa, and 118–134°N, respectively.

The stress determination for drill site 7 is the most reliable in terms of resolution of the stress field. The solution was also verified by the packer-induced fractures. To our knowledge, this is the first time anyone has produced an independent check on the validity of a stress determination and this is regarded as a unique aspect of quality assurance procedure.

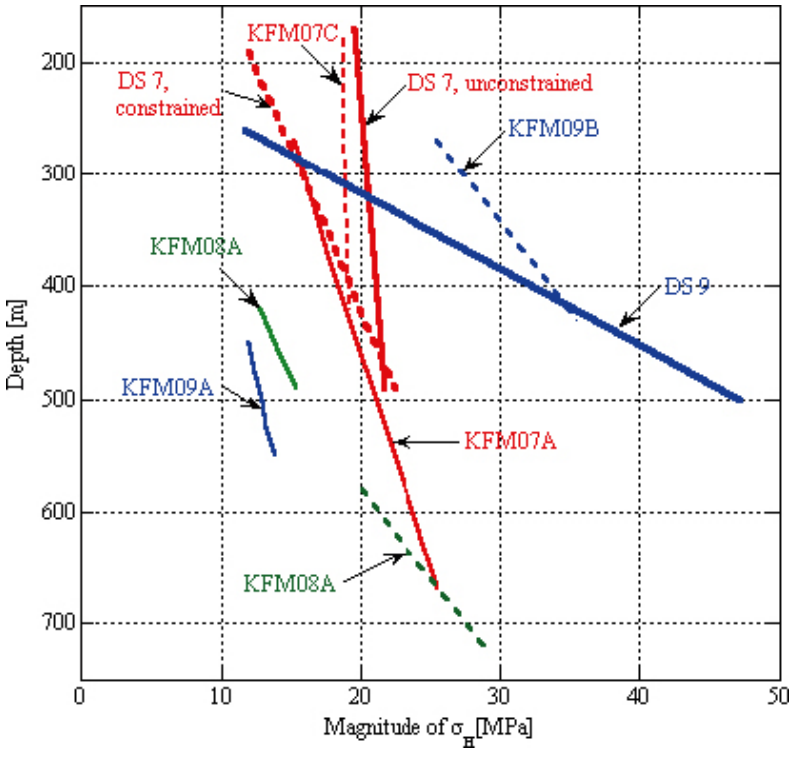

Figure 8-1. *Summary plot of solutions for individual boreholes and drill sites with respect to magnitude of maximum horizontal stress.*

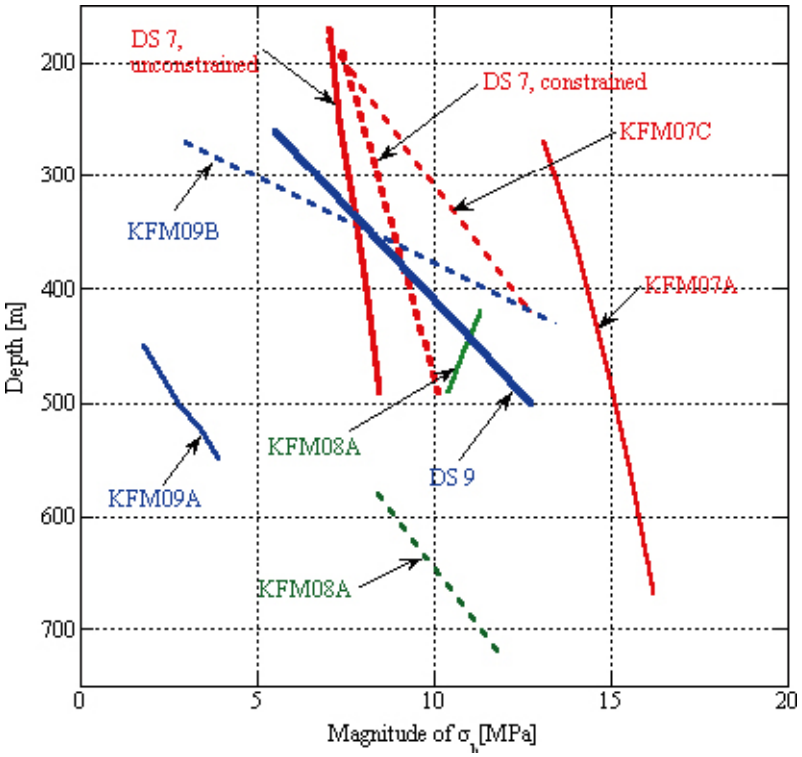

Figure 8-2. *Summary plot of solutions for individual boreholes and drill sites with respect to magnitude of minimum horizontal stress.*

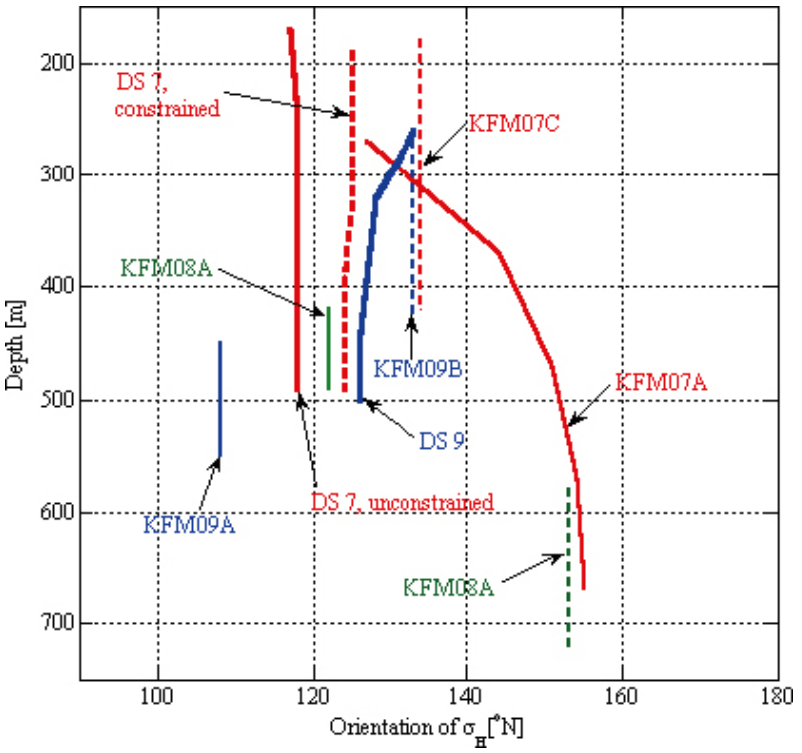

Figure 8-3. *Summary plot of solutions for individual boreholes and drill sites with respect to orientation of magnitude of maximum horizontal stress.*

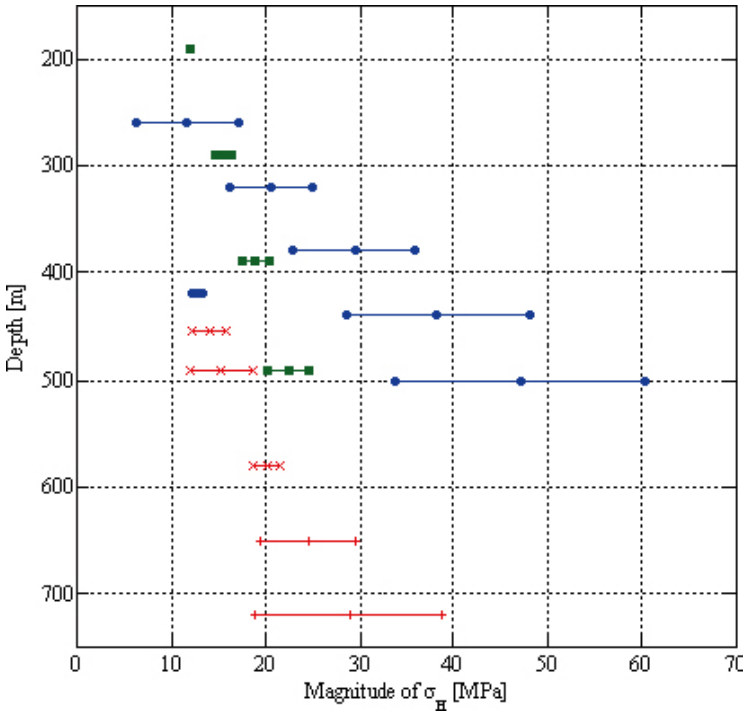

Figure 8-4. *Summary plot of best solutions with respect to magnitude of maximum horizontal stress for drill site 7 (green line and green filled squares), 8 (red line and red crosses; red line and red plus signs), and 9 (blue line and blue filled circles). The results for each drill site are presented with central value and 90% confidence level.*

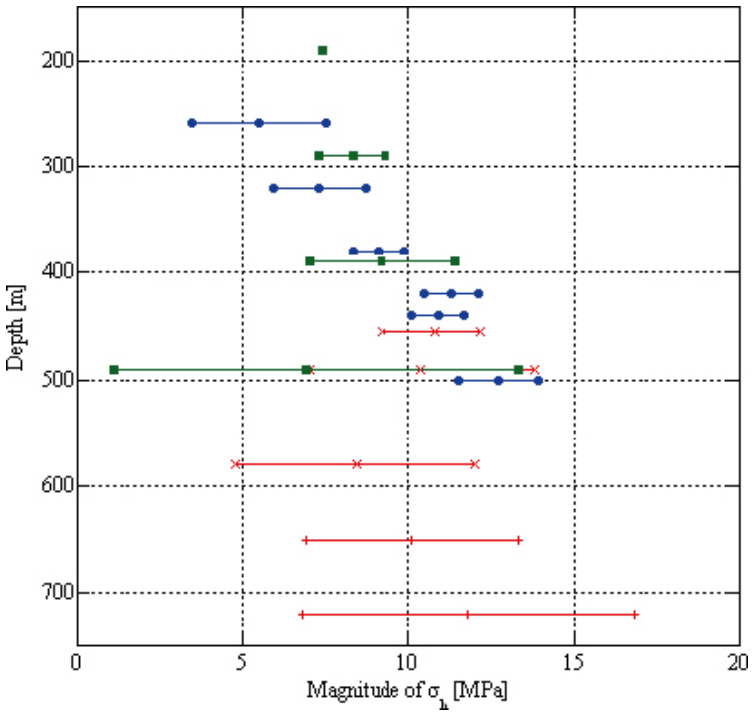

Figure 8-5. *Summary plot of best solutions with respect to magnitude of minimum horizontal stress for drill site 7 (green line and green filled squares), 8 (red line and red crosses; red line and red plus signs), and 9 (blue line and blue filled circles). The results for each drill site are presented with central value and 90% confidence level.*

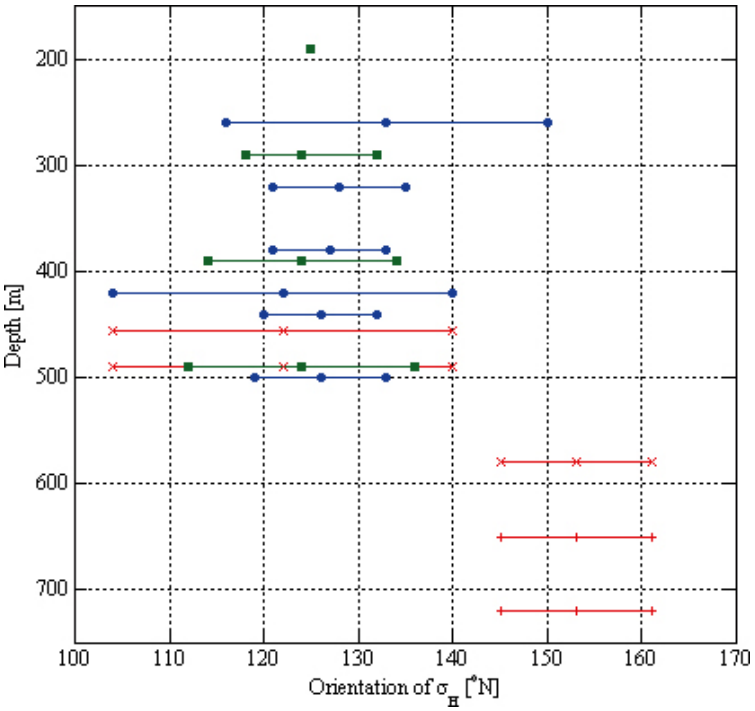

Figure 8-6. *Summary plot of best solutions with respect to orientation of maximum horizontal stress for drill site 7 (green line and green filled squares), 8 (red line and red crosses; red line and red plus signs), and 9 (blue line and blue filled circles). The results for each drill site are presented with central value and 90% confidence level.*

8.2 Uncertainties in stress determination results

The uncertainties in the stress determination results may be divided into two categories; those associated with the collected data used for stress determination and those associated with the parameterization/mathematical model used to describe the stress field.

8.2.1 Uncertainties associated with collected data

The uncertainties in collected data are visualized in Appendices I to III and for e.g. normal stresses it involves an uncertainty of a few bars. These uncertainties are completely normal in hydraulic stress measurement campaigns. However, of the 87 tests conducted, only 45 involve unambiguous data, i.e. have a reliable normal stress and a well defined fracture geometry (but only nine of these exhibit one single fracture plane). Note that the stress determinations are based on almost entirely unambiguous data (the exception is borehole KFM08A). The reasons for the ambiguity in the data are described below in decreasing order or importance.

The primary reason for the reduced success rate was the strong fracture sealing that prevailed at the Forsmark site, combined with strongly inclined boreholes. Early on in the injection testing, it became clear that sub-horizontal fractures were induced at pressures just moderately higher than the corresponding theoretical vertical stress at the location in question. Hence, unless the chosen pre-existing fracture could be re-activated before reaching the level of the theoretical vertical stress (a few bars), sub-horizontal fractures would be induced. This implies that a major constraint for injection testing prevailed and that sub-horizontal fractures were induced in all cases where the fracture did not re-activate before reaching this critical pressure. The physical explanation for these fractures is not yet fully understood (although a successful interpretation methodology is presented in Chapter 7). Often, these tests also resulted in a poor flow-back after completed testing, which in many cases is explained by that the fractures are located underneath

the packer elements. Although the sub-horizontal fractures significantly reduced the number of unambiguous tests, they contain very useful information as described in Chapter 7.

Two additional problems existed during the field measurements; noise in the HTPF tool and tool displacement during testing.

A noise in the HTPF tool was outlined in the quality procedure and consisted of a systematic magnetic discrepancy above about 250 m depth at the Forsmark site. This discrepancy is due to a 50 Hz electrical noise that is collected by our HTPF tool resulting from ground currents. Hence, for tests conducted above 250 m, collected data had to be given special attention.

The tool displacement during injection testing appeared in the deepest tests in borehole KFM08A (Appendix II; but also in borehole KLX12A /Ask et al. 2007/) as a result of pressure build-up behind the downhole tool. The reason for this pressure build-up is not fully understood but it is probably a combination of several factors. First of all, the bedrock is completely impervious (i.e. all pre-existing fractures are sealed) and pressure cannot escape if trapped below the tool. Hence, already the inflation of the packer would increase the pressure behind the tool, although not to such a degree that the tool would move. During injection into the test section, additional pressure build-up behind the tool could result from: (i) short-circuiting through fractures. Because the well is inclined about 60° (at the collaring) from the horizontal and the dominating fracture sets are sub-vertical and sub-horizontal, there is a possibility for the injected water to pass through these fractures and below the tool; and (ii) leakage through the packer. A common observation at the Forsmark site is spiral grooves on the cores and borehole walls. Hence, the packers may not have sealed the test section properly, allowing water to enter the well section behind the tool.

8.2.2 Uncertainties associated with the parameterization and determination of the stress field

As previously noted, the difficulties during data collection in the various boreholes reduced the number of unambiguous data. Yet, the state of stress could be determined in all investigated boreholes, although the resolution of the stress field is not always optimal. An exception is drill site 7 (Appendix I), which involved both true hydraulic fracturing data and hydraulic tests on pre-existing fractures.

Because the notion of rock stress is a concept of continuum mechanics, it is necessary to identify volumes where the continuity hypothesis is verified. In other words, bodies that may be approximated by a continuum need to be identified. Moreover, because the stress at a specific point involves six components, the determination of the regional stress field includes determination of six functions for the domain under consideration. This requires integrating measurements conducted at points that sample properly the continuum volume of interest.

In the methodology of Vattenfall Power Consultant AB, the first interpretation of the continuity hypothesis is given by the reconnaissance log with the HTPF tool (Appendices I to III). The first evaluation provided by the HTPF tool is also used for selection of suitable test sections.

Given the non-linear and scattered stress profiles derived from previous overcoring stress data /e.g. Sjöberg et al. 2005/, application of a standard profiling approach was believed to be hampered by the non-linearity. Instead, the methodology chosen for the tests at Forsmark involved the cluster approach /e.g. Ask and Cornet 2006, 2007/. This implies that measurements are grouped in clusters with the aim of collecting a sufficient number of HF and HTPF data in a small enough volume to permit complete stress determination without considering stress gradients. Such an approach would result in a minimum of parameters at each cluster but also have the benefit of that the continuity hypothesis would be more easily evaluated by comparisons of full tensors from multiple clusters along a borehole.

However, although a first interpretation of the continuity aspect was available and although a new and more robust testing methodology was employed, the stress determinations for the

various boreholes were not optimal. Obviously, the large amount of ambiguous data does not help in this respect. In many cases, the cluster methodology for testing could not be followed by cluster methodology in interpretation because there were not a sufficient number of unambiguous tests to enable cluster interpretation. In fact, a completely successful cluster methodology was only made in borehole KLX12A /Ask et al. 2007/. The cluster methodology was employed also in borehole KFM08A (Appendix II), but, regrettably, the solution had to be based on partly ambiguous data when presently disregarding information from packer-induced fractures. It is the authors' opinion that much work could still be accomplished in this respect.

Given that the cluster approach could not be utilized, profiling was employed. This implies that stresses are solved as a function of depth, involving stress gradients. However, it became clear that the stress field at the Forsmark site is non-linear, which can be visualized simply by investigating the variation of the normal stress with depth of any fracture of given orientation. During stress inversion, the non-linear stress distribution is directly visualized by the poor resolution of the unknown parameters and by convergence problems. In other words, the interpolation of stress data during profiling over long depth intervals is not optimal. The non-linearity is especially pronounced at drill site 8 (Appendix II), but is believed to cause dispersion at all drill sites. With this respect, the cluster methodology /Ask and Cornet 2006, 2007/ for data collection is indeed favourable, but it failed in the absence of sufficient number of unambiguous data in each cluster. However, if the packer-induced fractures would be used, the cluster approach could most likely be employed.

Moreover, as displayed by the HTPF Mosnier logs, the electrical resistivity of the bedrock is strongly varying in the investigated boreholes, which is correlated to the material properties. For example, in the high-resistivity zone at about 200 mvd in borehole KFM07C, the tensile strength was as high as 21.6 MPa (Appendix I). Clearly, if this would be the overall tensile strength at the Forsmark site, we would not encounter sub-horizontal fractures that develop when the injection or packer pressure just barely exceeds the vertical stress. Generally during the cluster data collection, it was clear that the pressure required for inducement of sub-horizontal fractures increased when the electrical resistivity, as displayed by the HTPF Mosnier tool, increased.

8.3 Stress variation within the Forsmark site

As noted above, the stress field variation versus depth at the Forsmark site is non-linear. This non-linear variation is also confirmed by the vast amount of overcoring data collected at the site /e.g. Lindfors et al. 2007/. To get orders of magnitude of lateral stress variations, the various solutions from drill sites 7, 8, and 9 were compared.

The parameter that has proven most difficult to constrain is the magnitude of maximum horizontal stress, which is normally the case at all sites independent of measurement method. As a result, this parameter also displays the largest scatter between the various solutions at the three drill sites.

When comparing the results for the magnitude of σ_H for drill sites 7 and 9, the differences are significant. Drill sites 7 and 9 display the following general trends for maximum horizontal stress (z starts from 200 mvd):

DS 7:

$\sigma_H = 12.4 + 0.035*z$, where z is the vertical depth

DS 9:

$\sigma_H = 3.0 + 0.148*z$, where z is the vertical depth

Keeping in mind that drill sites 7 and 9 are only located 400 m apart, and that borehole KFM07A extends below drill site 9, raises a question about these results. In principle, there are two options for this result. The first is that the solution for drill site 9 is not optimal, which is also indicated by the relatively pronounced standard deviations for σ_H maximum for the entire interval between 260 and 500 mvd. Interestingly, when excluding results where the standard deviation is larger than 3 MPa for σ_H (from about 350 mvd and below), the solution for drill site 9 falls within the verified solution of drill site 7 at the 90% confidence level. The second option is influence of geology. However, because the data from borehole KFM09A do not significantly affect the magnitude of σ_H in the joint solution of boreholes KFM09A and KFM09B, we interpret the differences in σ_H–magnitude between drill site 7 and 9 as a result of a non-optimal solution for drill site 9.

If we then turn to drill site 8, the solution for the deeper level (580–720 mvd) shows a close resemblance with the extension of the verified, constrained solution at drill site 7 that is valid between 190 and 490 mvd. Thus, this suggests, if the data in these two solutions belong to the same continuum, that no lateral stress gradient exists from drill site 7 towards drill site 8, i.e. towards North.

The solution for the interval 420–490 at drill site 8, on the other hand, displays a σ_H–magnitude about 5 MPa lower, but with a similar vertical gradient. Assuming that the data in these two solutions belong to the same continuum would suggest the following lateral stress gradient, moving from drill site 7 towards drill site 8 (i.e. North):

$\alpha_H = 0.014 \cdot x_{H,N}$, where $x_{H,N}$ is the lateral distance from DS 7 towards North.

However, note that the reasoning concerning lateral gradients between drill sites is only meaningful if the data indeed belong to the same continuum. If not, the comparison becomes completely pointless. Only careful site reconnaissance, which is outside the scope of this study, may help answer if lateral gradients of maximum horizontal stress exist or not.

Minimum horizontal stress magnitudes also display some scatter when comparing the various solutions for the three drill sites, but it is considerably less pronounced compared with maximum horizontal stress magnitude. Common for all solutions is that the magnitude reaches about 10–13 MPa at 500 mvd. In fact, the equation (starting at z = 0):

$\sigma_h = 4.6 + 0.0135 \cdot z$, where z is the vertical depth

fits almost all solutions obtained for the three sites at the 90% confidence level in the interval 190 to 720 mvd.

This result speaks in favour of that no or small lateral variations of the magnitude of σ_h exist at the Forsmark site. Possibly, the magnitude of σ_h is smaller at shallow depth (above 400 mvd) at drill site 9, compared with those at drill sites 7 and 8.

As opposed to stress magnitudes, the stress determinations at the various sites are very consistent with respect to orientation of maximum horizontal stress. The only outlier is the deeper solution in borehole KFM08A, which indicates an orientation of 153 ± 4°N. All other orientations fall within the interval 122–133°N, and the maximum standard deviation in the individual solutions reaches 9°, but the average standard deviation is about 4°. This may be compared with the two true hydraulic fracturing tests in borehole KFM07C, indicating about 125°N. Hence, there is no evidence that variations in stress orientation exist between the three drill sites, apart from potential local variations.

Regarding the vertical stress component, the results suggest that it closely resembles the theoretical weight of the overburden of about 0.026 MPa/m. Some variability may naturally occur near local heterogeneities.

8.4 The estimated state of stress at repository depth at the Forsmark site

The outlined non-linear stress variation combined with the multiple fractures observed in the various tested interval is a severe limitation to integration of data over large volumes. However, given the satisfactory results obtained at drill site 7, thanks to the combination of a vertical well with an inclined well, it seems that, for the Forsmark site, only a combination of true hydraulic fractures in vertical wells together with nearby HTPF tests in inclined wells provides a sound methodology for a reliable stress determination. However, an even more reliable method is proposed by integrating simultaneously, on limited rock volumes, HF tests, HTPF tests and analysis of packer induced fractures. Further, the combination of sleeve fracturing with hydraulic testing has revealed a powerful method to develop axial fractures in vertical wells. This suggests that an optimum stress determination procedure could be proposed in order to determine, with the existing HTPF tool, the complete stress tensor at the scale of observed stress heterogeneity. It requires a combination of one vertical well and one inclined well within the volume of interest.

Because the best solution at repository depth at the Forsmark site corresponds to that of drill site 7, this solution is used for expressing the state of stress at repository depth:

400 mvd	**500 mvd**
$\sigma_h = 9.3 \pm 1.1$ MPa	$\sigma_h = 10.2 \pm 1.6$ MPa
$\sigma_H = 19.2 \pm 0.7$ MPa	$\sigma_H = 22.7 \pm 1.1$ MPa
$\sigma_v = 10.4$ MPa	$\sigma_v = 13.0$ MPa
Orientation of $\sigma_H = 124 \pm 6°$N	Orientation of $\sigma_H = 124 \pm 6°$N

Because of local disturbances, such as fractures and fracture zones, larger σ_H-magnitudes may be observed, implying that it is smaller in adjacent domains, in order to maintain equilibrium, when integration is made on larger rock mass volumes. As a result of this, an important question to discuss is the origin of the stress heterogeneity, e.g. a block effect, water circulation and correlated alteration, or temperature disturbances. This is though outside the scope of the present report.

9 References

Aamodt R L, Kuriyagawa M, 1981. Measurements of instantaneous shut-in pressure in crystalline rock. *Proc. Workshop on Hydraulic Fracture Stress Measurements* (Eds. Zoback MD, Haimson BC), Monterey, USA. USGS, pp. 139–42.

Ask D, 2004. New developments of the Integrated Stress Determination Method and application to the Äspö Hard Rock Laboratory, Sweden. PhD Thesis, Dept. Land and Water Resources Engineering, Royal Institute of Technology (KTH).

Ask D, 2006a. Manual for hydraulic rock stress measurements, version 1.32. Internal report, Vattenfall Power Consultant AB.

Ask D, 2006b. Quality operating procedures, hydraulic rock stress measurements, version 3. Internal report, Vattenfall Power Consultant AB.

Ask D, Cornet F H, 2006. Strategy for in situ rock stress measurements. *Proc. 4th Asian Rock Mechanics Symposium* (Eds. Leung CF, Zhou YX), Singapore. B & JO Enterprice, pp. 99–107.

Ask D, Cornet F H, 2007. The integrated stress determination method and suggested measurement strategy. *ISRM News Journal*, 3:9, pp. 24–27.

Ask D, Cornet F H, Fontbonne F, Brunet C, 2007. Oskarshamn site investigation. Stress measurements with hydraulic methods in borehole KLX12A. SKB P-07-232. Svensk Kärnbränslehantering AB.

Bredehoeft J D, Wolff R D, Keys W S, Schuter E, 1976. Hydraulic fracturing to determine the regional stress field, Piceance Basin, Colorado. *Bull.Geol. Soc. Am.*, 87, pp. 250–8.

Brudy M, Zoback M D, 1993. Compressive and tensile failure of boreholes arbitrary inclined to principal stress axis: application to the KTB boreholes, Germany. *Int. J. Rock. Mech. Min. Sci.*, 30, pp. 1035–8.

Cornet F H, 1993. The HTPF and the integrated stress determination methods. *Comprehensive Rock Engineering*, 3, (J. Hudson, Ed.). Pergamon Press, Oxford, pp. 413–432.

Cornet F H, Valette B, 1984. In situ determination from hydraulic injection test data. *J. Geophys. Res.*, 89, pp. 11527–37.

Cornet F H, Li L, Hulin J P, Ippolito I, Kurowski P, 2003. The hydromechanical behaviour of a fracture: an in situ experimental case study. *Int. J. Rock Mech. Min. Sci.*, 40, pp. 1257–70.

Daneshy A A, 1973. A study of inclined hydraulic fractures. *Proc. 47th SPE Annual Fall Meeting*, San Antonio Texas, Soc. Petrol. Eng, pp. 346–57.

Desroches J, Kurkjian A, 1999. Applications of wireline stress measurements, SPE 48960. *SPE Reserv. Eval. Eng.* 2(5), pp. 451–61.

Enever J, Chopra P N, 1989. Experience with hydraulic fracturing stress measurements in granites. *Proc. Int. Conf. On Rock Stress and Rock Stress Measurements* (Ed. Stephansson O), Stockholm. Centek Publisher, Luleå, pp. 411–20.

Haimson B C, Cornet F H, 2003. ISRM Suggested Methods for rock stress estimation – Part 3: hydraulic fracturing (HF) and/or hydraulic testing of pre-existing fractures (HTPF). *Int. J. Rock Mech. Min. Sci.*, 40, pp. 1011–20.

Hayashi K, Haimson B C, 1991. Characteristics of shut-in curves in hydraulic fracturing stress measurements and determination of in situ minimum compressive stress. *J. Geophys. Res.*, 96, pp. 18311–21.

Hiramatsu Y, Oka Y, 1968. Determination of the stress in rock unaffected by boreholes of drifts, from measured strains or deformations. *Int. J. Rock Mech. Min. Sci.*, 5, pp. 337–353.

Ito T, Evans K, Kawai K, Hayashi K, 1999. Hydraulic fracturing reopening pressure and the estimation of maximum horizontal stress. *Int. J. Rock Mech. & Geomech. Abstr.*, 36, pp. 811–26.

Klee G, Rummel F, 2004. Rock stress measurements with hydraulic fracturing and hydraulic testing of pre-existing fractures in borehole nos. KFM01A, KFM01B, KFM02A and KFM04A. Results of in situ tests. SKB P-04-311. Svensk Kärnbränslehantering AB.

Lindfors U, Berg S, Perman F, 2007. Forsmark site investigation. Overcoring rock stress measurements in borehole KFM02B. SKB P-07-205. Svensk Kärnbränslehantering AB.

Mosnier J, Cornet F H, 1989. Apparatus to provide an image of the wall of a borehole during hydraulic fracturing experiments. *Proc. 4th Europ. Gepth. Update – Int- Sem.,* Florence, Kluwer, Dordrecht, pp. 205–12.

Mosnier J, 1982. Détection électric des fractures naturelles ou artificielles dans un forage. *Ann. Géophs.,* 38, pp. 537–40.

Peska P, Zoback M D, 1995. Compressive and tensile failure of inclined well bores and determination of in situ stress and rock strength. *J. Geohys. Res.*, 100, pp. 12791–811.

Ratigan J L, 1992. The use of the fracture reopening pressure in hydraulic fracturing stress measurements. *Rock Mech. Rock Eng.*, 25, pp. 125–136.

Rutqvist J, 1995. Coupled stress-flow properties of rock joints from hydraulic field testing. Doctoral Thesis, Royal Institute of Technology, Stockholm.

Rutqvist J, Tsang C-F, Stephansson O, 2000. Uncertainty in the principal stress estimated from hydraulic fracturing measurements due to the presence of the induced fracture. *Int. J. Rock Mech. & Geomech. Abstr.*, 37, pp. 107–20.

Sjöberg J, Lindfors U, Perman F, Ask D, 2005. Evaluation of the state of stress at the Forsmark site. SKB R-05-35. Svensk Kärnbränslehantering AB.

Stephansson O, 1983a. Rock stress measurements by sleeve fracturing. *Proc. 5th Cong. Int. Soc. Rock Mech.,* Melbourne, Balkema, Rotterdam, pp. F129–37.

Stephansson O, 1983b. Sleeve fracturing for rock stress measurements in boreholes. *Proc. Int. Symp. Essais en Place, In Situ Testing,* Paris, Vol. 2, pp. 571–8.

Tarantola A, Valette B, 1982. Generalized non-linear inverse problem solved using the least square criterion. *Rev. Geophys. Space Phys.*, 20, pp. 219–32.

Zoback M D, Barton C A, Brudy M, Castillo D A, Finkbeiner T, Grollimund B R, Moos D B, Peska P, Ward C D, Wiprut D J, 2003. Determination of stress orientation and magnitude in deep wells. *Int. J. Rock. Mech. Min. Sci.*, 40, pp. 1049–76.

APPENDIX I

FORSMARK SITE INVESTIGATION. COLLECTION OF HYDRAULIC ROCK STRESS DATA IN BOREHOLES KFM07A AND KFM07C

Forsmark site investigation

Collection of hydraulic rock stress data in boreholes KFM07A and KFM07C

Daniel Ask, Vattenfall Power Consultant AB

Francois Cornet, Institut de Physique du Globe de Paris

Frederic Fontbonne, Geostress Co.

Christophe Brunet, Institut de Physique du Globe de Paris

November, 2007

SUMMARY

Hydraulic rock stress measurements were performed in boreholes KFM07A (13 tests) and KFM07C (15 tests) at the Forsmark candidate area, Sweden. The measurements were carried out in a single campaign and a total of 28 hydraulic fracturing tests and hydraulic tests on pre-existing fractures were conducted between the 2nd to the 21th of October, 2006.

The work involved cooperation between Vattenfall Power Consultant AB (Contractor), Institut de Physique du Globe de Paris (IPGP), and Geostress Co (both Sub-contractors). Vattenfall Power Consultant AB provided an MKW wireline system and field personnel, whereas IPGP supplied downhole equipment, data acquisition system, and field personnel. Finally, Geostress contributed with field personnel.

This document includes a detailed description of the observations made in the field, and results.

Of the 28 tests conducted at drill site 7, only 18 involve completely unambiguous data, i.e. have a reliable normal stress and a well defined fracture geometry (although only two of these tests involves a single fracture geometry). The success rate of testing was hence unusually low for this type of hydraulic stress measurement equipment, especially for KFM07A. The primary reason for the reduced success rate was that sub-horizontal fractures were induced. These fractures were created when the pressure in the test section was just moderately larger (a few bars) than the theoretical weight of the overburden rock mass. This implies that a major constraint for injection testing prevailed and that sub-horizontal fractures were induced in all cases where the fracture did not re-activate before reaching this critical pressure. The physical explanation for these fractures is yet to be determined, but the relatively moderate testing depth in combination with the inclined borehole KFM07A (about 59^o from the horizontal plane and flattening out to c 46^o towards the borehole bottom) is probably not favourable for hydraulic stress measurements. To our surprise however, the fractures also appear in the sub-vertical borehole KFM07C, although not to the same extent. We would like to emphasize that the observed sub-horizontal fractures contain very useful information. If a failure criterion for these fractures can be derived, they will contribute much to the knowledge of the present state of stress at the Forsmark site.

Two attempts to induce axial fracture with sleeve fracturing technique (Stephansson, 1983a;b) were attempted in the 175 - 200 m depth range in borehole KFM07C. Both of these tests were successful in that respect and indicate an average orientation of σ_H of about 127^{o}N.

SAMMANFATTNING

Hydrauliska bergspänningsmätningar har utförts i borrhål KFM07A (13 tester) och KFM07C (15 tester) i Forsmark. Totalt gjordes således 28 tester i en sammanhängande kampanj mellan den 2:a och 21:a oktober, 2006.

Aktiviteten var ett samarbetsprojekt mellan Vattenfall Power Consultant AB (huvudkonsult), Institute de Physique du Globe de Paris (IPGP), och Geostress Co (båda dessa organisationer underkonsulter). Vattenfall Power Consultant AB tillhandahöll ett MKW wireline-system samt fältpersonal, IPGP stod för borrhålsutrustning, datainsamlingssystem och fältpersonal, medan Geostress bidrog med fältpersonal.

Detta dokument innehåller en detaljerad beskrivning av fältobservationer och resultat.

Av de 28 utförda injektionstesterna vid borrplats 7 är endast 18 helt otvetydiga, dvs uppvisar tillförlitlig normalspänning och välbestämd sprickorientering (men bara två av dessa involverar en enskild sprickgeometri). Andelen lyckade tester är därför lägre än normalt för metoden och var en följd av att sub-horisontella sprickor skapats vid många av testerna. Dessa sprickor inducerades redan vid ett pålagt tryck som endast måttligt överstigeg den teoretiska vertikalspänningen och innebar därför en stark begränsning av metodens möjligheter. De bakomliggande fysikaliska orsakerna till uppkomsten av dessa sprickor återstår att förklara, men de relativt måttliga testdjupen i kombination med borrhålet KFM07As relativt stora lutning (ca 59^o från horisontalplanet i ytan som sedan flackar ut mot ca 46^o mot borrhålets botten) är sannolikt inte fördelaktiga för denna typ av mätningar. Vi fann dock överraskande nog dessa sprickor även i det sub-vertikala borrhålet KFM07C, om än inte i samma omfattning. Vi vill betona att om ett brottkriterium för dessa sprickor kan härledas, kan en systematisk analys av den datamängd som dessa sprickor representerar sannolikt ge ett mycket värdefullt bidrag till beskrivningen av det rådande spänningsfältet i Forsmark.

Två försök att inducera axiella sprickor med membranspräckningsteknik (Stephansson, 1983a; b) utfördes i borrhål KFM07C med lyckat resultat. De två axiella sprickorna indikerar en orientering av σ_H omkring 127^oN.

Contents

1 Collected data in boreholes KFM07A and KFM07C

The collected data comprise numerous parameters for determination of the stress field but also for verification of the data recording quality, which are described below.

1.1 Fracture orientation and groundwater data

The three alternative means of determining fracture orientations available in this activity are described in Chapter 4.2.5. Regarding fracture orientation by using the Mosnier tool, the reliability of the fracture orientation determination rests on three features:

- The proper recording of all parameters that characterize the position of the tool in the well (borehole length, and measurements from 3 magnetometers and 2 inclinometers).
- The good understanding of tool manufacturing and its consistency with data processing routines.
- The repeatability of orientations during comparisons of multiple scans of the same fracture.

There are a few independent means to verify that the overall data recording has been successful. One involves readings of orientation devices as the tool is lowered and hoisted in the borehole. The values of the magnetic field inclination, as determined from the magnetometers, offer a completely independent check on the digitization procedure used for the downhole data acquisition and surface data recording. The results from the magnetometers and inclinometers may also be used to verify reproducibility. This involves comparisons of derived fracture orientations with those of the BIPS, but more importantly, we compare our determination of magnetic field inclination (angle with vertical) with the Uppsala magnetic field observatory (Appendices 1 and 2). For boreholes KFM07A and KFM07C, below about 225 mvd, we are always within 3^o and 2°, respectively, with the Uppsala observatory results. Above this depth, electric noise is disturbing all downhole sensors. Moreover, the inclinometers are reproducible (comparison between pre- and post-logs) and it is always within 2^o and 1° for boreholes KFM07A and KFM07C, respectively. For well azimuth, the corresponding values are 5^o and 6°, respectively.

The reduced agreement for KFM07C has though limited consequences on fracture orientation determination due to the sub-verticality of the well (i.e. possibly a maximum 6^o to 7° error on fracture orientations). Note that the well orientation of the HTPF tool refers to the magnetic North, whereas the Maxibor refers to the geographical North ($N_{magnetic} = N_{geographical} + 2.464^o$ at the time of measurements). Thus, we have established that our orientation determination for the tool is reliable and reproducible and well within expected errors.

The other independent control of successful data recording is correlated with the observed variations in downhole pressure during lowering and hoisting in the borehole. These variations, which were investigated after completed field campaign, can be

compared with the theoretical weight of the water column in the borehole and indicate that no discrepancies were found during measurements at drill site 7.

1.2 Calibrations

1.2.1 Pressure transducers and flow meter

Prior to the measurements, the pressure transducers were calibrated against a reference load cell and the flow meters by volume (mass) determination per time unit prior to field measurements (Appendix 3). Note that response remains linear with time and that the calibration factor has not changed during the complete duration of all tests at the Forsmark site (calibrations were run in May, early June, late July, and in October, 2006). The apparent noise comes from the time response of the testing system, not from the transducers. If data would have been plotted with respect to time, all sensors would have been very stable. Also note that nowhere in the stress determination procedure do we require flow rate measurements. These are only used to control the re-opening of fractures, and the normal stress measurements are only based on shut-in.

1.2.2 Tilt meters and magnetometers

The orientation devices were checked for functionality and calibrated several times during the campaign: prior to departure to the field, before entering each borehole, and after completed measurements.

The calibration prior to descent in the well consists of two phases. In the first phase, the orientation device is placed in a special calibration support and both inclinometers and the three magnetometers are tested for various inclinations and orientations so that the readings are not saturated for any inclination/orientation.

In phase two, the orientation device is placed inside the HTPF tool (Mosnier, 1982, Mosnier and Cornet, 1989). Using a special calibration plate, the tool is first placed vertically and orientations are checked for every 20^{o} of rotation around the tool axis. Thereafter, the HTPF tool is inclined about 45^{o} towards the North, followed by verification of readings for every 20^{o} rotation around the tool axis. The latter is then repeated with the tool inclined 45^{o} towards East, South, and West. Finally, the HTPF tool is placed horizontally and is rotated around a vertical axis during which the output of the axial magnetometer is sampled. When the tool is fixed in the N, E, S, and W, the output of the perpendicular magnetometers is sampled during the corresponding rotation around the tool axis.

Phases one and two of the calibration before descent are repeated when the work in the well has been completed, to verify that the readings are systematic. Moreover, after the field campaign, the electrical imaging logs are used to provide independent data on dip and azimuth of the well (see 1.1 above).

The functionality of the tilt-and magnetometers at drill site 7 is verified by the good agreement with the magnetic inclination from the Uppsala magnetic field observatory as well as with the deviation data of the Maxibor (Appendices 1 and 2).

1.2.3 Length measurement

For the sake of stress determination, the knowledge of absolute depth to within a few metres is quite sufficient. But because the objective is to relate images of features on the HTPF logs with those observed on cores, an adjustment to some decimetres is necessary.

Initially, the reference grooves in the boreholes were intended to be identified with the HTPF tool. However, the grooves proved to be too small for identification and a different strategy had to be adopted.

Instead, we compared the electrical imaging log with the cores and the BIPS images for a few unique features in the well. Once identified, by interpolation, equivalence is proposed between HTPF logs and BIPS/Boremap depths for the complete borehole length. Thereafter, each pre-existing fracture tested was correlated with the equivalent fracture observed on the cores. In addition, the tested fracture was photo documented in the core boxes. This comparison entails that the length calibration between the two systems is within 2 dm for both wells.

KFM07A

During the measurements in KFM07A, the reference marks could not be detected with the HTPF tool. Instead, the length was calibrated using detailed comparisons with images, cores, and the BIPS for unique features at three locations.

The first depth correspondence is the bottom of the borehole cone between the percussion drilled and core drilled part of the borehole at about 100 mbl. The electrical log measure is 101.86 mbl and the corresponding BIPS measure is 101.94 mbl. The second mark is in a section of many parallel fractures of which one is chosen for exact correlation with BIPS. On BIPS, the bottom of two closely located fractures is at 384.72 mbl (CB 53) and the corresponding electrical log measure is 385.13 mbl. Fractures were correlated about 10 m in each direction from it. The third reference mark corresponds to a fracture at about 616.65 mbl (CB 94) on the electrical log, which is 616.13 mbl on the BIPS. Fractures were positively correlated about 10 m in each direction from it.

A gradient for the borehole was determined and the correspondence between the HTPF log and the length calibrated BIPS was within 5-10 cm. Together, these allowed exact determination of the fracture tested in each test section. This leads us to propose the following approximation:

BIPS length = 1.001 * electrical imaging length.

KFM07C

Similarly to borehole KFM07A, the calibration was conducted by comparison with unique features on the electrical images, BIPS, and cores at two different depths. However, at the time of the work, the BIPS file is not yet completed and only recorded depths are available. This work was as a result undertaken after completed campaign.

The first depth correspondence is the bottom of the borehole cone at about 98 mbl. The electrical log measure is 98.29 mbl and the corresponding BIPS measure is 98.46 mbl. The second mark is a unique fracture 408.21 mbl according to the BIPS measure (the upper limit of an approximately 1 m long fracture), for which the electrical log measure is 408.20 mbl. Fractures were positively correlated about 10 m in each direction from the second reference mark.

A gradient for the borehole was determined and the correspondence between the HTPF log and the length calibrated BIPS was within 10 cm for the interval where data were collected. Together, these allowed exact determination of the fracture tested in each test section. This leads us to propose the following approximation:

BIPS length = 1.000 * electrical imaging length.

1.3 Reconnaissance logs

Because the notion of rock stress is a concept of continuum mechanics, it is necessary to identify volumes where the continuity hypothesis is verified. The first interpretation of the continuity hypothesis is given by the reconnaissance log with the HTPF tool (Appendices 4 and 5). During the reconnaissance log, the intensity of the injected electrical current is adjusted to highlight very tiny fractures (which are suitable for hydraulic injection testing), which means that very conductive fractures, i.e. potential stress decoupling zones, are clearly outlined by a significant change of resistivity. The first evaluation provided by the HTPF tool is used for selection of suitable test sections.

Note that the borehole lengths as displayed in the reconnaissance log may be somewhat shifted as compared with the lengths given in the various tables of this document. This is a length calibration problem with no significance for the interpretation of data.

1.4 Testing results

The results of testing are presented in Appendices 6 and 7. For each test the following is presented:

- The downhole pressures in the chamber (test section) and in the packers versus time are displayed and below, in a separate plot, the fluid flow rate versus time.
- Blow-ups of the shut-in curves for each cycle are presented on the second page.
- The third page displays the pressure versus flow rate during the jacking tests for all cycles (if conducted).
- The fourth and fifth pages include the post-frac log with the test section marked. Note that this log starts at the bottom and moves upwards, implying that the fracture is “up-side down” compared to the following detailed plots.
- The next pages include detailed plots of the test section with: (i) results of the reconnaissance log; (ii) results of the post-log, which may be multiple when different electrical gains have been applied to enhance visibility and/or when the fracture is located underneath the packers; (iii) interpretation of fracture one; (iv) interpretation of fracture two; etc.

The borehole lengths as displayed in the reconnaissance log and in the post-log may be somewhat shifted as compared with the lengths given in the various tables of this document. This is a length calibration problem with no significance for the interpretation of data. The correct borehole length and vertical depth for each test are found in the tables.

1.5 Interpreted data

The analysis of data is based on the ISRM suggested methods for rock stress estimation by hydraulic fracturing and hydraulic tests on pre-existing fractures (Haimson and Cornet, 2003).

The interpreted data in Appendices 8 and 9 are presented in tabular form so that full traceability is achieved. This means that the appendices cover the collected raw data, the first interpretation of the data (e.g. normal stresses for each cycle in the injection testing), and the final interpretation of e.g. the normal stress acting on the fracture.

Normal stresses are denoted using a geomechanical sign convention with compressive stresses taken as positive. Measurement positions are given as the borehole length of the centre of the test section. The corresponding vertical depth is based on recalculation of the borehole length using the deviation file delivered from Sicada. All orientation data represent the normal of the fracture plane, positive downwards, and are given with respect to geographic North according to coordinate system RT90 2.5 gon W 0:-15 for x and y and RHB70 for z, using a right-hand rule notation.

1.5.1 Fracture orientation data

In principle, the fracture orientations (i.e. the normal to the fracture plane) can in this specific assignment be determined with three different methods:

- Based on magnetometers and inclinometers of the HTPF tool
- Based on SKB´s deviation measurements of the well (the optical Maxibor method or the magnetic Flexit method) and tool face (inclinometers) of the HTPF tool
- Based on SKB´s BOREMAP system (Maxibor or Flexit deviation measurements) and tool face of the BIPS tool.

However, it must be pointed out that the third method is not available for fractures induced during the HF-/HTPF-campaign, because they were induced after the logging with the BIPS tool.

In the result files (Appendices 8 and 9), the results using method 2 are displayed (i.e. based on the Maxibor method).

Fracture orientation determined from the HTPF tool is obtained by fitting a sinusoid to the electrical image seen on the log. Special zooming techniques are used to identify more precisely the fracture. Two sinusoids are fitted to the image so as to identify domains of uncertainty. The central value is taken as the dip and azimuth values and the width of the interval on the values is selected as the 90% confidence level (to be compared with 99% confidence interval for pressure data).

For sub-vertical fractures, the electrical signals are seen on two neighbouring electrodes. Each electrode covers an azimuth range of 15°, implying that the domain of uncertainty (99% confidence level) is 30°. Hence, the standard deviation is 5° for axial fractures.

1.5.2 Normal stresses

Because Cornet et al. (2003) observed that the normal stress may be overestimated when based on opening phases of hydraulic jacking tests, only shut-in values have been used. The shut-in pressure determinations have been made using two methods: (i) an overestimate of the shut-in pressure is provided by the Hayashi and Haimson procedure (1991) that indicates when the fracture stops being “opened”; and (ii) an underestimate is provided by the Aamodt and Kuriyagawa procedure (1981) that indicates the first

pressure for which the fracture may be regarded as “closed”. The normal stress, or shut-in value, is taken equal to the mean of these methods, i.e.

$$\sigma_n = \frac{\sigma_{n,Aa\,\mathrm{mod}\,t,\min} + \sigma_{n,Aa\,\mathrm{mod}\,t,\max} + \sigma_{n,Hayashi,\min} + \sigma_{n,Hayashi,\max}}{4} \quad (1)$$

Moreover, the tangent method of Enever and Chopra (1989) is used to allow comparisons (Appendices 8 and 9). The extreme values for the Hayashi and Haimson (1991) and the Aamodt and Kuriyagawa procedure (1981) are taken as bounds of the 99% confidence interval.

1.6 Comparison of fracture orientations determined with different methods

In appendices 10 and 11, the fracture orientations as observed in the Boremap-system are compared with those of the HTPF tool. Note that these appendices present the truly tested fractures, as opposed to the fractures aimed for testing presented in Chapter 1.9. After this comparative study was initiated, a decision was taken to up-date SKB´s well deviation measurements, entailing that for many boreholes Maxibor measurement will be exchanged to Flexit measurements as the official deviation measurement files in SKB´s database Sicada. This up-date also affects the fracture orientations in Boremap as they are based on deviation data. In Appendices 10 and 11, the Boremap orientations based on the new Flexit well deviation data are presented, whereas the orientations of the HTPF tool is based on Maxibor.

For borehole KFM07A, the correspondence between methods yields an average deviation for azimuth and dip of the normal to the fracture plane of 11.6^o and 3.6^o, respectively.

For borehole KFM07C, the correspondence between methods yields an average deviation for azimuth and dip of the normal to the fracture plane of 34.4^o and 3.8^o, respectively. Three tests reduce the agreement with respect to azimuth (at 388.0, 271.5 and 173.5 mvd). When excluded, the average difference between both methods is reduced to 11.8^o and 3.5^o, respectively.

1.7 Analysis of errors in well orientation data on fracture orientation determination

Because the results of the electrical imaging system is dependent upon the well deviation data, the up-date of deviation data from Maxibor to Flexit introduces errors in the fracture orientation data of the electrical imaging system. As a result of this, a study was initiated attempting to quantify this error. The result is presented in Appendix 12 and indicates that the error is very small and negligible for the sake of stress determination. Hence, HTPF orientations based on Maxibor well deviation data were not updated with the new Flexit well deviation data.

1.8 General trends in collected data

1.8.1 KFM07A

The normal stresses of the tests in borehole KFM07A indicate that quite a few measurements are fairly close, or even below, the corresponding theoretical weight of the overburden rock mass (0.026 MPa/m; Figure 1-1 and Figure 1-2). However, given

the variations in normal stresses and orientations (Figure 1-3), the data are promising for the subsequent stress determination.

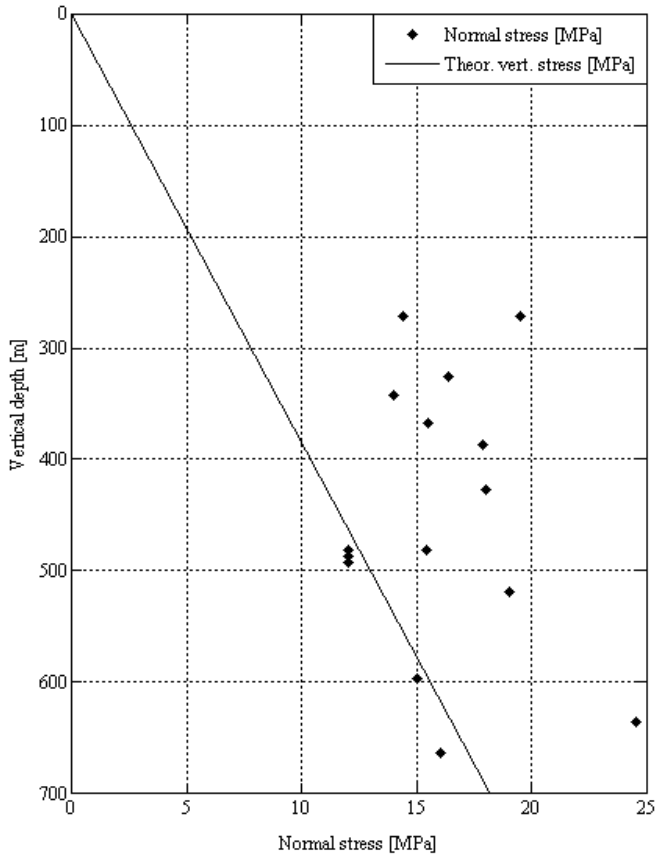

Figure 1-1. *Normal stresses versus depth in borehole KFM07A.*

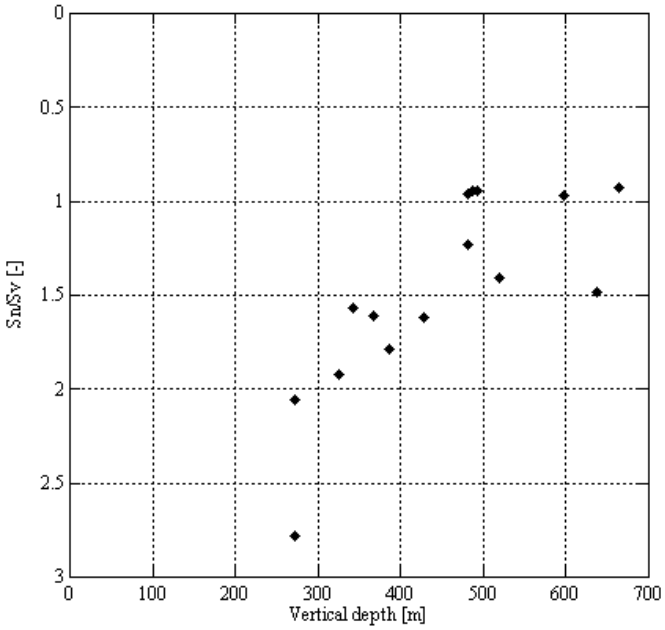

Figure 1-2. *Normal stresses divided by theoretical vertical stress versus depth in borehole KFM07A.*

Polar plots of the fractures aimed for testing versus the observed distribution of the normal to the tested fractures are presented in Figure 1-3. The result indicates that a large number of sub-horizontal fractures exist. Because only 5 tests have a normal stress close to the overburden weight, it seems that some sub-horizontal fractures have not controlled the result of the injection test.

A **B**

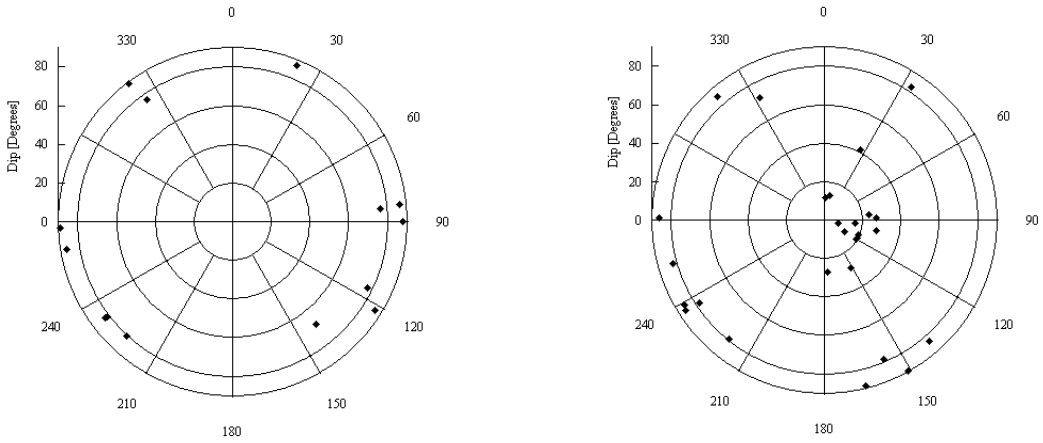

Figure 1-3. *Polar plot of normal to the fracture planes in borehole KFM07A: A) Fractures aimed for testing; B) Resulting fracture orientations.*

1.8.2 KFM07C

Also in borehole KFM07C, the normal stresses of the tests indicate that most measurements have a normal stress somewhat higher but still close to the theoretical weight of the overburden rock mass (0.026 MPa/m; Figure 1-4 and Figure 1-5).

Polar plots of the fractures aimed for testing versus the observed distribution of the normal to the tested fractures are presented in Figure 1-6. The result indicates that an overwhelming majority of sub-horizontal fractures have been tested. However, two successful axial fractures from the two sleeve fracturing tests indicate an orientation of σ_H between 121 and 128^{o}N. Hence, this information, together with the data in KFM07C are indeed useful for stress determination.

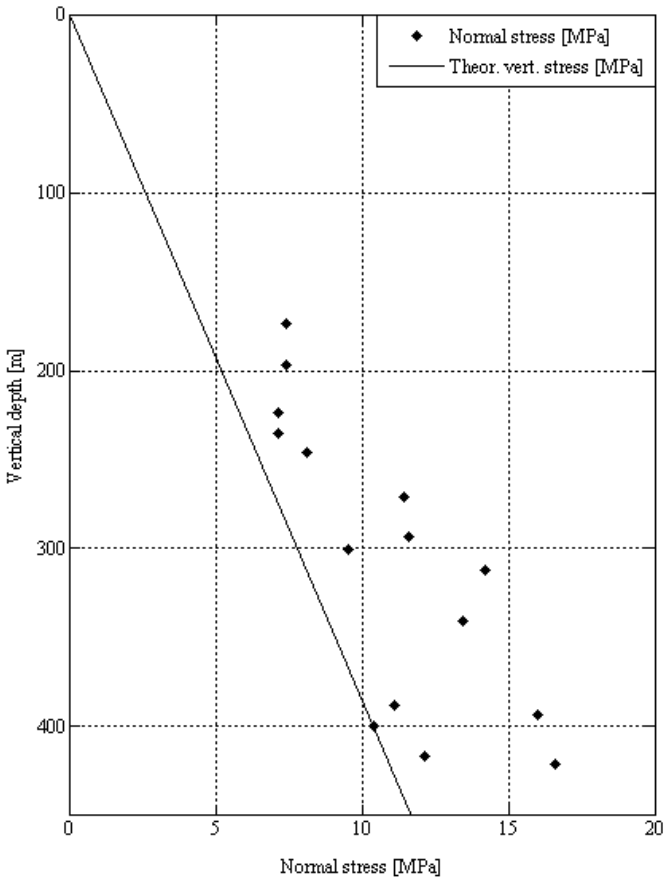

Figure 1-4. *Normal stresses versus depth in borehole KFM07C.*

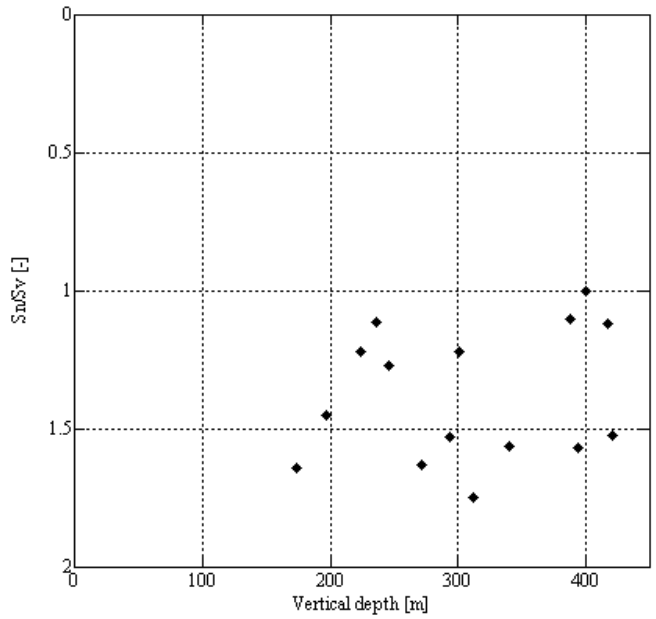

Figure 1-5. *Normal stresses divided by theoretical vertical stress versus depth in borehole KFM07C.*

A **B**

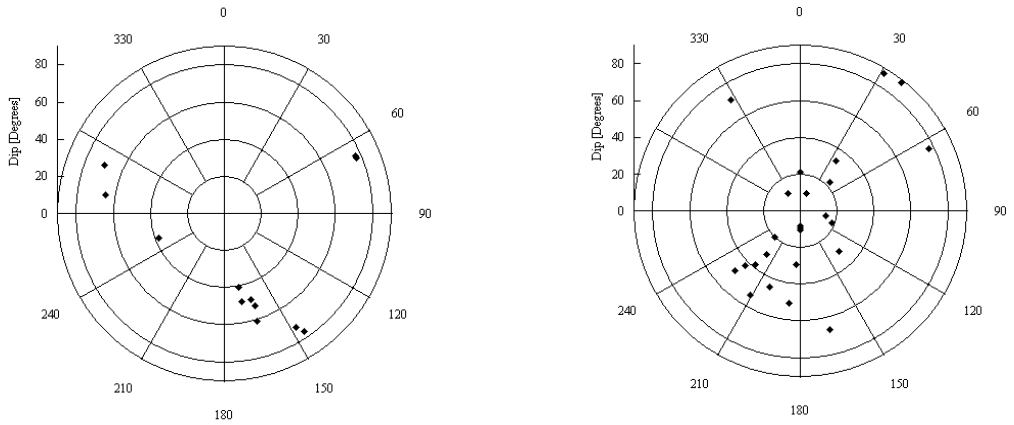

Figure 1-6. *Polar plot of normal to the fracture planes in borehole KFM07C: A) Fractures aimed for testing; B) Resulting fracture orientations.*

1.9 Individual tests

The fractures aimed for testing in boreholes KFM07A and KFM07C are presented in Table 1-1 and Table 1-2, respectively, and indicate that a large number of sub-horizontal fractures have been induced. These fractures sometimes appear in the test section, although they are more commonly located at the end of the test section (i.e. at the packer ends) and sometimes underneath the packers. Hence, a majority of the fractures are packer induced.

The induced sub-horizontal fractures cause a significant problem in the evaluation of the tests. The reason for this is that the opening of a fracture changes the stress field locally, but leaves the normal stress unaffected. Hence, for multiple fractures in the test section, the fracture normal stresses can be unambiguously determined only when the fractures are parallel.

By the appearance of the sub-horizontal fractures on the electrical imaging logs, many fractures seem to have experienced no or very limited propagation or fluid percolation, although visual inspection is a somewhat speculative approach. This would imply that, similar to drilling induced fractures (Brudy and Zoback, 1993; Peska and Zoback, 1995; Zoback et al., 2003) or fractures induced by sleeve fracturing technique (Stephansson, 1983a; b), they do not extend far into the rock. If this would be true, they would not distort the stress field as much as fully propagated fractures. Because the effect of the sub-horizontal fractures has not been investigated fully at this stage, HTPF tests that have changed the resistivity image of the aimed pre-existing fracture but that also include sub-horizontal fractures, have been assigned “potentially successful re-opening” in Table 1-1 and Table 1-2 below.

In some tests, the shut-in pressure was found to be dependent on the packer pressure, i.e. when increasing the packer pressure, the normal stress increased. The most pronounced examples were at 762.6 and 616.4 mbl in borehole KFM07A, and are a result of a sub-horizontal fracture underneath the packers. These data cannot be used for normal interpretation.

Table 1-1. Results from individual injection tests in borehole KFM07A.

			Aimed fracture (BOREMAP)					
Test [No]	**Bh length [m]**	**Depth [m]**	**Azimuth [^{o}N]**	**Dip [^{o}]**	**σ_n [Bar]**	**$\sigma_{v,theory}$ [Bar]**	**Successful re-opening**	**Additional fractures**
1*	796.2	663.5	140	69	160	172	Potentially	Sub-horizontal fracture^{EoP}
2	762.6	636.5	321	89	245	165	No	Sub-horizontal fracture^{UP}
3*	713.6	597.0	329	89	150	155	No	Sub-horizontal fracture^{EoP}
4*	616.4	518.5	232	82	190	135	Potentially	Sub-horizontal fracture^{UP}
5*	585.3	493.0	252	79	120	128	No	Sub-horizontal fracture^{TS}
			253	81				
6*	578.5	487.5	233	82	120	127	No	Sub-horizontal fracture^{TS}
7*	570.3	481.0	258	86	154	125	Potentially	Sub-horizontal fracture^{TS}
					120			
8	505.4	427.5	323	76	180	111	No	Sub-horizontal fractures^{EoP}
9*	455.9	387.0	125	88	179	100	Potentially	Sub-horizontal fracture^{EoP}
10*	433.4	368.0	266	88	155	96	Potentially	Sub-horizontal fractures$^{EoP, TS}$
			267	89				
11*	403.2	343.0	21	87	140	89	Potentially	Sub-horizontal fractures$^{EoP, TS}$
12*	383.0	326.0	141	86	164	85	Potentially	Sub-horizontal fracture^{TS}
13*	317.4	271.5	114	78	195	70	Potentially	Sub-horizontal fracture^{TS}
					144			

Note: “TS”, “EoP”, and “BP” denote sub-horizontal fracture in the Test Section, at the End of the Packer, and Underneath the Packer, respectively. Unambiguous data are marked with “*” in the first column. Theoretical vertical stress based on a vertical gradient of 0.026 MPa/m.

Table 1-2. Results from individual injection tests in borehole KFM07C.

			Aimed fracture (BOREMAP)					
Test [No]	**Bh length [m]**	**Depth [m]**	**Azimuth [°N]**	**Dip [°]**	**σ_n [Bar]**	**$\sigma_{v,theory}$ [Bar]**	**Successful re-opening**	**Additional fractures**
1	423.6	421.0	-	-	166	109	Unsuccessful HF	Sub-horizontal fractures^{TS}
2*	418.6	416.5	182	49	121	108	Potentially	Sub-horizontal fracture^{TS}
3*	402.2	400.0	169	52	104	104	Potentially	Sub-horizontal fracture^{TS}
4	396.2	394.0	-	-	160	102	Unsuccessful HF	Multiple fractures^{EoP,TS}
5*	390.3	388.0	246	38	111	101	Potentially	Sub-horizontal fracture^{TS}
6*	342.3	340.5	282	65	134	86	No	Sub-horizontal fracture^{EoP,TS}
7	313.6	312.0	70/71	77/78	142	81	Yes	Vague indication of other pre-existing features
8	302.0	300.5	-	-	95	78	Unsuccessful HF	Sub-horizontal fracture^{EoP}
9	294.4	293.0	158	72	116	76	No	Sub-horizontal fracture^{TS}
			157	76				
10	272.7	271.5	-	-	114	71	Unsuccessful HF	Multiple sub-horizontal fractures^{EoP,TS}
11	247.0	246.0	339	88	81	64	No	Sub-horizontal fracture^{EoP}
12*	237.6	235.5	-	-	71	61	Unsuccessful HF	Sub-horizontal fracture^{EoP}
13	224.5	223.5	-	-	71	58	Unsuccessful HF	Sub-horizontal fracture^{TS}
14*	197.5	196.5	-	-	74	51	Successful sleeve fracturing and HF	Sub-horizontal fracture^{EoP}
15*	174.5	173.5	-	-	74	45	Successful sleeve fracturing and HF	Sub-horizontal fracture^{BP}

Note: “TS”, “EoP”, and “BP” denote sub-horizontal fracture in the Test Section, at the End of the Packer, and Underneath the Packer, respectively. Unambiguous data are marked with “*” in the first column. Theoretical vertical stress based on a vertical gradient of 0.026 MPa/m.

2 Discussion and summary

2.1 General

Hydraulic rock stress measurements were performed in boreholes KFM07A and KFM07C at the Forsmark candidate area. Of the 28 tests conducted at drill site 7, only 18 involved completely unambiguous data, i.e. have a reliable normal stress and a well defined fracture geometry (but only two of these involve a single fracture geometry). The success rate of testing was hence unusually low for this type of hydraulic stress measurement equipment.

The primary reason for the reduced success rate was that sub-horizontal fractures frequently were induced. These fractures sometimes appear in the test section, although they are more commonly located at the end of the test section (i.e. at the packer ends) and underneath the packers. Hence, a majority of the fractures are packer induced. In a few tests, multiple sub-horizontal fractures were created.

The sub-horizontal fractures were induced when the pressure in the test section was just moderately higher (a few bars) than the theoretical weight of the overburden rock mass. This implies that a major constraint for injection testing prevailed at the site and that sub-horizontal fractures were induced in all cases where the fracture did not re-activate before reaching this critical pressure. The physical explanation for these fractures is not yet fully understood but we would like to emphasize that the observed sub-horizontal fractures contain very useful information. If a failure criterion for these fractures is derived, they will contribute much to the knowledge of the present state of stress at the Forsmark site.

The induced sub-horizontal fractures as well as the other test sections with multiple fractures cause a significant problem in the normal evaluation of the injection tests. The reason for this is that the opening of a fracture changes the stress field locally, but leaves the normal stress unaffected. Hence, for multiple fractures in the test section, the fracture normal stresses can be unambiguously determined only when the fractures are parallel.

For the somewhat surprising result of normal stresses lower than the theoretical vertical stress (Figure 1-2 and Figure 1-5), the most reasonable explanation is that the normal stress corresponds to a sub-horizontal fracture located near the end of the packer element. The fracture is thereby prevented from closing when pressure drops in the interval and affects the shut-in measurement. This is manifested by poor flow back tests that help detect this difficulty. In practice, flow back tests are part of the quality assurance procedure for selecting completely unambiguous tests. This phenomenon has, as far as we know, not been found outside the Forsmark or Oskarshamn sites (Ask et al., 2007). This means that it is either specific to these sites, or perhaps more likely, it has not been detected before due to limitations in fracture determination methods (which normally involve impression packer technique).

2.2 Borehole specific objectives

The objectives of the hydraulic stress measurements at drill site 7 were to (i) decrease uncertainty in data on in-situ state of stress, (ii) increase the understanding of how local

geological site conditions may affect the state of stress, and (iii) provide input for site descriptive modelling on the state of stress at the site.

The borehole specific objectives involved:

- Identify what types of fractures that seem feasible for HTPF.
- Identify possible decoupling zones along the borehole.
- Determine the state of stress at the borehole location, from 100 m depth and down to depths were measurements could be carried out without jeopardizing the borehole equipment.

These objectives and how they have been fulfilled are described below.

2.2.1 Identification of fractures suitable for HTPF testing

The effectiveness of the HTPF tool is clear when looking at the result of the reconnaissance and post-logs (Appendices 4 to 7). A large number of electrically conductive features exist in the boreholes, and they are repeated for each new log performed, which implied that they might be opened using a suitable injection testing strategy. The HTPF tool was also successful with respect to post-log images, which also include the entire packer sections. Indeed, this feature has proven most valuable given the very common observation of packer induced fractures. The only reduced imaging result obtained is for the most shallow located test in borehole KFM07C, where the ground currents are disturbing the downhole sensors. For this reason, the most shallow located data in KFM07C involved a special analysis to attempt to improve data quality.

2.2.2 Identify possible decoupling zones along the borehole.

The electrical imaging tool is very useful for identification of possible decoupling zones. Such zones are clearly displayed as electrical anomalies (red coloured in the logs).

2.2.3 Determine the state of stress from c. 100-1000 mbl

The stress determinations are undertaken in the main report.

APPENDIX II

FORSMARK SITE INVESTIGATION. COLLECTION OF HYDRAULIC ROCK STRESS DATA IN BOREHOLE KFM08A

Forsmark site investigation

Collection of hydraulic rock stress data in borehole KFM08A

Daniel Ask, Vattenfall Power Consultant AB

Francois Cornet, Institut de Physique du Globe de Paris

Frederic Fontbonne, Geostress Co.

Christophe Brunet, Institut de Physique du Globe de Paris

November, 2007

SUMMARY

Hydraulic rock stress measurements were performed in borehole KFM08A at the Forsmark candidate area, Sweden. The measurements were carried out in one single campaign and a total of 23 hydraulic fracturing tests and hydraulic tests on pre-existing fractures were conducted between the 11th and the 23rd of September, 2006.

The work involved cooperation between Vattenfall Power Consultant AB (Contractor), Institut de Physique du Globe de Paris (IPGP), and Geostress Co (both Sub-contractors). Vattenfall Power Consultant AB provided an MKW wireline system and field personnel, whereas IPGP supplied downhole equipment, data acquisition system, and field personnel. Finally, Geostress contributed with field personnel.

This document includes a detailed description of observations made in the field, and results.

Of the 23 tests conducted in borehole KFM08A, only 6 involve completely unambiguous data, i.e. have a reliable normal stress and a well defined fracture geometry (although only two of these involve a single fracture geometry). The success rate of testing was hence lower than expected for this type of hydraulic stress measurement equipment. The primary reasons for the reduced success rate was that sub-horizontal fractures were induced and additional pre-existing fractures were stimulated. The sub-horizontal fractures were created when the pressure in the test section was just moderately larger (a few bars) than the theoretical weight of the overburden rock mass. This implies that a major constraint for injection testing prevailed and that sub-horizontal fractures were induced in all cases where the fracture did not re-activate before reaching this critical pressure. The physical explanation for these fractures is yet to be determined, but the relatively moderate testing depth in combination with the inclined boreholes (about 61° from the horizontal plane at surface and flattening out to c 38° towards the borehole bottom) is probably not favourable for hydraulic stress measurements. We would like to emphasize that the observed sub-horizontal fractures contain very useful information. If a failure criterion for these fractures is derived, they will contribute much to the knowledge of the present state of stress at the Forsmark site.

SAMMANFATTNING

Hydrauliska bergspänningsmätningar har utförts i borrhål KFM08A i Forsmark. Totalt gjordes 23 tester i en sammanhållande kampanj mellan den 11:e och den 23:e september, 2006.

Aktiviteten var ett samarbetsprojekt mellan Vattenfall Power Consultant AB (huvudkonsult), Institute de Physique du Globe de Paris (IPGP), och Geostress Co (båda dessa organisationer underkonsulter). Vattenfall Power Consultant AB tillhandahöll ett MKW wireline-system samt fältpersonal, IPGP stod för borrhålsutrustning, datainsamlingssystem och fältpersonal, medan Geostress bidrog med fältpersonal.

Detta dokument innehåller en detaljerad beskrivning av fältobservationer och resultat.

Av de 23 utförda injektionstesterna i borrhål KFM08A är 6 helt otvetydiga, dvs uppvisar tillförlitlig normalspänning och välbestämd sprickorientering (men endast två av dessa involverar en enskild sprickgeometri). Andelen lyckade tester är därför lägre än normalt för metoden. De sub-horisontella sprickorna inducerades redan vid ett pålagt tryck som endast måttligt översteg den teoretiska vertikalspänningen och innebar därför en stark begränsning av metodens möjligheter. De bakomliggande fysikaliska orsakerna till uppkomsten av dessa sprickor återstår att förklara, men de relativt måttliga testdjupen i kombination med borrhålets relativt stora lutning (ca 61^{o} från horisontalplanet vid ytan till ca 38° mot botten) är sannolikt inte fördelaktiga för denna typ av mätningar. Vi vill dock betona att om ett brottkriterium för dessa sprickor kan härledas, kan en systematisk analys av den datamängd som dessa sprickor representerar sannolikt ge ett mycket värdefullt bidrag till beskrivningen av det rådande spänningsfältet i Forsmark.

Contents

1 Collected data in borehole KFM08A

The collected data comprise of numerous parameters for determination of the stress field but also for verification of the data recording quality, which are described below.

1.1 Fracture orientation and groundwater pressure data

The three alternative means of determining fracture orientations available in this activity are described in Chapter 4.2.5. Regarding fracture orientation by using the Mosnier tool the reliability of the fracture orientation determination rests on three features:

- The proper recording of all parameters that characterize the position of the tool in the well (borehole length, and measurement results from 3 magnetometers and 2 inclinometers).
- The good understanding of tool manufacturing and its consistency with data processing routines.
- The repeatability of orientations during comparisons of multiple scans of the same fracture.

There are a few independent means to verify that the overall data recording has been successful. One involves readings of orientation devices as the tool is lowered and hoisted in the borehole. The values of the magnetic field inclination, as determined from magnetometers, offer a completely independent check on the digitization procedure used for the downhole data acquisition and surface data recording. The results of the measurements of well azimuth and well inclination are compared with those obtained with Maxibor as well as with the Uppsala magnetic field observatory are presented in Appendices 1. Repeatability of well inclination and azimuth is within a few degrees and the magnetic field inclination determinations are always within 2.5° of Uppsala observatory measurements, for all depths greater than 400 m (Appendix 1). Position in well is calibrated on that of the BIPS and cores. Note that the well orientation of the HTPF tool refers to the magnetic North, whereas the Maxibor refers to the geographical North ($N_{magnetic} = N_{geographical} + 2.464^{o}$ at the time of measurements).

The other independent control of successful data recording is correlated with the observed variations in downhole pressure during lowering and hoisting in the borehole. These variations, which were investigated after completed field campaign, can be compared with the theoretical weight of the water column in the borehole and indicate that no discrepancies were found during measurements at drill site 8.

The functionality of the tilt-and magnetometers in borehole KFM08A is verified by the good agreement with the magnetic inclination from the Uppsala magnetic field observatory as well as with the deviation data of the Maxibor below 350 mbl. However, above this depth, a noise starts to appear on the orientation data as well as the magnetic inclination data. At about 100 mbl, the magnetic deviation is about 7-8^{o} off the observation from the Uppsala magnetic field observatory, but stabilizes in the uppermost 50 mbl. A similar pattern can be observed on well azimuth data. On the other hand, well inclination is stable over the entire borehole but starts to deviate from the

Maxibor data above 400 mbl and reaches some 8^{o} at surface. However, this noise does not affect the collected data because the most superficial test was made at 333 mbl.

1.2 Calibration of equipment

1.2.1 Pressure transducers and flow meter

Prior to the measurements, the pressure transducers were calibrated against a reference load cell and the flow meters by volume (mass) determination per time unit prior to field measurements (Appendix 2). Note that response remains linear with time and that the calibration factor has not changed during the complete duration of all tests at the Forsmark site (calibrations were run in May, early June, late July, and in October, 2006). The apparent noise comes from the time response of the testing system, not from the transducers. If data would have been plotted with respect to time, all sensors would have been very stable. Also note that nowhere in the stress determination procedure do we require flow rate measurements. These are only used to control the re-opening of fractures, and the normal stress measurements are only based on shut-in.

1.2.2 Tilt meters and magnetometers

The orientation devices were checked for functionality and calibrated several times during the campaign: prior to departure to the field, before entering each borehole, and after completed measurements.

The calibration prior to descent in the well consists of two phases. In the first phase, the orientation device is placed in a special calibration support and both inclinometers and the three magnetometers are tested for various inclinations and orientations so that the readings are not saturated for any inclination/orientation.

In phase two, the orientation device is placed inside the HTPF tool (Mosnier, 1982; Mosnier and Cornet, 1989). Using a special calibration plate, the tool is first placed vertically and orientations are checked for every 20^{o} of rotation around the tool axis. Thereafter, the HTPF tool is inclined about 45^{o} towards the North, followed by verification of readings for every 20^{o} rotation around the tool axis. The latter is then repeated with the tool inclined 45^{o} towards East, South, and West. Finally, the HTPF tool is placed horizontally and is rotated around a vertical axis during which the output of the axial magnetometer is sampled. When the tool is fixed in the N, E, S, and W, the output of the perpendicular magnetometers is sampled during the corresponding rotation around the tool axis.

Phases one and two of the calibration before descent are repeated when the work in the well has been completed, to verify that the readings are systematic. Moreover, after the field campaign, the electrical imaging logs are used to provide independent data on dip and azimuth of the well (see Chapter 1.1 above).

1.2.3 Length measurement

For the sake of stress determination, the knowledge of absolute depth to within a few metres is quite sufficient. But because the objective is to relate images of features on the HTPF logs with those observed on cores, an adjustment to some decimetre is necessary.

Initially, the reference grooves in the borehole were intended to be identified with the HTPF tool. However, the grooves proved to be too small for identification and a

different strategy had to be adopted.

Instead, we compared the electrical imaging log with the cores and the BIPS images for a few unique features in the well. Once identified, by interpolation, equivalence is proposed between HTPF logs and BIPS/Boremap depths for the complete borehole length. Thereafter, each pre-existing fracture tested was correlated with the equivalent fracture observed on the cores. In addition, the tested fracture was photo documented in the core boxes. This comparison entails that the length calibration between the two systems is within 2 dm for KFM08A.

Because the reference grooves could not be detected with the HTFP tool, the length was calibrated using detailed comparisons with images, cores, and the BIPS for unique features. Two sections, both involving about 20 m of core, were carefully mapped to achieve an accurate correspondence between fractures observed on the HTPF log and of those seen on cores and mapped in BIPS.

The first depth correspondence consisted of the bottom of the borehole cone between the percussion drilled and core drilled part of the borehole at about 100 mbl. The electrical log measure is 102.06 mbl and the corresponding BIPS measure is 102.28 mbl. The second mark was found near a very conductive zone at about 409 to 412 mbl, where fractures were correlated about 10 m in each direction from it. The reference fracture at 404.10 mbl on the electrical log was used for calibration, which corresponds to 404.43 mbl on the BIPS. The third reference mark corresponds to a fracture at about 751.16 mbl on the electrical log, which is 751.62 mbl on the BIPS. Fractures were positively correlated about 10 m in each direction from it.

A gradient for the borehole was determined and the correspondence between the HTPF log and the length calibrated BIPS was within 5-10 cm. This leads us to propose the following approximation:

BIPS length = 1.005 * electrical imaging length.

1.3 Reconnaissance logs

Because the notion of rock stress is a concept of continuum mechanics, it is necessary to identify volumes where the continuity hypothesis is verified. The first interpretation of the continuity hypothesis is given by the reconnaissance log with the HTPF tool (Appendices 3). During the reconnaissance log, the intensity of the injected electrical current is adjusted to highlight very tiny fractures (which are suitable for hydraulic injection testing), which means that very conductive fractures, i.e. potential stress decoupling zones, are clearly outlined by a significant change of resistivity. The first evaluation provided by the HTPF tool is used for selection of suitable test sections.

Note that the borehole lengths as displayed in the reconnaissance log may be somewhat shifted as compared with the lengths given in the various tables of this document. This is a length calibration problem with no significance for the interpretation of data.

1.4 Testing results

The results of testing are presented in Appendix 3. For each test the following is presented:

- The downhole pressures in the chamber (test section) and in the packers versus time are displayed and below, in a separate plot, the fluid flow rate versus time.

- Blow-ups of the shut-in curves for each cycle are presented on the second page.

- The third page displays the pressure versus flow rate during the jacking tests for all cycles (if conducted).

- The fourth and fifth pages include the post-frac log with the test section marked. Note that this log starts at the bottom and moves upwards, implying that the fracture is “up-side down” compared to the following detailed plots.

- The next pages include detailed plots of the test section with: (i) results of the reconnaissance log; (ii) results of the post-log, which may be multiple when different electrical gains have been applied to enhance visibility and/or when the fracture is located underneath the packers; (iii) interpretation of fracture one; (iv) interpretation of fracture two; etc.

The borehole lengths as displayed in the reconnaissance log and in the post-log may be somewhat shifted as compared with the lengths given in the various tables of this document. This is a length calibration problem with no significance for the interpretation of data. The correct borehole length and vertical depth for each test are found in the tables.

1.5 Interpreted data

The analysis of data is based on the ISRM suggested methods for rock stress estimation by hydraulic fracturing and hydraulic tests on pre-existing fractures (Haimson and Cornet, 2003).

The interpreted data in Appendix 4 are presented in tabular form so that full traceability is achieved. This means that the appendices cover the collected raw data, the first interpretation of the data (e.g. normal stresses for each cycle in the injection testing), and the final interpretation of e.g. the normal stress acting on the fracture.

Normal stresses are denoted using a geomechanical sign convention with compressive stresses taken as positive. Measurement positions are given as the borehole length of the centre of the test section. The corresponding vertical depth is based on recalculation of the borehole length using the deviation file delivered from Sicada. All orientation data represent the normal of the fracture plane, positive downwards, and are given with respect to geographic North according to coordinate system RT90 2.5 gon W 0:-15 for x and y and RHB70 for z, using a right-hand rule notation.

1.5.1 Fracture orientation data

In principle, the fracture orientations (i.e. the normal to the fracture plane) can in this specific assignment be determined with three different methods:

- Based on magnetometers and inclinometers of the HTPF tool

- Based on SKB´s deviation measurements of the well (the optical Maxibor

method or the magnetic Flexit method) and tool face (inclinometers) of the HTPF tool

- Based on SKB´s BOREMAP system (Maxibor or Flexit deviation measurements) and tool face of the BIPS tool.

However, it must be pointed out that the third method is not available for fractures induced during the HF-/HTPF-campaign, because they were induced after the logging with the BIPS tool.

In the result files (Appendix 4), the results using method 2 are displayed (i.e. based on the Maxibor method).

Fracture orientation determined with the HTPF tool is obtained by fitting a sinusoid to the electrical image seen on the log. Special zooming techniques are used to identify more precisely the fracture. Two sinusoids are fitted to the image so as to identify domains of uncertainty. The central value is taken as the dip and azimuth values and the width of the interval on the values is selected as the 90% confidence level (to be compared with 99% confidence interval for pressure data).

1.5.2 Normal stresses

Because Cornet et al., (2003) observed that the normal stress may be overestimated when based on opening phases of hydraulic jacking tests, only shut-in values have been used. The shut-in pressure determinations have been made using two methods: (i) an overestimate of the shut-in pressure is provided by the Hayashi and Haimson procedure (1991) that indicates when the fracture stops being “opened”; and (ii) an underestimate is provided by the Aamodt and Kuriyagawa procedure (1981) that indicates the first pressure for which the fracture may be regarded as “closed”. The normal stress, or shut-in value, is taken equal to the mean of these methods, i.e.

$$\sigma_n = \frac{\sigma_{n,Aa\,\mathrm{mod}\,t,\min} + \sigma_{n,Aa\,\mathrm{mod}\,t,\max} + \sigma_{n,Hayashi,\min} + \sigma_{n,Hayashi,\max}}{4} \quad (1)$$

Moreover, the tangent method of Enever and Chopra (1989) is used to allow comparisons (Appendix 4). The extreme values for the Hayashi and Haimson (1991) and the Aamodt and Kuriyagawa procedure (1981) are taken as bounds of the 99% confidence interval.

1.6 Comparison of fracture orientations determined with different methods

In Appendix 5, the fracture orientations as observed in the Boremap-system are compared with those of the HTPF tool. Note that this appendix presents the truly tested fractures, as opposed to the fractures aimed for testing presented in Chapter 1.9. After this comparative study was initiated, a decision was taken to up-date SKB´s well deviation measurements, entailing that for many boreholes Maxibor measurement will be exchanged to Flexit measurements as the official deviation measurement files in SKB´s database Sicada. This up-date also affects the fracture orientations in Boremap as they are based on deviation data. In Appendix 5, the Boremap orientations based on the new Flexit well deviation data are presented, whereas the orientations of the HTPF tool

is based on Maxibor.

For borehole KFM08A, the correspondence between methods yields an average deviation for azimuth and dip of the normal to the fracture plane of 9.6^{o} and 7.6^{o}, respectively. For all matched fractures, the corresponding values are 8.7^{o} and 6.7^{o}, respectively.

1.7 Analysis of errors in well orientation data on fracture orientation determination

Because the results of the electrical imaging system is dependent upon the well deviation data, the up-date of deviation data from Maxibor to Flexit introduces errors in the fracture orientation data of the electrical imaging system. As a result of this, a study was initiated attempting to quantify this error. The result is presented in Appendix 6 and indicates that the error is very small and negligible for the sake of stress determination. Hence, HTPF orientations based on Maxibor well deviation data were not updated with the new Flexit well deviation data.

1.8 General trends in collected data

The normal stresses of the tests in borehole KFM08A indicate that all measurements are evenly distributed around the theoretical weight of the overburden rock mass (0.026 MPa/m; Figure 1-1 and Figure 1-2). Noticeable is that 11 tests show a normal stress lower than the theoretical weight of the overburden rock mass. This result will be discussed in Chapter 1.9.

Polar plots of the fractures aimed for testing versus the observed distribution of the normal to the tested fractures are presented in Figure 1-3. The result indicates that 7 sub-horizontal fractures have been tested, which is in accordance with observed normal stresses. It is a large variety of fracture orientations, which is promising for stress inversion.

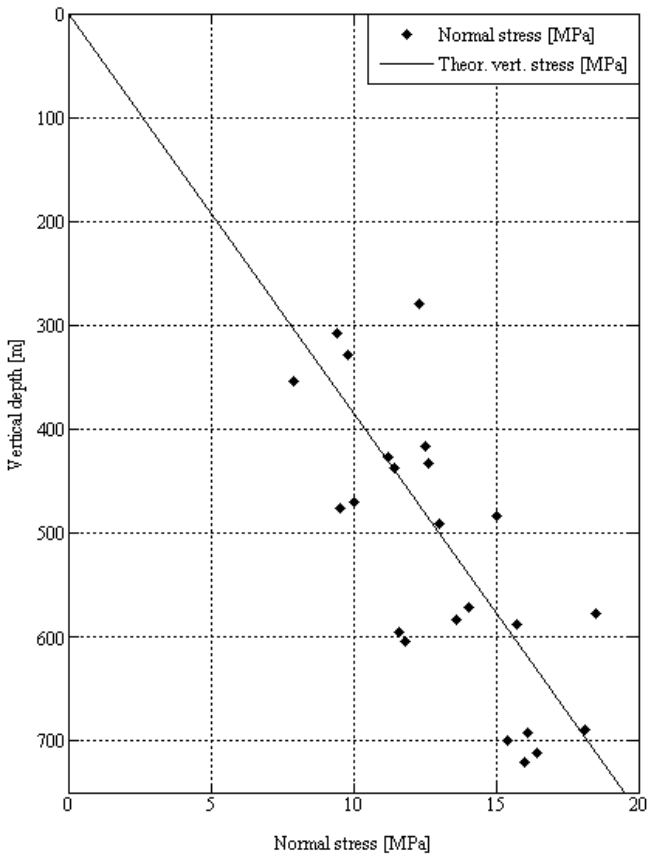

Figure 1-1. *Normal stresses versus depth in borehole KFM08A.*

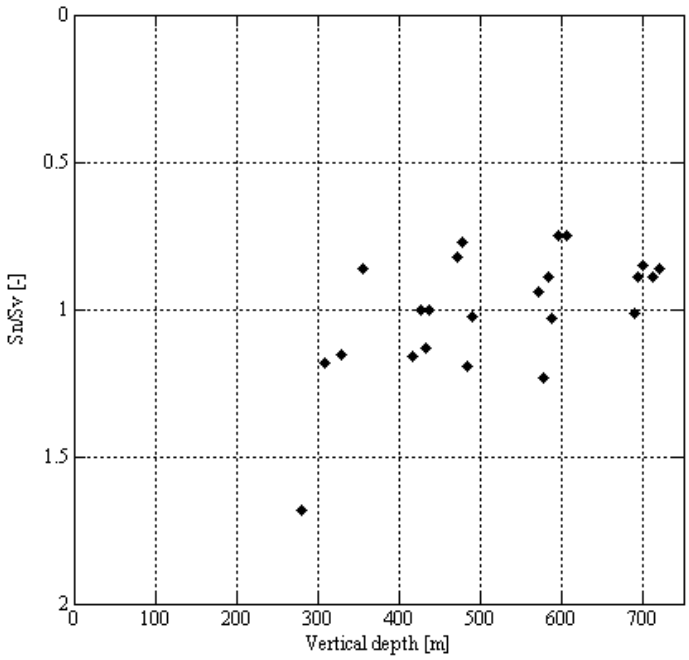

Figure 1-2. *Normal stresses divided by theoretical vertical stress versus depth in borehole KFM08A.*

A **B**

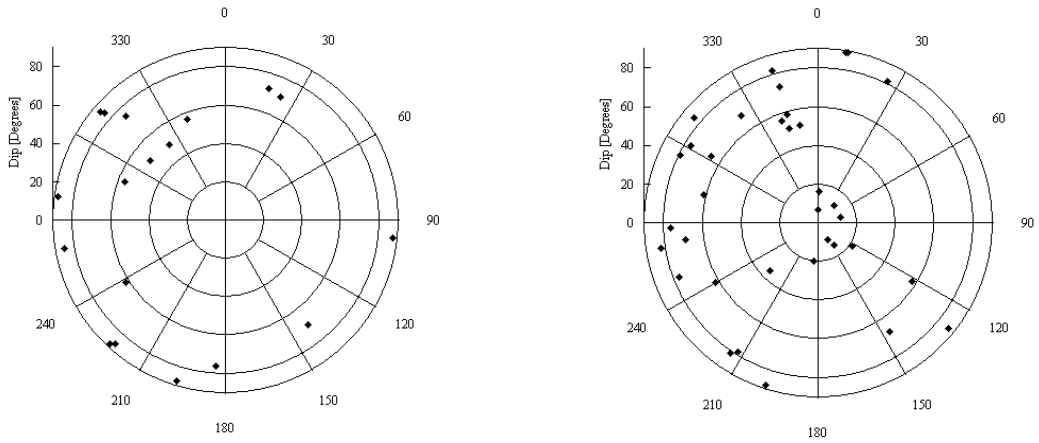

Figure 1-3. *Polar plot of normal to the fracture planes in borehole KFM08A: A) Fractures aimed for testing; B) Resulting fracture orientations.*

1.9 Individual tests

The individual tests results for borehole KFM08A are presented in Table 1-1, and indicate that some sub-horizontal fractures have been induced and that several additional pre-existing fractures were stimulated during testing. The sub-horizontal fractures sometimes appear in the test section, although they are more commonly located at the end of the test section (i.e. at the packer ends) and sometimes underneath the packers. Hence, a majority of the sub-horizontal fractures are packer induced.

The additional fractures cause a significant problem in the evaluation of the tests. The reason for this is that the opening of a fracture changes the stress field locally, but leaves the normal stress unaffected. Hence, for multiple fractures in the test section, the fracture normal stresses can be unambiguously determined only when the fractures are parallel.

By the appearance of the sub-horizontal fractures on the electrical imaging logs, many fractures seem to have experienced no or very limited propagation or fluid percolation, although visual inspection is a somewhat speculative approach. This would imply that, similar to drilling induced fractures (Brudy and Zoback, 1993; Peska and Zoback, 1995; Zoback et al., 2003) or fractures induced by sleeve fracturing technique (Stephansson, 1983a; b), they do not extend far into the rock. If this would be true, they would not distort the stress field as much as fully propagated fractures. Because the effect of the sub-horizontal fractures has not been investigated fully at this stage, HTPF tests that have changed the resistivity image of the aimed pre-existing fracture but that also include sub-horizontal fractures, have been assigned “potentially successful re-opening” in Table 1-1 below. This denomination has also been given the tests with multiple pre-existing fractures in the test section.

Table 1-1. Results from individual injection tests in borehole KFM08A.								
			Aimed fracture (BOREMAP)					
Test [No]	**Bh length [m]**	**Depth [m]**	**Azimuth [^{o}N]**	**Dip [^{o}]**	**σ_n [Bar]**	**$\sigma_{v,theory}$ [Bar]**	**Successful re-opening**	**Additional fractures**
1*	942.7	719.5	**223**	**87**	160	187	Yes	
2	928.4	711.0			164	185	Potentially, HF	Three pre-existing fractures in test section
3	910.7	699.5	**325-326**	**48**	154	182	Potentially	Sub-horizontal fracture^{EoP}
4*	901.0	692.5	**-**	-	161	180	HF	Multiple sub-horizontal fracture^{EoP,TS}
5	893.7	689.0	**21**	**71**	181	179	Yes	No
6*	766.8	604.5	**341**	**54**	118	157	Potentially	Sub-horizontal fracture^{EoP}
7	753.7	595.5	**26**	**69**	116	155	Potentially	Another, but vaguely defined pre-existing fracture in the test section
8*	741.9	587.5	**308/318**	**82/83**	157	153	Potentially	Sub-horizontal fracture^{EoP}
9	735.7	583.0			136	152	Potentially, HF	Two pre-existing fractures in test section
10	725.9	576.5			185	150	Yes, HF	Pre-existing fracture in test section
11	717.9	571.0	**278**	**87**	140	148	Yes	No
12*	606.0	490.0	**273**	**89**	130	127	Potentially	Sub-horizontal fracture^{TS}
13	595.4	482.5			150	125	HF	Sub-horizontal fracture^{UP}
14	586.7	476.0	**172**	**76**	95	124	Potentially	Sub-horizontal fracture^{TS}
15*	578.5	470.0	**139**	**70**	100	122	Potentially	Multiple sub-horizontal fracture^{EoP,TS}
16	534.2	436.5	**195**	**86**	114	113	Yes	No
17	527.8	432.0	**307**	**48**	126	112	Yes	No
18	520.6	426.5	**220**	**84**	112	111	Yes	No
19	508.0	416.5	**316**	**73**	125	108	Yes	No
20	427.2	354.0	**314**	**87**	79	92	Potentially	Sub-horizontal fracture^{EoP}
21	395.1	328.5	**238**	**61**	98	85	Yes	No

Table 6-1. Results from individual injection tests in borehole KFM08A (continued).								
			Aimed fracture (BOREMAP)					
Test [No]	**Bh length [m]**	**Depth [m]**	**Azimuth [^{o}N]**	**Dip [^{o}]**	**σ_n [Bar]**	**$\sigma_{v,theory}$ [Bar]**	**Successful re-opening**	**Additional fractures**
22	365.8	307.0	**261**	**84**	94	80	Potentially	Another inclined fracture is observed in the test section
23	333.5	279.5	**312**	**85**	123	73	Yes	No

Note: “TS”, “EoP”, and “BP” denote sub-horizontal fracture in the Test Section, at the End of the Packer, and Underneath the Packer, respectively. Theoretical vertical stress based on a vertical gradient of 0.026 MPa/m. Unambiguous data are marked with “*” in the first column.

2 Discussion and summary

2.1 General

Hydraulic rock stress measurements were performed in borehole KFM08A at the Forsmark candidate area. Of the 23 tests conducted in the borehole, 6 involved completely unambiguous data, i.e. have a reliable normal stress and a well defined fracture geometry but only two of these involve a single fracture geometry. The success rate of testing was hence unusually low for this type of hydraulic stress measurement equipment.

The primary reason for the reduced success rate was that sub-horizontal fractures frequently were induced or that additional pre-existing fractures were stimulated. The sub-horizontal fractures sometimes appear in the test section, although they are more commonly located at the end of the test section (i.e. at the packer ends) and underneath the packers. Hence, a majority of the sub-horizontal fractures are packer induced.

The sub-horizontal fractures were induced when the pressure in the test section was just moderately higher (a few bars) than the theoretical weight of the overburden rock mass. This implies that a major constraint for injection testing prevailed at the site and that sub-horizontal fractures were induced in all cases where the fracture did not re-activate before reaching this critical pressure. The physical explanation for these fractures is not yet fully understood but we would like to emphasize that the observed sub-horizontal fractures contain very useful information. If a failure criterion for these fractures is derived, they will contribute much to the knowledge of the present state of stress at the Forsmark site.

The multiple fractures in the test section cause a significant problem in the normal evaluation of the injection tests. The reason for this is that the opening of a fracture changes the stress field locally, but leaves the normal stress unaffected. Hence, for multiple fractures in the test section, the fracture normal stresses can be unambiguously determined only when the fractures are parallel.

For the somewhat surprising result of normal stresses lower than the theoretical vertical stress (Figure 1-2), the most reasonable explanation is that the normal stress corresponds to a sub-horizontal fracture located near the end of the packer element. The fracture is thereby prevented from closing when pressure drops in the interval and affects the shut-in measurement. This is manifested by poor flow back tests that help detect this difficulty. In practice, flow back tests are part of the quality assurance procedure for selecting completely unambiguous tests. This phenomenon has, as far as we know, not been found outside the Forsmark or Oskarshamn sites (Ask et al., 2007). This means that it is either specific to these sites, or perhaps more likely, it has not been detected before due to limitations in fracture determination methods (which normally involve impression packer technique).

2.2 Borehole specific objectives

The objectives of the hydraulic stress measurements at drill site 8 were to (i) decrease uncertainty in data on in-situ state of stress, (ii) increase the understanding of how local

geological site conditions may affect the state of stress, and (iii) provide input for site descriptive modelling of the state of stress at the Forsmark site.

The borehole specific objectives involved:

- Identify what types of fractures that seem feasible for HTPF.
- Identify possible decoupling zones along the borehole.
- Determine the state of stress at the borehole location, from c. 100 m borehole length down to levels close to the borehole bottom at c. 1000 m borehole length. The consultant is responsible for the choice of method at each test location (HF or HTPF).

These objectives and how they have been fulfilled are described below.

2.2.1 Identification of fractures suitable for HTPF testing

The effectiveness of the HTPF tool is clear when looking at the result of the reconnaissance and post-logs (Appendices 3 and 4). A large number of electrically conductive features exist in the boreholes, and they are repeated for each new log performed, which implied that they might be opened using a suitable injection testing strategy. The HTPF tool was also successful with respect to post-log images, which also include the entire packer sections. Indeed, this feature has proven most valuable given the very common observation of packer induced fractures.

2.2.2 Identify possible decoupling zones along the borehole.

The electrical imaging tool is very useful for identification of possible decoupling zones. Such zones are clearly displayed as electrical anomalies (red coloured in the logs).

2.2.3 Determine the state of stress from c. 100-1000 mbl

The stress determination is undertaken in the main report.

APPENDIX III

FORSMARK SITE INVESTIGATION. COLLECTION OF HYDRAULIC ROCK STRESS DATA IN BOREHOLES KFM09A AND KFM09B

Forsmark site investigation

Collection of hydraulic rock stress data in boreholes KFM09A and KFM09B

Daniel Ask, Vattenfall Power Consultant AB

Francois Cornet, Institut de Physique du Globe de Paris

Frederic Fontbonne, Geostress Co.

Christophe Brunet, Institut de Physique du Globe de Paris

November, 2007

SUMMARY

Hydraulic rock stress measurements were performed in boreholes KFM09B (18 tests) and KFM09A (16 tests) at the Forsmark candidate area, Sweden. The measurements were carried out in two separate campaigns and a total of 34 hydraulic fracturing tests and hydraulic tests on pre-existing fractures were conducted between the 6th of June and the 20th of July, 2006.

The work involved cooperation between Vattenfall Power Consultant AB (Contractor), Institut de Physique du Globe de Paris (IPGP), and Geostress Co (both Sub-contractors). Vattenfall Power Consultant AB provided an MKW wireline system and field personnel, whereas IPGP supplied downhole equipment, data acquisition system, and field personnel. Finally, Geostress contributed with field personnel.

This document includes a detailed description of observations made in the field, and results.

Of the 34 tests conducted at drill site 9, only 21 involve unambiguous data, i.e. have a reliable normal stress and a well-defined fracture geometry (although only five of these exhibit one single fracture plane). The success rate of testing was hence unusually low for this type of hydraulic stress measurement equipment. The primary reason for the reduced success rate was that sub-horizontal fractures were induced. These fractures were created when the pressure in the test section was just moderately larger (a few bars) than the theoretical weight of the overburden rock mass. This implies that a major constraint for injection testing prevailed and that sub-horizontal fractures were induced in all cases where the fracture did not re-activate before reaching this critical pressure. The physical explanation for these fractures is yet to be determined, but the relatively moderate testing depth in combination with the inclined boreholes (KFM09A is inclined c 59^{o} at surface, flattening out to c 41° at the borehole bottom, whereas KFM09B is inclined c 55^{o} at surface and 43° at the borehole bottom) is probably not favorable for hydraulic stress measurements. We would like to emphasize that the observed sub-horizontal fractures contain very useful information. If a failure criterion for these fractures is derived, they will contribute much to the knowledge of the present state of stress at the Forsmark site.

SAMMANFATTNING

Hydrauliska bergspänningsmätningar har utförts i borrhål KFM09B (18 tester) och KFM09A (16 tester) i Forsmark. Totalt gjordes således 34 tester i två separata kampanjer mellan den 6:e juni och 20:e juli, 2006.

Aktiviteten var ett samarbetsprojekt mellan Vattenfall Power Consultant AB (huvudkonsult), Institute de Physique du Globe de Paris (IPGP), och Geostress Co (båda dessa organisationer underkonsulter). Vattenfall Power Consultant AB tillhandahöll ett MKW wireline-system samt fältpersonal, IPGP stod för borrhålsutrustning, datainsamlingssystem och fältpersonal, medan Geostress bidrog med fältpersonal.

Detta dokument innehåller en detaljerad beskrivning av fältobservationer och resultat.

Av de 34 utförda injektionstesterna vid borrplats 9 är endast 21 otvetydiga, dvs uppvisar tillförlitlig normalspänning och välbestämd sprickgeometri (men endast fem av dessa har en enskild spricka i testsektion). Andelen otvetydiga tester är därför lägre än normalt för metoden och är en följd av att sub-horisontella sprickor skapats vid många av testerna. Dessa sprickor inducerades redan vid ett pålagt tryck som endast måttligt översteg den teoretiska vertikalspänningen och innebar därför en stark begränsning av metodens möjligheter. De bakomliggande fysikaliska orsakerna till uppkomsten av dessa sprickor återstår att förklara, men de relativt måttliga testdjupen i kombination med borrhålens relativt stora lutning (KFM09A har lutningen ca 59^{o} vid ytan och flackar sedan ut till ca 41° vid borrhålets, medan motsvarande siffror för KFM09B är ca 55^{o} vid ytan och 43° vid botten) är sannolikt inte fördelaktiga för denna typ av mätningar. Vi vill dock betona att om ett brottkriterium för dessa sprickor kan härledas, kan en systematisk analys av den datamängd som dessa sprickor representerar sannolikt ge ett mycket värdefullt bidrag till beskrivningen av det rådande spänningsfältet i Forsmark.

Contents

1 Collected data in boreholes KFM09A and KFM09B

The collected data comprise numerous parameters for determination of the stress field but also for verification of the data recording quality, which are described below.

1.1 Fracture orientation and groundwater pressure data

The three alternative means of determining fracture orientations available in this activity are described in Chapter 4.2.5. Regarding fracture orientation by using the Mosnier tool the reliability of the fracture orientation determination rests on three features:

- The proper recording of all parameters that characterize the position of the tool in the well (borehole length, and measurements results from 3 magnetometers and 2 inclinometers).
- The good understanding of tool manufacturing and its consistency with data processing routines.
- The repeatability of orientations during comparisons of multiple scans of the same fracture.

There are a few independent means to verify that the overall data recording has been successful. One involves readings of orientation devices as the tool is lowered and hoisted in the borehole. The values of the magnetic field inclination, as determined from magnetometers, offer a completely independent check on the digitization procedure used for the downhole data acquisition and surface data recording. The results of the measurements of well azimuth and well inclination are compared with those obtained with Maxibor as well as with the Uppsala magnetic field observatory are presented in Appendices 1 and 2. For both wells, we are always within 2° with the Uppsala observatory results below about 250 mbl. Above this depth, electric noise is disturbing all downhole sensors. Moreover, the inclinometer results are reproducible (comparison between pre- and post-logs) within 2°. Note that the well orientation of the HTPF tool refers to the magnetic North, whereas the Maxibor refers to the geographical North ($N_{magnetic} = N_{geographical} + 2.464^{o}$ at the time of measurements).

The other independent control of successful data recording is correlated with the observed variations in downhole pressure during lowering and hoisting in the borehole. These variations, which were investigated after completed field campaign, can be compared with the theoretical weight of the water column in the borehole and indicate that no discrepancies were found during measurements at drill site 9.

The reliability of orienting sensors (inclinometers and magnetometers) is provided by the repeatability of observations. Further comparison with independent data provides evaluation of accuracy of tool orientation. Repeatability is better than 2° on inclinations and 6° on borehole azimuth between the various reconnaissance logs and post logs. Magnetic field inclination determinations are always within 2.5° of Uppsala observatory measurements, for all depths greater than 300 m (Appendices 1 and 2). Position in well is calibrated on that of the BIPS and cores.

1.2 Calibrations

1.2.1 Pressure transducers and flow meter

Prior to the measurements, the pressure transducers were calibrated against a reference load cell and the flow meters by volume (mass) determination per time unit prior to field measurements (Appendix 3). Note that response remains linear with time and that the calibration factor has not changed during the complete duration of all tests at the Forsmark site (calibrations were run in May, early June, late July, and in October, 2006). The apparent noise comes from the time response of the testing system, not from the transducers. If data would have been plotted with respect to time, all sensors would have been very stable. Also note that nowhere in the stress determination procedure do we require flow rate measurements. These are only used to control the re-opening of fractures, and the normal stress measurements are only based on shut-in.

1.2.2 Tilt meters and magnetometers

The orientation devices were checked for functionality and calibrated several times during the campaign: prior to departure to the field, before entering each borehole, and after completed measurements.

The calibration prior to descent in the well consists of two phases. In the first phase, the orientation device is placed in a special calibration support and both inclinometers and the three magnetometers are tested for various inclinations and orientations so that the readings are not saturated for any inclination/orientation.

In phase two, the orientation device is placed inside the HTPF tool (Mosnier, 1982; Mosnier and Cornet, 1989). Using a special calibration plate, the tool is first placed vertically and orientations are checked for every 20^{o} of rotation around the tool axis. Thereafter, the HTPF tool is inclined about 45^{o} towards the North, followed by verification of readings for every 20^{o} rotation around the tool axis. The latter is then repeated with the tool inclined 45^{o} towards East, South, and West. Finally, the HTPF tool is placed horizontally and is rotated around a vertical axis during which the output of the axial magnetometer is sampled. When the tool is fixed in the N, E, S, and W, the output of the perpendicular magnetometers is sampled during the corresponding rotation around the tool axis.

Phases one and two of the calibration before descent are repeated when the work in the well has been completed, to verify that the readings are systematic. Moreover, after the field campaign, the electrical imaging logs are used to provide independent data on dip and azimuth of the well (see 1.1 above).

For borehole KFM09B, there is a small problem with the magnetometers, whereas the inclinometers are functional and the comparison of magnetic inclination from the Uppsala magnetic field observatory is good. We have repeatedly observed that magnetometers have some drift, during the motion in the wells, but this generally poses no problem because the tool rotates by itself as it moves up or down. These rotations are used to obtain the exact compensation factors. For borehole KFM09B, however, the tool did not rotate fully but only for around 90°. Hence, the tool does not cover all azimuthal ranges, and compensation factors cannot be determined precisely. The outcome of this problem is that the fracture orientations are dependent upon the deviation measurements conducted by SKB, i.e. a completely independent fracture orientation determination cannot be made for this borehole.

1.2.3 Length measurements

For the sake of stress determination, the knowledge of absolute depth to within a few metres is quite sufficient. But because the objective is to relate images of features on the HTPF logs with those observed on cores, an adjustment to some decimetre is necessary.

Initially, the reference grooves in the borehole were intended to be identified with the HTPF tool. However, the grooves proved to be too small for identification and a different strategy had to be adopted.

Instead, we compared the electrical imaging log with the cores and the BIPS images for a few unique features in the well. Once identified, by interpolation, equivalence is proposed between HTPF logs and BIPS/Boremap depths for the complete borehole length. Thereafter, each pre-existing fracture tested was correlated with the equivalent fracture observed on the cores. In addition, the tested fracture was photo documented in the core boxes. This comparison entails that the length calibration between the two systems is within 2 dm for drill site 9.

KFM09A

During the measurements in KFM09A, which were made after testing in borehole KFM09B, attempts were made to scan most reference marks with a reduced logging speed of about 0.5 m/min. However, the reference marks could still not be detected with the HTPF tool. Instead, similar as for borehole KFM09B, the length was calibrated using detailed comparisons with images, cores, and the BIPS for unique features.

Two sections, both involving about 20 m of core, were carefully mapped to achieve an accurate correspondence between fractures observed on the HTPF log and of those seen on cores and mapped in BIPS. The two depth intervals were located at 669.78 mbl on the BIPS log, which corresponds to 673.24 m on the imaging log, and at 354.06 mbl on the BIPS log, which corresponds to 355.55 mbl on the imaging log. Once established, a gradient for the borehole was determined and the correspondence between the HTPF log and the length calibrated BIPS was within 10 cm. This allowed exact determination of the pre-existing fracture tested in each test section. According to these fits, the electrical imaging depth is 1.49 m off the BIPS at 354.06 mbl and 3.46 m off BIPS at 669.78 mbl. This leads us to propose the following approximation:

BIPS length = 0.7 + 0.994 * electrical imaging length.

KFM09B

The calibration was conducted by comparison with electrical images, BIPS, and cores at two different depths, around 250 m and around 570 mbl. At both depths, the electrical imaging log has been exactly (to the very centimetre) matched with cores by fitting precisely fractures over a borehole length equal to about 6 m between 570 m and 576 mbl (log depth), and about 10 m between 221 m and 231 mbl (log depth). The exact fit is demonstrated by the very same fracture pattern as identified on the log and on the cores. Then, precise fit between cores and BIPS was established by identifying large crystalline structures or veins on both the cores and the BIPS images. This provides an accurate fit between BIPS and electrical imaging.

Between 231 and 221 mbl, the following has been first grossly fitted: fractures between 230.5 and 231 mbl, then the fractured zone between 228.5 and 226.9 mbl. Then the three fractures seen at 225.49, 224.50, 223.72 mbl on the imaging log have been used to

adjust to the very centimetre the cores and the imaging log. The core recovery is continuous at this depth and a very clear white vein is identified on both the cores and the BIPS at 231.12 mbl (BIPS length). This provides the exact match between imaging log and BIPS between 231 and 223 mbl.

Around 572 mbl, a very characteristic altered zone, about 4 m thick, is very easily identified on the electrical imaging log (575.0 and 570.4 mbl), on the cores (between 573 and 569 mbl) and on the BIPS images (around 570 mbl). This ensures a first matching to a few tens of centimetres. Then the exact match, to the very centimetre, between cores and imaging log is provided by two fractures that intersect each other, thus producing a characteristic X-shape on the electrical imaging log (569.8 mbl), also easily identifiable on the cores. According to these fits, the electrical imaging depth is 0.9 m off the BIPS at 231 mbl and 2.9 m off at 570 mbl. This leads us to propose the following approximation:

BIPS length = 0.995 * electrical imaging length.

1.3 Reconnaissance logs

Because the notion of rock stress is a concept of continuum mechanics, it is necessary to identify volumes where the continuity hypothesis is verified. The first interpretation of the continuity hypothesis is given by the reconnaissance log with the HTPF tool (Appendices 4 and 5). During the reconnaissance log, the intensity of the injected electrical current is adjusted to highlight very tiny fractures (which are suitable for hydraulic injection testing), which means that very conductive fractures, i.e. potential stress decoupling zones, are clearly outlined by a significant change of resistivity. The first evaluation provided by the HTPF tool is used for selection of suitable test sections.

Note that the borehole lengths as displayed in the reconnaissance log may be somewhat shifted as compared with the lengths given in the various tables of this document. This is a length calibration problem with no significance for the interpretation of data.

1.4 Testing results

The results of testing are presented in Appendices 6 and 7. For each test the following is presented:

- The downhole pressures in the chamber (test section) and in the packers versus time are displayed and below, in a separate plot, the fluid flow rate versus time.
- Blow-ups of the shut-in curves for each cycle are presented on the second page.
- The third page displays the pressure versus flow rate during the jacking tests for all cycles (if conducted).
- The fourth and fifth pages include the post-frac log with the test section marked. Note that this log starts at the bottom and moves upwards, implying that the fracture is “up-side down” compared to the following detailed plots.
- The next pages include detailed plots of the test section with: (i) results of the reconnaissance log; (ii) results of the post-log, which may be multiple when different electrical gains have been applied to enhance visibility and/or

when the fracture is located underneath the packers; (iii) interpretation of fracture one; (iv) interpretation of fracture two; etc.

The borehole lengths as displayed in the reconnaissance log and in the post-log may be somewhat shifted as compared with the lengths given in the various tables of this document. This is a length calibration problem with no significance for the interpretation of data. The correct borehole length and vertical depth for each test are found in the tables.

1.5 Interpreted data

The analysis of data is based on the ISRM suggested methods for rock stress estimation by hydraulic fracturing and hydraulic tests on pre-existing fractures (Haimson and Cornet, 2003).

The interpreted data in Appendices 8 and 9 are presented in tabular form so that full traceability is achieved. This means that the appendices cover the collected raw data, the first interpretation of the data (e.g. normal stresses for each cycle in the injection testing), and the final interpretation of e.g. the normal stress acting on the fracture.

Normal stresses are denoted using a geomechanical sign convention with compressive stresses taken as positive. Measurement positions are given as the borehole length of the centre of the test section. The corresponding vertical depth is based on recalculation of the borehole length using the deviation file delivered from Sicada. All orientation data represent the normal of the fracture plane, positive downwards, and are given with respect to geographic North according to coordinate system RT90 2.5 gon W 0:-15 for x and y and RHB70 for z, using a right-hand rule notation.

1.5.1 Fracture orientation data

In principle, the fracture orientations (i.e. the normal to the fracture plane) can in this specific assignment be determined with three different methods:

- Based on magnetometers and inclinometers of the HTPF tool
- Based on SKB´s deviation measurements of the well (the optical Maxibor method or the magnetic Flexit method) and tool face (inclinometers) of the HTPF tool
- Based on SKB´s BOREMAP system (Maxibor or Flexit deviation measurements) and tool face of the BIPS tool.

However, it must be pointed out that the third method is not available for fractures induced during the HF-/HTPF-campaign, because they were induced after the logging with the BIPS tool.

In the result files (Appendices 8 and 9), the results using method 2 are displayed (i.e. based on the Maxibor method).

Fracture orientation determined with the HTPF tool is obtained by fitting a sinusoid to the electrical image seen on the log. Special zooming techniques are used to identify more precisely the fracture. Two sinusoids are fitted to the image so as to identify domains of uncertainty. The central value is taken as the dip and azimuth values and the

width of the interval on the values is selected as the 90% confidence level (to be compared with 99% confidence interval for pressure data).

1.5.2 Normal stresses

Because Cornet et al. (2003) observed that the normal stress may be overestimated when based on opening phases of hydraulic jacking tests, only shut-in values have been used. The shut-in pressure determinations have been made using two methods: (i) an overestimate of the shut-in pressure is provided by the Hayashi and Haimson procedure (1991) that indicates when the fracture stops being "opened"; and (ii) an underestimate is provided by the Aamodt and Kuriyagawa procedure (1981) that indicates the first pressure for which the fracture may be regarded as "closed". The normal stress, or shut-in value, is taken equal to the mean of these methods, i.e.

$$\sigma_n = \frac{\sigma_{n,Aa\,\mathrm{mod}\,t,\min} + \sigma_{n,Aa\,\mathrm{mod}\,t,\max} + \sigma_{n,Hayashi,\min} + \sigma_{n,Hayashi,\max}}{4} \quad (1)$$

Moreover, the tangent method of Enever and Chopra (1989) is used to allow comparisons (Appendices 8 and 9). The extreme values for the Hayashi and Haimson (1991) and the Aamodt and Kuriyagawa procedure (1981) are taken as bounds of the 99% confidence interval.

1.6 Comparison of fracture orientations determined with different methods

In appendices 10 and 11, the fracture orientations as observed in the Boremap system are compared with those of the HTPF tool. Note that these appendices present the truly tested fractures, as opposed to the fractures aimed for testing presented in Chapter 1.9. After this comparative study was initiated, a decision was taken to up-date SKB´s well deviation measurements, entailing that for many boreholes Maxibor measurement will be exchanged to Flexit measurements as the official deviation measurement files in SKB´s database Sicada. This up-date also affects the fracture orientations in Boremap as they are based on deviation data. In Appendices 10 and 11, the Boremap orientations based on the new Flexit well deviation data are presented, whereas the orientations of the HTPF tool is based on Maxibor.

For borehole KFM09A, the correspondence between methods yields an average deviation for azimuth and dip of the normal to the fracture plane of 13.5^o and 3.5^o, respectively. Only one test (at 557.9 mbl) displays a significantly different fracture orientation between the methods. When excluded, the average difference between methods is reduced to 11.2^o and 3.1^o, respectively.

For borehole KFM09B, the correspondence between methods yields an average deviation for azimuth and dip of the normal to the fracture plane of 20.2^o and 4.9^o, respectively. Two tests (at 523.0 and 368.6 mbl) display a significantly different orientation fracture between both methods. When excluded, the average difference between methods is reduced to 10.4^o and 4.0^o, respectively.

1.7 Analysis of errors in well orientation data on fracture orientation determination

Because the results of the electrical imaging system is dependent upon the well deviation data, the up-date of deviation data from Maxibor to Flexit introduces errors in

the fracture orientation data of the electrical imaging system. As a result of this, a study was initiated attempting to quantify this error. The result is presented in Appendix 12 and indicates that the error is very small and negligible for the sake of stress determination. Hence, HTPF orientations based on Maxibor well deviation data were not updated with the new Flexit well deviation data.

1.8 General trends in collected data

1.8.1 KFM09A

The normal stresses of the tests in borehole KFM09A indicate that all measurements are fairly close to the theoretical weight of the overburden rock mass (0.026 MPa/m; Figure 1-1 and Figure 1-2). Noticeable is that eight tests show a normal stress significantly lower than the theoretical weight of the overburden rock mass. This result will be discussed in Chapter 1.9.

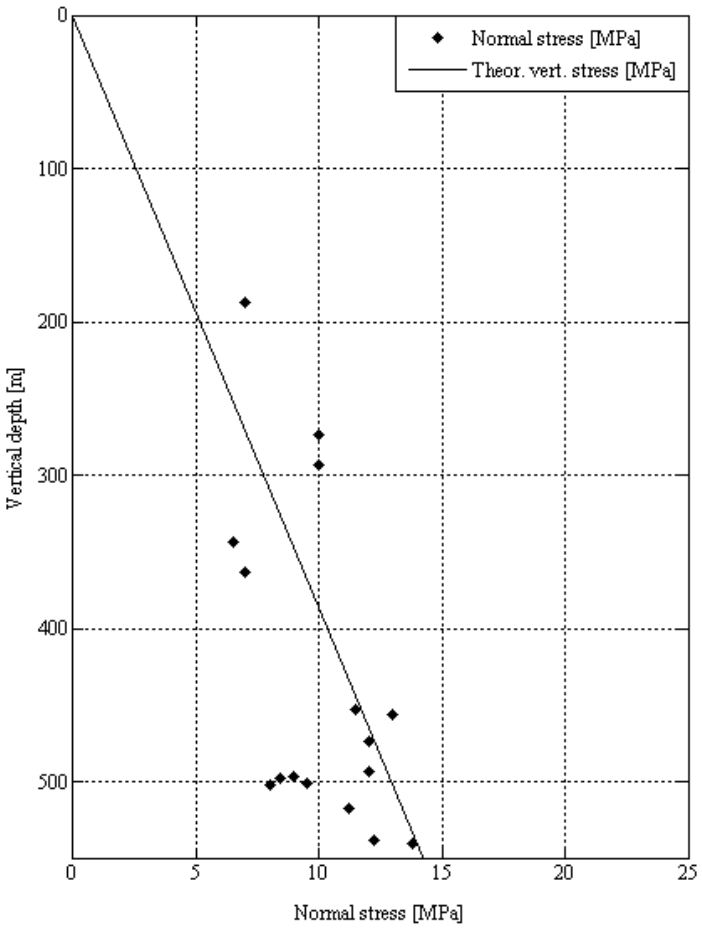

Figure 1-1. *Normal stresses versus depth in borehole KFM09A.*

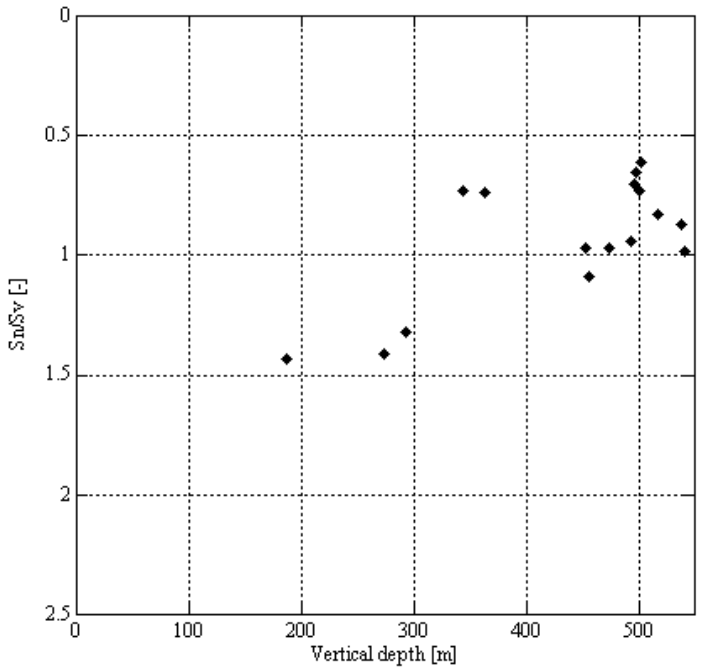

Figure 1-2. *Normal stresses divided by theoretical vertical stress versus depth in borehole KFM09A.*

Polar plots of the fractures aimed for testing versus the observed distribution of the normal to the tested fractures are presented in Figure 1-3A. The result indicates that a large number of sub-horizontal fractures have been tested, which is in accordance with observed normal stresses. However, in the tested fractures (Figure 1-3B), three other groups can be identified: (i) one group of steeply inclined fractures with a normal oriented about NE-SW; (ii) one group of moderately inclined fractures with a normal oriented about SE; and (iii) one group of steeply inclined fractures oriented about E-W. Given that previous determinations of maximum horizontal stress orientation has been found in average close to 140^{o}N, these fractures would constrain minimum and maximum horizontal stress, respectively. This will be further discussed in Chapter 1.9.

1.8.2 KFM09B

Also in borehole KFM09B, the normal stresses of the tests indicate that most measurements are close to the theoretical weight of the overburden rock mass (0.026 MPa/m; Figure 1-4 and Figure 1-5). This result will be discussed in Chapter 1.9.

Polar plots of the fractures aimed for testing versus the observed distribution of the normal to the tested fractures are presented in Figure 1-6A. The result indicates that an overwhelming majority of sub-horizontal fractures has been tested. However, a set of moderately inclined fractures with a normal oriented NE-SW as well as a few steeply inclined fractures with a normal oriented NW-SE have also been tested.

A **B**

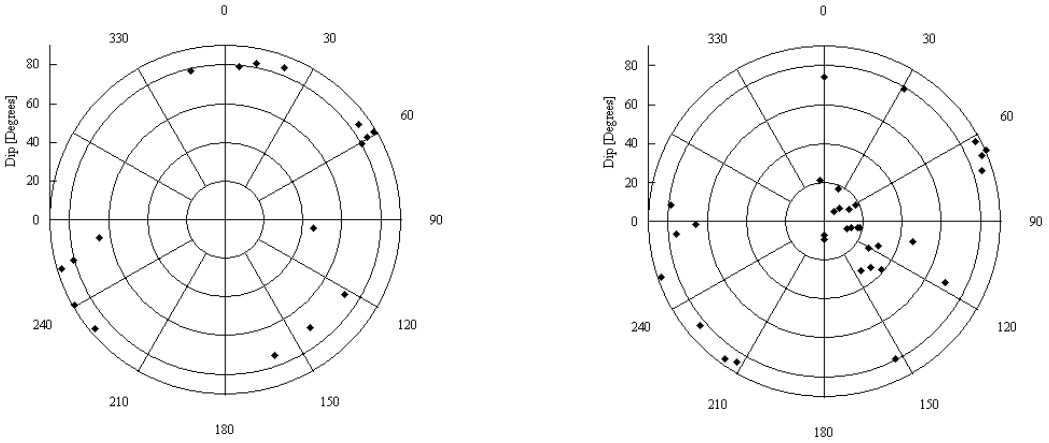

Figure 1-3. *Polar plot of normal to the fracture planes in borehole KFM09A: A) Fractures aimed for testing; B) Resulting fracture orientations.*

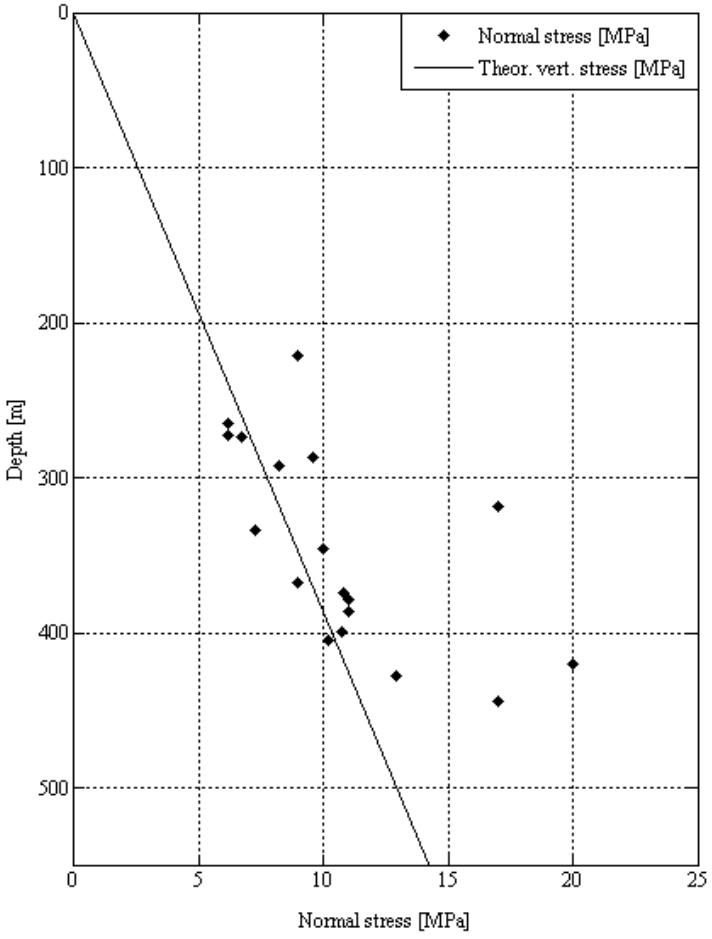

Figure 1-4. *Normal stresses versus depth in borehole KFM09B.*

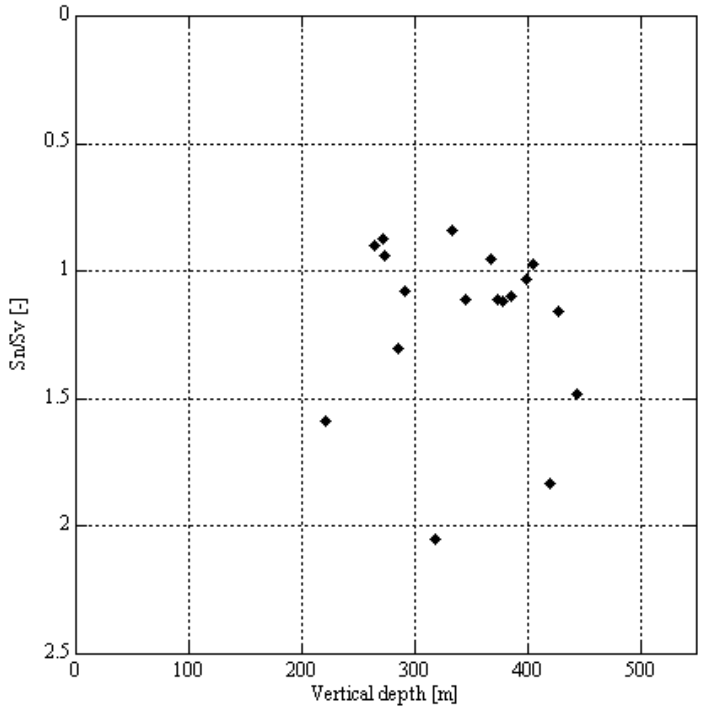

Figure 1-5. *Normal stresses divided by theoretical vertical stress versus depth in borehole KFM09A.*

A **B**

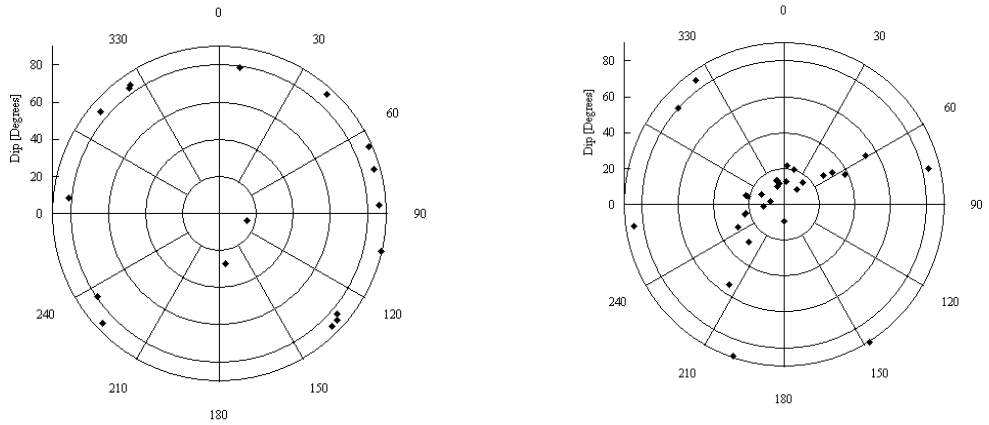

Figure 1-6. *Polar plot of normal to the fracture planes in borehole KFM09B: A) Fractures aimed for testing; B) Resulting fracture orientations.*

1.9 Individual tests

The fractures aimed for testing in boreholes KFM09A and KFM09B are presented in Table 1-1 and Table 1-2, respectively, and indicate that a large number of sub-horizontal fractures have been induced. These fractures sometimes appear in the test section, although they are more commonly located at the end of the test section (i.e. at the packer ends) and sometimes underneath the packers. Hence, a majority of the

fractures are packer induced. In a few tests, multiple sub-horizontal fractures were created (e.g. about 14 fractures in test 4 in borehole KFM09B).

The induced sub-horizontal fractures cause a significant problem in the evaluation of the tests. The reason for this is that the opening of a fracture changes the stress field locally, but leaves the normal stress unaffected. Hence, for multiple fractures in the test section, the fracture normal stresses can be unambiguously determined only when the fractures are parallel.

By the appearance of the sub-horizontal fractures on the electrical imaging logs, many fractures seem to have experienced no or very limited propagation or fluid percolation, although visual inspection is a somewhat speculative approach. This would imply that, similar to drilling induced fractures (Brudy and Zoback, 1993; Peska and Zoback, 1995; Zoback et al., 2003) or fractures induced by sleeve fracturing technique (Stephansson, 1983a; b), they do not extend far into the rock. If this would be true, they would not distort the stress field as much as fully propagated fractures. Because the effect of the sub-horizontal fractures has not been investigated fully at this stage, HTPF tests that have changed the resistivity image of the aimed pre-existing fracture but that also include sub-horizontal fractures, have been assigned “potentially successful re-opening” in Table 1-1 and Table 1-2 below.

Table 1-1. Results from individual injection tests in borehole KFM09A.

			Aimed fracture (BOREMAP)					
Test [No]	**Bh length [m]**	**Depth [m]**	**Azimuth [^{o}N]**	**Dip [^{o}]**	**σ_n [Bar]**	**$\sigma_{v,theory}$ [Bar]**	**Successful re-opening**	**Additional fractures**
1*	672.6	540.5	23 232	84 87	117	141	No No	Two sub-horizontal fractures^{EoP}
2*	669.7	538.5	97	46	119	140	Potentially	Two, possibly three, sub-horizontal fractures^{EoP,UP}
3*	640.6	517.5	60-61 242	88-89 89	100	135	Yes	No
4*	619.8	502.0	56	85	81	131	Potentially	Two sub-horizontal fractures^{EoP}
5	613.9	498.0	-	-	84	130	HF	Multiple sub-horizontal fractures^{EoP,UP}
6*	611.0	496.0	144	70	79	129	Yes	No
7	617.0	500.5	-	-	107	130	HF	Sub-horizontal fracture^{EoP}
8*	606.5	493.0	254-257	87-88	120	128	Potentially	Sub-horizontal fracture^{TS}
9*	580.8	473.5	60-63	78-82	95	123	Yes	No
10	557.9	456.0	162	74	117	119	Potentially	Two sub-horizontal fractures^{EoP}
11	553.7	453.0	7 12	82 79	112	118	Potentially	Sub-horizontal fracture^{EoP}
12*	437.0	363.0	349	79	70	94	No	Two sub-horizontal fractures^{EoP}
13	412.6	343.5	252-261	78-83	65	89	Yes	No
14	348.9	293.0	58-63	83-85	83	76	Potentially	Two sub-horizontal fractures^{EoP}
15*	325.2	273.5	263	65	90	71	Potentially	Sub-horizontal fracture^{EoP}
16*	221.3	187.5	122	72	66	49	Potentially	Sub-horizontal fracture^{UP}

Note: “TS”, “EoP”, and “BP” denote sub-horizontal fracture in the Test Section, at the End of the Packer, and Underneath the Packer, respectively. Theoretical vertical stress based on a vertical gradient of 0.026 MPa/m. Unambiguous data are marked with “*”.

Table 1-2. Results from individual injection tests in borehole KFM09B.

			Aimed fracture (BOREMAP)					
Test [No]	**Bh length [m]**	**Depth [m]**	**Azimuth [^{o}N]**	**Dip [^{o}]**	**σ_n [Bar]**	**$\sigma_{v,theory}$ [Bar]**	**Successful re-opening**	**Additional fractures**
1*	555.5	428.2	65	87	129	111	No	Multiple inclined fracture$^{TS, UP}$
2*	542.8	419.8	87	86	200	109	Potentially	Multiple inclined fracture$^{TS, EoP}$
3*	523.0	405.5	112	14	102	105	Potentially	Two sub-horizontal fractures^{TS,EoP}
4	514.9	399.0	62	31	107	104	Potentially	Multiple inclined fracture$^{TS, EoP, UP}$
5*	477.9	374.0	42 227	89 86	100	97	No	Sub-horizontal fracture and complex geometry
6*	469.0	367.0	236	79	90	95	No	Multiple inclined fracture$^{TS, EoP, UP}$
7*	439.2	345.0	324	84	100	90	Potentially	Multiple inclined fracture$^{TS, EoP, UP}$
8	424.5	334.0	74	85	73	87	Potentially	Multiple inclined fracture$^{TS, EoP, UP}$
9*	403.3	318.0	275-277	81-84	150	83	Potentially	Multiple inclined fracture$^{TS, EoP, UP}$
10*	368.6	292.5	174	26	82	76	Potentially	Sub-horizontal fracture^{EoP}
11*	359.7	286.0	130	82	92	74	No	Sub-horizontal fracture^{TS}
12*	342.7	273.0	8	80	67	71	No	Sub-horizontal fracture^{TS}
13*	333.2	265.5	145	81-85	59	69	No	Sub-horizontal fracture^{TS}
14	579.2	444.5	-	-	166	116	HF	Sub-horizontal fracture^{TS}
15	495.6	386.0	-	-	114	100	HF	Sub-horizontal fractures^{TS,UP}
16	484.7	378.5	-	-	110	98	HF	Sub-horizontal fractures^{TS,UP}
17	276.2	221.0	131 134	86 84	87	57	No	Sub-horizontal fractures^{TS,UP}
18	272.2	218.5	102	88	62	57	No	Sub-horizontal fractures^{TS}

Note: “TS”, “EoP”, and “BP” denote sub-horizontal fracture in the Test Section, at the End of the Packer, and Underneath the Packer, respectively. Theoretical vertical stress based on a vertical gradient of 0.026 MPa/m. Unambiguous data are marked with “*” in the first column.

2 Discussion and summary

2.1 General

Hydraulic rock stress measurements were performed in boreholes KFM09B and KFM09A at the Forsmark candidate area. Of the 34 tests conducted at drill site 9, only 21 of them involved completely unambiguous data, i.e. have a reliable normal stress and a well defined fracture geometry. Of these, only five involve a single fracture geometry in the test section. The success rate of testing was hence unusually low for this type of hydraulic stress measurement equipment.

The primary reason for the reduced success rate was that sub-horizontal fractures frequently were induced. These fractures sometimes appear in the test section, although they are more commonly located at the end of the test section (i.e. at the packer ends) and underneath the packers. Hence, a majority of the fractures are packer induced. In a few tests, multiple sub-horizontal fractures were created (e.g. about 14 fractures in test 4 in borehole KFM09B; Appendix 7).

The sub-horizontal fractures were induced when the pressure in the test section was just moderately higher (a few bars) than the theoretical weight of the overburden rock mass. This implies that a major constraint for injection testing prevailed at the site and that sub-horizontal fractures were induced in all cases where the fracture did not re-activate before reaching this critical pressure. The physical explanation for these fractures is not yet fully understood but we would like to emphasize that the observed sub-horizontal fractures contain very useful information. If a failure criterion for these fractures is derived, they will contribute much to the knowledge of the present state of stress at the Forsmark site.

The induced sub-horizontal fractures cause a significant problem in the normal evaluation of the injection tests. The reason for this is that the opening of a fracture changes the stress field locally, but leaves the normal stress unaffected. Hence, for multiple fractures in the test section, the fracture normal stresses can be unambiguously determined only when the fractures are parallel.

For the somewhat surprising result of normal stresses lower than the theoretical vertical stress (Figure 1-2 and Figure 1-5), the most reasonable explanation is that the normal stress corresponds to a sub-horizontal fracture located near the end of the packer element. The fracture is thereby prevented from closing when pressure drops in the interval and affects the shut-in measurement. This is manifested by poor flow back tests that help detect this difficulty. In practice, flow back tests are part of the quality assurance procedure for selecting completely unambiguous tests. This phenomenon has, as far as we know, not been found outside the Forsmark or Oskarshamn sites (Ask et al., 2007). This means that it is either specific to these sites, or perhaps more likely, it has not been detected before due to limitations in fracture determination methods (which normally involve impression packer technique).

2.2 Borehole specific objectives

The borehole specific objectives of the hydraulic stress measurements at drill site 9 were to (i) decrease uncertainty in data on in-situ state of stress, (ii) increase the

understanding of how local geological site conditions may affect the state of stress, and (iii) provide input for site descriptive modelling on the state of stress at the site.

The borehole specific objectives were slightly different, and for KFM09B they involved:

- Test the effectiveness of the HTPF tool in the rock mass at the Forsmark site.
- Work out an effective strategy for stress determination with the hydraulic methods within the SKB Site Investigation Program.
- Identify what types of fractures that seem feasible for HTPF.
- Test the capacity of the equipment for HF in competent, unfractured rock at a vertical depth of at least 400 – 500 m.
- If feasible, also determine the state of stress at the borehole location, at least down to a vertical depth of 500 m.

For borehole KFM09A, the objectives were to:

- Identify what types of fractures that seem feasible for HTPF.
- Identify possible decoupling zones along the borehole.
- Determine the state of stress at the borehole location, from 100 m depth and at least down to a vertical depth of 500 m.

These objectives and how they have been fulfilled are described below.

2.2.1 Effectiveness of the HTPF tool and identification of suitable test sections

The effectiveness of the HTPF tool is clear when looking at the result of the reconnaissance and post-logs (Appendices 4 to 7). A large number of electrically conductive features exist in the boreholes, and they are repeated for each new log performed, which implied that they might be opened using a suitable injection testing strategy. The HTPF tool was also successful with respect to post-log images, which also include the entire packer sections. Indeed, this feature has proven most valuable given the very common observation of packer induced fractures. Only in one occasion, in the homogeneous rock formation at about 574 mbl in borehole KFM09B, the imaging tool provided data with reduced quality. This homogeneous formation is located immediately below a large alteration zone in which the electrical signal is completely saturated. This was marked also on the pre-log image by an imprecise/blurry appearance. We interpret the absence of signal as that the alteration zone causes a short-circuit for the electrical signal, preventing a large enough intensity to be detected by the electrodes on the tool. This result thus entails that alteration zones may mask electrical signatures below the zone corresponding to the length of the bridle (the about 20 m long insulated geophysical cable).

2.2.2 Strategy for stress determination with the hydraulic methods.

The testing program was successful in the aspects of finding suitable test sections and to stimulate and open pre-existing fracture planes. During the first injection tests in borehole KFM09B, it became clear that sub-horizontal fractures were induced. Once

this could be established, the following injection tests were modified to include a longer percolation process. However, this did not improve the situation much due to the strong sealing of the pre-existing fractures. We believe that in this respect, the inclination of the well was not optimal for HTPF testing (they were far less numerous in the sub-vertical wells KFM07C (Appendix I) and KLX12A (Ask et al., 2007)) as the weight of the overburden and the tensile strength completely govern the pressure level that can be used during the first quasi-static re-opening of the pre-existing plane of weakness. Hence, this cannot be controlled by modifications of testing procedure or strategy.

2.2.3 Test the capacity of the equipment for HF in competent, unfractured rock at a vertical depth of at least 400 - 500 m

Due to the inducement of sub-horizontal fractures, the capacity of the equipment was never near its limit, which is 380 bars differential pressure. Normally, this is sufficient for measurements at least down to 1000 m vertical depth. Thus, problems to fracture the rock, as experienced by Klee and Rummel (2004), were not encountered.

2.2.4 Identify possible decoupling zones along the borehole.

The electrical imaging tool is very useful for identification of possible decoupling zones. Such zones are clearly displayed as electrical anomalies (red coloured in the logs).